
20th International Symposium on Nonlinear
Acoustics

—
2nd International Sonic Boom Forum

BOOK OF ABSTRACTS

20th ISNA

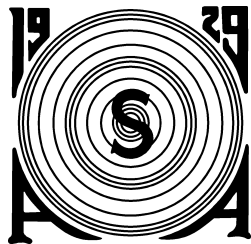
LYON, FRANCE - JUNE 29, JULY 3



ÉCOLE
CENTRALE LYON

Sponsors

We would like to thank our sponsors:



Program of the conference

14

Table of contents

Monday 29 june, 2015 - Plenary lecture 1: Robin Cleveland

Amphi 2

- 15:10 **Nonlinear acoustics in biomedical ultrasound** 17
R. Cleveland

Monday 29 june, 2015 - General nonlinear acoustics 1

Amphi 1 bis

- 16:20 **Standing Shear Waves in Anisotropic Viscoelastic Media** 18
T. Krit, I. Golubkova and V. Andreev
- 16:40 **Second-Harmonic Generation in Shear Wave Beams with Different Polarizations** 19
K. Spratt, Y. Ilinskii, E. Zabolotskaya and M. Hamilton
- 17:00 **Effect of Nanostructuring on the Elastic Properties of Aluminum Alloy AMg6.** 20
V. Prokhorov, A. Korobov, A. Kokshaiskii, S. Perfilov and A. Volkov
- 17:20 **Application of Weak Shock Theory to Transient Plane Shear Waves** 21
J. Cormack and M. Hamilton

Monday 29 june, 2015 - Therapeutic applications 1

Amphi 2

- 16:20 **Histotripsy: Nonlinearities Essential for Therapeutic Lesion Formation** 22
C. Cain
- 17:00 **Use of Shock-Wave Heating for Faster and Safer Ablation of Tissue Volumes in High Intensity Focused Ultrasound Therapy** 23
V. Khokhlova, P. Yuldashev, I. Sinilshchikov, A. Partanen, T. Khokhlova, N. Farr, W. Kreider, A. Maxwell and O. Sapozhnikov
- 17:20 **Nonlinear effects in ultrasound fields of diagnostic-type transducers used for kidney stone propulsion: characterization in water and derating to clinically relevant depth in tissue** 24
M. Karzova, B. Cunitz, P. Yuldashev, Y. Andriyakhina, W. Kreider, O. Sapozhnikov, M. Bailey and V. Khokhlova
- 17:40 **Quantitative Assessment of Reactive Oxygen Species Generation by Cavitation Incepted Efficiently Using Nonlinear Propagation Effect** 25
Y. Jun, S. Yoshizawa and S.-I. Umemura

Monday 29 june, 2015 - Thermoacoustics 1

Amphi 3

- 16:20 **Nonlinear Diffusion-Wave Equation for a Gas in a Regenerator Subject to Temperature Gradient** 26
N. Sugimoto
- 16:40 **Magnetoacoustic Nonlinear Waves in a Heat-Releasing Plasma** 27
D. Ryashchikov, N. Molevich and D. Zavershinskiy

17:00	Lagrangian description of energy conversion in the Taconis oscillations	28
	K. Ishii, S. Adachi, H. Hayashi and I. Menshov	
17:20	Experiments on the acoustic solitary wave generated thermoacoustically in a looped tube	29
	D. Shimizu and N. Sugimoto	
17:40	Acoustic Agglomeration of Fine Particles Based on a High Intensity Acoustical Resonator	30
	Y. Zhao, X. Zeng and Z. Tian	

Tuesday 30 june, 2015 - Plenary lecture 2: Vincent Tournat

Amphi 2

11:00	Nonlinear acoustic wave processes in granular media	31
	V. Tournat	

Tuesday 30 june, 2015 - Computational methods in Nonlinear Acoustics 1

Amphi 1 bis

9:00	Three dimensional full-wave nonlinear acoustic simulations: applications to ultrasound imaging	32
	G. Pinton	
9:20	Numerical Modelling of Nonlinear Full-Wave Acoustic Propagation	33
	P.L. Rendón and R. Velasco	
9:40	GPU Simulation of Nonlinear Propagation of Dual Band Ultrasound Pulse Complexes	34
	J. Kvam, B. Angelsen and A. Elster	
10:00	Simulation of Nonlinear Ultrasound Wave Propagation in Fourier Domain	35
	F. Varray, O. Basset and C. Cachard	

Tuesday 30 june, 2015 - Therapeutic applications 2

Amphi 2

9:00	Enhancement of Cavitation Inception by Second-harmonic Superimposition for Focused Ultrasound Treatment	36
	S.-I. Umemura, S. Yoshizawa, R. Takagi and J. Yasuda	
9:40	Numerical Study of a Confocal Ultrasonic Setup for Creation of Cavitation	37
	M. Lafond, F. Chavrier, F. Prieur, J.-L. Mestas and C. Lafon	
10:00	Enhanced focus steering abilities of multi-element therapeutic arrays operating in non-linear regimes	38
	P. Yuldashev, S. Ilyin, L. Gavrilov, O. Sapozhnikov, W. Kreider and V. Khokhlova	

Tuesday 30 june, 2015 - Thermoacoustics 2

Amphi 3

9:00	Analogy between the One-dimensional Acoustic Waveguide and the Electrical Transmission Line in the Cases of Nonlinearity and Relaxation	39
	D. Yang, H. Zhang, S. Shi, J. Shi, D. Li and B. Hu	
9:20	Suppression of Oscillations in a Coupled Thermoacoustic Oscillators	40
	T. Biwa	

- 9:40 Theoretical Study of a Thermo-acousto-electric Engine equipped with an Electroacoustic Feedback Loop** 41
C. Olivier, G. Penelet, G. Poignand and P. Lotton
- 10:00 Evolution equation of subcritical Hopf bifurcation in thermoacoustic oscillations** 42
H. Hyodo and T. Biwa

Tuesday 30 june, 2015 - General nonlinear acoustics 2

Amphi 1 bis

- 13:40 Fatigue Crack Detection based on Change of Linear Ultrasonic Features caused by Structural Nonlinearity** 43
H.J. Lim and H. Sohn
- 14:00 Finite Element Modeling of the Non Collinear Mixing Method for Detection and Characterization of Closed Cracks** 44
A. Meziane and P. Blanloeuil
- 14:20 Numerical and Experimental Analysis of harmonic generation method for detection of closed cracks** 45
A. Saidoun, A. Meziane, M. Rénier, F. Zhang and H. Walaszek
- 14:40 Nonlinear Ultrasonic Imaging of Thermal Fatigue Cracks of Several Tens nm Gap in Glass Plates** 46
M. Hertl, K. Kawashima, K. Sekino, H. Yasui and T. Aida

Tuesday 30 june, 2015 - Radiation force in biology and medicine

Amphi 2

- 13:40 Nonlinear Aspects of Acoustic Radiation Force in Biomedical Applications** 47
L. Ostrovsky and A. Sarvazyan
- 14:00 Effect of particle-particle interactions on the acoustic radiation force in an ultrasonic standing wave** 48
B. Lipkens, Y. Ilinskii and E. Zabolotskaya
- 14:20 Acoustic Radiation Force due to Arbitrary Incident Fields on Spherical Particles in Soft Tissue** 49
B. Treweek, Y. Ilinskii, E. Zabolotskaya and M. Hamilton
- 14:40 Experimental Study of Acoustic Radiation Force of an Ultrasound Beam on Absorbing and Scattering Objects** 50
A. Nikolaeva, M. Kryzhanovskiy, S. Tsysar, W. Kreider and O. Sapozhnikov

Tuesday 30 june, 2015 - Thermoacoustics 3

Amphi 3

- 13:40 Oscillating viscous boundary layer at high Reynolds number : Experiments and numerical calculations** 51
I. Reyt, H. Bailliet, E. Foucault and J.-C. Valière
- 14:00 Measurements of acoustic minor loss in a tube with geometrical irregularities** 52
Y. Ueda, S. Yonemitsu and T. Saito
- 14:20 LDV measurements of Rayleigh streaming in narrow channels** 53
R. Bessis, H. Bailliet, I. Reyt and J.-C. Valière
- 14:40 New Method to Increase the Energy Conversion Efficiency of Thermoacoustic Engine.** 54
A. Kido, S.-I. Sakamoto, K. Taga and Y. Watanabe

Tuesday 30 june, 2015 - Poster session - 15:00

Velocity Measurement Method to Control the Coagulation Enzymatic	55
M. Derra, A. Amghar and H. Sahrah	
Acoustic field distribution of sawtooth wave with nonlinear SBE model	56
X. Liu, L. Zhang, X. Wang and X. Gong	
Acoustic analysis of voices from students with speech disorders	57
B. Sabir	
Cavitation Activity Enhancement by Nanoparticles in Sonodynamic Therapy of Melanoma B16	58
A. Nikolaev, A. Gopin, N. Andronova, N. Dezhkunov and E. Treshalina	
Axial acoustic radiation force on a sphere in a Gaussian beam	59
R. Wu, X. Liu and X. Gong	
Sound beam manipulation based on temperature gradients	60
F. Qian, L. Quan, X. Liu and X. Gong	
Acoustic Characteristics of the Medium with Gradient Change of Impedance	61
B. Hu, D. Yang, Y. Sun, J. Shi, S. Shi and H. Zhang	
Elastic Waves in a Wedge of Aluminum Alloy with Permanent Residual Deformations	62
A. Korobov, M. Izosimova and A. Kokshaiskii	
Influence of a low flow rate on an acoustic cavitation bubble cloud	63
A. Seck, C. Inserra, S. Ollivier, J.-C. Béra and P. Blanc-Benon	
Flow Velocity Measurement with the Nonlinear Acoustic Wave Scattering	64
I. Didenkulov and N. Pronchatov-Rubtsov	
Experimental Nonlinearity in Soft Crystals	65
N. Vilchinska	
Nonlinear Interaction of Air Bubbles and Ultrasonic Field: an Analysis of some Physical Aspects	66
C. Vanhille and C. Campos-Pozuelo	
Laser velocimetry for non-linear acoustics : an overview over two decades of research	67
J.-C. Valière and H. Bailliet	

Tuesday 30 june, 2015 - General nonlinear acoustics 3**Amphi 1 bis**

16:00 Acoustic Streaming Jets: a Scaling and Dimensional Analysis.	68
V. Botton, B. Moudjed, D. Henry, S. Millet, H. Ben Hadid and J.-P. Garandet	
16:20 Inertial effects on non linear acoustic streaming	69
V. Daru, D. Baltean-Carlès and C. Weisman	
16:40 Control of droplet temperature on disposable digital microfluidic system based on acoustic streaming	70
J. Kondoh and N. Ohashi	
17:00 Tunable Optical Lens Array Using Viscoelastic Material and Acoustic Radiation Force	71
D. Koyama, Y. Kashihara, M. Hatanaka, K. Nakamura and M. Matsukawa	
17:20 Pitch Glide Effect Induced by a Nonlinear String-Barrier Interaction	72
D. Kartofelev, A. Stulov and V. Välimäki	

Tuesday 30 june, 2015 - Imaging and tissue characterization 1**Amphi 2**

- 16:00 Implications of Superharmonic Ultrasound Contrast Agent Imaging** 73
M. Verweij, D. Peruzzini, P. Tortoli, N. De Jong and H. Vos
- 16:20 Cumulative Phase Delay Imaging - a new contrast enhanced ultrasound modality** 74
L. Demi, R.J.G. Van Sloun, H. Wijkstra and M. Mischi
- 16:40 Experimental Study of Transmission of a Pulsed Focused Beam through a Skull Phantom in Nonlinear Regime** 75
S. Tsysar, A. Nikolaeva, V. Svet, V. Khokhlova, P. Yuldashev and O. Sapozhnikov
- 17:00 Simulation of nonlinear propagation of biomedical ultrasound using PZFlex and the KZK Texas code** 76
S. Qiao, E. Jackson and R. Cleveland
- 17:20 Ultrasound Tissue Characterization: Comparison of Statistical Results using Fundamental and Harmonic Signals** 77
F. Lin, A. Cristea, C. Cachard and O. Basset

Tuesday 30 june, 2015 - Computational methods in Nonlinear Acoustics 2**Amphi 3**

- 16:00 The development of a hybrid finite difference solution of the Westervelt equation using the Fast Nearfield Method as a boundary condition for focused sources** 78
K. Bader and C. Holland
- 16:20 A boundary condition to the Khokhlov-Zabolotskaya equation for modeling strongly focused nonlinear ultrasound fields** 79
P. Rosnitskiy, P. Yuldashev and V. Khokhlova
- 16:40 Acoustic characterization of high intensity focused ultrasound fields generated from a transmitter with a large aperture** 80
D. Zhang and T. Fan
- 17:00 Experimental Validation of Computational Models for Large-scale Nonlinear Ultrasound Simulations in Heterogeneous, Absorbing Fluid Media** 81
E. Martin, J. Jaros and B. Treeby
- 17:20 A robust time-base transformation scheme for computing waveform deformation during nonlinear propagation of ultrasound** 82
B. De Graaf, S.B. Raghunathan and M.D. Verweij
- 17:40 Efficient, Adaptive Mesh Distributions for Spectral Methods Applied to Nonlinear Acoustics** 83
E. Wise, B. Cox and B. Treeby

Wednesday 1 july, 2015 - Computational methods in Nonlinear Acoustics 3**Amphi 1 bis**

- 9:00 3D Numerical Simulation of the Long Range Propagation of Acoustical Shock Waves Through a Heterogeneous and Moving Medium.** 84
D. Luquet, F. Coulouvrat and R. Marchiano
- 9:20 Modeling of strongly-nonlinear wave propagation using the extended Rankine-Hugoniot shock relations** 85
J.-W. Lee, W.-S. Ohm and W. Shim

- 9:40 Time-domain simulation of constitutive relations for nonlinear acoustics including relaxation for frequency power law attenuation media modelling** 86
N. Jimenez, F. Camarena, V. Sanchez-Morcillo, J. Redondo and E.E. Konofagou
- 10:00 Nonlinear Propagation and Decay of Intense Regular and Random Waves in Relaxing Media** 87
S. Gurbatov, O. Rudenko and I. Demin

Wednesday 1 July, 2015 - Imaging and tissue characterization 2

Amphi 2

- 9:00 Nonlinearity parameter B/A of biological tissue ultrasound imaging in echo mode** 88
M. Toulemonde, F. Varray, A. Bernard, O. Basset and C. Cachard
- 9:20 Symmetry Analysis for Nonlinear Time Reversal methods applied to Nonlinear Acoustic Imaging** 89
S. Dos Santos and J. Chaline
- 9:40 Feasibility of Low-frequency Ultrasound Imaging Using Parametric Sound** 90
H. Nomura, H. Adachi and T. Kamakura
- 10:00 Focused Shear Shock Waves in Soft Solids and the Brain: Simulations and Experiments** 91
B. Giammarinaro, F. Coulouvrat and G. Pinton

Wednesday 1 July, 2015 - Non-linear propagation in heterogeneous media 1

Amphi 3

- 9:40 Acoustic solitary waves in a lattice of Helmholtz resonators** 92
B. Lombard, J.-F. Mercier and O. Richoux
- 10:00 Nonlinear ultrasonic testing by Rayleigh waves on control of concrete cover - Application in thermal damage evaluation** 93
Q.A. Vu, V. Garnier, C. Payan, J.-F. Chaix and M. Lott

Wednesday 1 July, 2015 - Plenary lecture 3: Robert Mettin

Amphi 2

- 11:00 Bubble dynamics in high-power ultrasonic fields** 94
R. Mettin

Wednesday 1 July, 2015 - Computational methods in Nonlinear Acoustics 4

Amphi 1 bis

- 13:40 Modeling elastic wave propagation in a solid with distributed damage and kissing bonds using the Discontinuous Galerkin Finite Element Method** 95
O. Bou Matar, A. Trifonov and V. Aleshin
- 14:00 Evolution of bulk strain solitons in cylindrical inhomogeneous shells** 96
A. Shvartz, A. Samsonov, G. Dreiden and I. Semenova
- 14:20 Discontinuous Galerkin Method with Gaussian Artificial Viscosity on Graphical Processing Units for Nonlinear Acoustics** 97
B. Tripathi, B. Sambandam, F. Coulouvrat and R. Marchiano
- 14:40 Simulation of the interaction between a bubble and a ultrasound wave by implementing a two-phase compressible solver adapted to low Mach number regime.** 98
G. Huber, S. Tanguy, J.-C. Béra and B. Gilles

Wednesday 1 July, 2015 - Modeling in biology and medicine**Amphi 2**

- 13:40 Numerical Investigation of Bubble Nonlinear Dynamics Characteristics** 99
J. Shi, D. Yang, H. Zhang, S. Shi, B. Hu and S. Jin
- 14:00 A model for acoustic vaporization of encapsulated droplets** 100
F. Coulouvrat and M. Guédra
- 14:20 Nonlinear Dynamics of a Vapor Bubble Expanding in a Superheated Region of a Finite Size** 101
E. Annenkova, W. Kreider and O. Sapozhnikov
- 14:40 Numerical Study on the Effective Heating due to Inertial Cavitation in Microbubble-enhanced HIFU Therapy** 102
K. Okita, K. Sugiyama, S. Takagi and Y. Matsumoto

Wednesday 1 July, 2015 - Non-linear propagation in heterogeneous media 1**Amphi 3**

- 13:40 Simulation of blast wave propagation from source to long distance with topography and atmospheric effects** 103
M. Nguyen-Dinh, O. Gainville and N. Lardjane
- 14:00 Revisiting Geometrical Shock Dynamics for blast wave propagation in complex environment** 104
J. Ridoux, N. Lardjane, T. Gomez and F. Coulouvrat
- 14:20 Numerical Study of Heterogeneous Mean Temperature and Shock Wave in a Resonator** 105
T. Yano
- 14:40 Nonlinear reflection of a spherically divergent N-wave from a plane surface: optical interferometry measurements in air** 106
P. Blanc-Benon, M. Karzova, S. Ollivier, V. Khokhlova and P. Yuldashev

Wednesday 1 July, 2015 - Plenary lecture 4: Igor Solodov**Amphi 2**

- 15:30 Resonant Acoustic Nonlinearity for Sensitive Defect-Selective Imaging and NDT** 107
I. Solodov

Wednesday 1 July, 2015 - General nonlinear acoustics 4**Amphi 1 bis**

- 16:40 High Frequency calibration of MEMS microphones using spherical N-waves** 108
S. Ollivier, C. Desjoux, P. Yuldashev, A. Koumela, E. Salze, L. Rufer and P. Blanc-Benon
- 17:00 Acoustic emission and magnification of atomic lines resolution for laser breakdown of salt water in ultrasound field** 109
A. Bulanov
- 17:20 Novel NWV Procedure for Characterizing Nonlinear Systems with Memory for Combating and Reducing the Curse of Dimensionality** 110
A. Nuttall, R. Katz, D. Hughes and R. Koch
- 17:40 Hydrodynamic aspects of explosive volcanic eruptions** 111
V. Kedrinskiy

Wednesday 1 july, 2015 - Non-destructive evaluation methods**Amphi 2**

- 16:40 Multimode Nonlinear Resonant Ultrasound Spectroscopy (NRUS): From the 1D to 3D Characterization of the Elastic Nonlinearity** 112
M. Remillieux, T. Ulrich, C. Lake, C. Payan and P.-Y. Le Bas
- 17:00 Coda Wave Interferometry Technique for Nonlinear Defects' Localization in composite plates** 113
A. Trifonov, O. Bou Matar, N. Smagin and V. Aleshin
- 17:20 DAET Monitoring Targeting Quality Control of Complex Industrial Products Manufacturing** 114
C. Trarieux, M. Defontaine, H. Moreschi and S. Callé
- 17:40 Nonlinear Ultrasonic Phased Array Imaging of Closed Cracks Using Global Preheating and Local Cooling** 115
Y. Ohara, K. Takahashi, Y. Ino and K. Yamanaka

Wednesday 1 july, 2015 - Non-linear propagation in heterogeneous media 2**Amphi 3**

- 16:40 Numerical simulation of weakly nonlinear acoustic propagation in bubbly liquid** 116
J.-B. Doc, J.-M. Conoir, R. Marchiano and D. Fuster
- 17:00 Second-Harmonic Generation by a Single Layer of Bubbles** 117
O. Lombard, C. Barriere and V. Leroy
- 17:20 Cavitation inception by the backscattering of pressure waves from a bubble interface** 118
H. Takahira, T. Ogasawara, N. Mori and M. Tanaka
- 17:40 The sessile liquid droplet as a geometrically self-reconstructed nonlinear acoustic resonator** 119
A. Begar, V. Mozhaev and I. Nedospasov

Thursday 2 july, 2015 - Bubbles and cavitation 1**Amphi 1 bis**

- 9:00 Theory and experimental demonstration of a single beam acoustical tweezers** 120
D. Baresch, J.-L. Thomas and R. Marchiano
- 9:20 Rotating small solid objects in liquids by a focused vortex ultrasound beam** 121
O. Sapozhnikov, M. Terzi, A. Nikolaeva, S. Tsysar and A. Maxwell
- 9:40 Theoretical investigation of the mechanisms involved in the modification of the cavitation threshold by multifrequency excitations** 122
M. Guédra, C. Desjoux, C. Insera, J.-C. Béra and B. Gilles
- 10:00 Factors Affecting the Cavitation Conditions Reproducibility** 123
N. Dezhkunov, A. Francescutto, A. Nikolaev and A. Kotukhov

Thursday 2 july, 2015 - Nonlinear propagation in fluids 1**Amphi 2**

- 9:20 Propagation of acoustic shock waves between parallel rigid boundaries and into shadow zones** 124
C. Desjoux, S. Ollivier, O. Marsden, D. Dagna and P. Blanc-Benon
- 9:40 Benchmark problems for long range atmospheric infrasound propagation** 125
R. Sabatini, O. Marsden, C. Bogey and C. Bailly
- 10:00 Quantitative nonlinearity analysis of model-scale jet noise** 126
B.O. Reichman, K.G. Miller, K.L. Gee, T.B. Neilsen and A.A. Atchley

Thursday 2 july, 2015 - Solids and soft matter**Amphi 3**

- 9:00 Soil Plate Oscillator: Modeling Nonlinear Mesoscopic Elastic Behavior and Hysteresis in Nonlinear Acoustic Landmine Detection** 127
M.S. Korman, D.V. Duong and A.E. Kalsbeek
- 9:40 3D TREND for crack orientation characterization** 128
P.-Y. Le Bas, T. Ulrich and B. Anderson
- 10:00 Bulk strain solitons in rods, plates and shells** 129
A. Samsonov, G. Dreiden, I. Semenova and A. Shvartz

Thursday 2 july, 2015 - Plenary lecture 5: Douglas Drob**Amphi 2**

- 11:00 Infrasound remote sensing of the atmosphere** 130
D. Drob

Thursday 2 july, 2015 - Bubbles and cavitation 2**Amphi 1 bis**

- 13:40 Acoustic wave equation in bubbly liquid** 131
B. Miao and Y. An
- 14:00 Dynamics of an aspherical bubble oscillating near a rigid sphere** 132
E. Kurihara
- 14:20 Nonlinear activity of acoustically driven gas bubble near a rigid boundary** 133
A. Maksimov
- 14:40 Derivation of the nonlinearity parameter B/A of saturated, unconsolidated marine sediments via a statistical approach** 134
H. Lee, E. Noh, W.-S. Ohm and O.-C. Kwon

Thursday 2 july, 2015 - Nonlinear propagation in fluids 2**Amphi 2**

- 13:40 Development of Nonlinear Acoustic Propagation Analysis Tool toward Realization of Loud Noise Environment in Aeronautics** 135
M. Kanamori, T. Takahashi and T. Aoyama
- 14:00 Structures of lee waves over combined topography** 136
J. Maltseva and N. Makarenko
- 14:20 Second Harmonic Coupling Coefficient in Resonant Nonlinear Generation of Water Surface Waves** 137
A. Bettucci, A. Alippi and M. Germano
- 14:40 The Study of Some Factors on Sound Wave Propagation in the Air** 138
K. Han, X. Zeng, D. Chen and X. Ma

Thursday 2 july, 2015 - Granular media 1**Amphi 3**

- 13:40 Irreversible Nonlinear Sound-Matter Interaction in Granular Media** 139
X. Jia
- 14:20 Modeling of non-linear interaction of waves in rocks** 140
C. Larmat, R. Guyer, P.-Y. Le Bas, P. Johnson and J. Ten Cate
- 14:40 Modulation of P-waves by S-waves in rocks** 141
A. Malcolm, J. Ten Cate, X. Feng and M. Fehler

Thursday 2 july, 2015 - Sonic boom propagation**Amphi 2**

- 15:40 Lateral Cutoff Analysis and Results from NASA's Farfield Investigation of No-boom Thresholds** 142
L. Cliatt, E. Haering, S. Arnac and M. Hill
- 16:00 Numerical Model of Sonic Boom in 3D Kinematic Turbulence.** 143
F. Coulouvrat, D. Luquet and R. Marchiano
- 16:20 Measured N-Wave Sonic Boom Events and Sensitivity in Sonic Boom Metrics** 144
J. Palmer and V.W. Sparrow

Thursday 2 july, 2015 - Granular media 2**Amphi 3**

- 15:40 Slow Dynamics in Granular Media: Theoretical Models and Experiments** 145
P. Johnson, A. Lebedev, L. Ostrovsky and J. Riviere
- 16:00 In Situ Acoustoelastic Testing: A Passive Monitoring Approach to Study Crustal and Fault Zone Rocks** 146
G. Hillers
- 16:20 Observations of the Nonlinear Interaction of Two Waves Intersecting at Angles in Earth Materials** 147
J. Ten Cate, P.-Y. Le Bas, C. Larmat, P. Johnson and R. Guyer

Friday 3 july, 2015 - Plenary lecture 6: Peter Coen**Amphi 3**

- 9:00** **Breaking the Sound Barrier: Achieving Overland Supersonic Flight without Sonic Boom Disturbance** 148
P. Coen

Friday 3 july, 2015 - Perception of sonic boom**Amphi 3**

- 10:00** **An investigation into the effect of playback environment on perception of sonic booms when heard indoors** 149
D. Carr and P. Davies
- 10:20** **Influence of chair vibrations on indoor sonic boom annoyance** 150
J. Rathsam, J. Klos and A. Loubeau
- 11:00** **A New Evaluation of Noise Metrics for Sonic Booms Using Existing Data** 151
A. Loubeau, Y. Naka, B.G. Cook, V.W. Sparrow and J.M. Morgenstern
- 11:20** **Understanding Sources of Uncertainty and Bias Error in Models of Human Response to Low Amplitude Sonic Booms** 152
J. Gavin, M. Collmar, B.G. Cook, R. Cowart and D. Freund

Program of the conference

Monday 29 June		Tuesday 30 June		Wednesday 1 July		Thursday 2 July		Friday 3 July	
		09:00 - 10:20	Technical sessions	09:00 - 10:20	Technical sessions	09:00 - 10:20	Technical sessions	09:00 - 10:00	Plenary lecture 6: P. Coen
09:00 - 13:00		10:20 - 11:00	Coffee break	10:20 - 11:00	Coffee break	10:20 - 11:00	Coffee break	10:00 - 10:20	Technical session
		11:00 - 12:00	Plenary lecture 2: V. Tournat	11:00 - 12:00	Plenary lecture 3: R. Mettin	11:00 - 12:00	Plenary lecture 5: D. Drob	10:40 - 11:00	Coffee break
			Lunch	12:00 - 13:40	Lunch	12:00 - 13:40	Lunch	11:00 - 11:40	Technical session
13:00 - 14:50	Registration	13:40 - 15:00	Technical sessions	13:40 - 15:00	Technical sessions	13:40 - 15:00	Technical sessions	11:40 - 12:30	Sonic Boom Industry Panel
14:50 - 15:10	Welcome and opening ceremony	15:00 - 16:00	Coffee break / Poster session	15:00 - 15:30	Coffee break	15:00 - 15:40	Coffee break	12:30 - 14:00	Lunch
15:10 - 16:10	Plenary lecture 1: R. Cleveland	16:00 - 18:00	Technical sessions	15:30 - 16:30	Plenary lecture 4: I. Solodov	15:40 - 16:40	Technical sessions	14:00 - 16:00	Q and A with Concorde/Air France Experts
16:20 - 18:00	Technical sessions		Technical sessions	16:40 - 18:00	Technical sessions	17:00	Closing ceremony	16:00	Concluding remarks
18:00 - 20:00	Welcome reception					17:20 - 20:00	Time off		
						20:00 - 23:00	Dinner cruise		

Abstracts

Mo. 15:10 Amphi 2

Plenary lecture 1: Robin Cleveland

Nonlinear acoustics in biomedical ultrasound

R. Cleveland

Institute of Biomedical Engineering, Dep. of Engineering Science, University of Oxford, Old Road Campus Research Building, Headington, OX3 7DQ Oxford, UK

robin.cleveland@eng.ox.ac.uk

Ultrasound is widely used to image inside the body; it is also used therapeutically to treat certain medical conditions. In both imaging and therapy applications the amplitudes employed in biomedical ultrasound are often high enough that nonlinear acoustic effects are present in the propagation: the effects have the potential to be advantageous in some scenarios but a hindrance in others. In the case of ultrasound imaging the nonlinearity produces higher harmonics that result in images of greater quality. However, nonlinear effects interfere with the imaging of ultrasound contrast agents (typically micron sized bubbles with a strong nonlinear response of their own) and nonlinear effects also result in complications when derating of pressure measurements in water to in situ values in tissue. High intensity focused ultrasound (HIFU) is emerging as a non-invasive therapeutic modality which can result in thermal ablation of tissue. For thermal ablation, the extra effective attenuation resulting from nonlinear effects can result in enhanced heating of tissue if shock formation occurs in the target region for ablation - a highly desirable effect. However, if nonlinearity is too strong it can also result in undesired near-field heating and reduced ablation in the target region. The disruption of tissue (histotripsy) and fragmentation of kidney stones (lithotripsy) exploits shock waves to produce mechanically based effects, with minimal heating present. In these scenarios it is necessary for the waves to be of sufficient amplitude that a shock exists when the waveform reaches the target region. This talk will discuss how underlying nonlinear phenomenon act in all the diagnostic and therapeutic applications described above.

Standing Shear Waves in Anisotropic Viscoelastic Media

T. Krit, I. Golubkova and V. Andreev

MSU, Leninskie Gory 1/2, GSP-1, 119991 Moscow, Russian Federation

timofey@acs366.phys.msu.ru

We studied standing shear waves in anisotropic resonator represented by a rectangular parallelepiped (layer) fixed without slipping between two wooden plates of finite mass. The viscoelastic layer with edges of 70 mm x 40 mm x 15 mm was made of a rubber-like polymer plastisol with rubber bands inside. The bands were placed between 40 mm x 15 mm side faces along the 70 mm edge equidistantly from each other.

Mechanical properties of the plastisol itself were carefully measured previously. It was found that plastisol shows a cubic nonlinear behavior, i.e. the stress-strain curve could be represented as: $\sigma = \mu\varepsilon + \beta\mu\varepsilon^3$, where ε stands for shear strain and σ is an applied shear stress. The value of shear modulus μ depends on frequency and was found to be several kilopascals which is common for such soft solids. Nonlinear parameter β is frequency dependent too and varies in range from tenths to unity at 1-100 Hz frequency range, decreasing with frequency growth. Stretching the rubber bands inside the layer leads to change of elastic properties in resonator. Such effect could be noticed due to frequency response of the resonator.

The numerical model of the resonator was based on finite elements method (FEM) and performed in MatLab. The resonator was cut in hundreds of right triangular prisms. Each prism was provided with viscoelastic properties of the layer except for the top prisms provided with the wooden plate properties and the prisms at the site of the rubber bands provided with the rubber properties. The boundary conditions on each prism satisfied the requirements that resonator is inseparable and all its boundaries but bottom are free. The bottom boundary was set to move horizontally with constant acceleration amplitude. It was shown numerically that the resonator shows anisotropic behavior expressed in different frequency response to oscillations applied to a bottom boundary in different directions. The rubber bands stretching inside the resonator was also taken into account and it appeared that stretching leads to plastisol properties change: plastisol hardens near the bands and its hardening makes the first resonance frequency grow.

Measurements of the shear modulus were conducted applying static deformation. The lower boundary of a resonator was fixed and a certain force was applied to the upper plate, producing shear stress in the layer. According to the approximation of a measured dependence of shear deformation on the applied stress by a cubic parabola, the linear shear modulus and nonlinear parameter values were obtained. The frequency dependence of the upper plate acceleration was measured in the frequency range 1-400 Hz. The accelerations of the upper and lower resonator plates were measured by miniature uniaxial accelerometers. The mass of accelerometers was 1 g; i.e., their effect on the process of resonator oscillations was ignorable. Accelerometer signals were transmitted to a computer through a GPIB interface. Experimental setup control and data acquisition were performed using a computer code written in the LabVIEW. The frequency step of 0.1 Hz provided sufficient precision.

This work was supported by RFBR grant No. 14-02-00426.

Second-Harmonic Generation in Shear Wave Beams with Different Polarizations

K. Spratt, Y. Ilinskii, E. Zabolotskaya and M. Hamilton

Applied Research Laboratories, University of Texas at Austin, 10000 Burnett Road, Austin, TX 78758, USA

sprattkyle@gmail.com

A coupled pair of nonlinear parabolic equations was derived by Zabolotskaya [*Sov. Phys. Acoust.* **32**, 296-299 (1986)] that model the transverse components of the particle motion in a collimated shear wave beam propagating in an isotropic elastic solid. Like the KZK equation, the parabolic equation for shear wave beams accounts consistently for the leading-order effects of diffraction, viscosity and nonlinearity. The nonlinearity includes a cubic nonlinear term that is equivalent to that present in plane shear waves, as well as a quadratic nonlinear term that is unique to diffracting beams. The work by Wochner et al. [*J. Acoust. Soc. Am.* **125**, 2488-2495 (2008)] considered shear wave beams with translational polarizations (linear, circular and elliptical), wherein second-order nonlinear effects vanish and the leading-order nonlinear effect is third-harmonic generation by the cubic nonlinearity. The purpose of the current work is to investigate the quadratic nonlinear term present in the parabolic equation for shear wave beams by considering second-harmonic generation in Gaussian beams as a second-order nonlinear effect using standard perturbation theory. In order for second-order nonlinear effects to be present, a broader class of source polarizations must be considered that includes not only the familiar translational polarizations, but also polarizations accounting for stretching, shearing and rotation of the source plane. It is found that the polarization of the second harmonic generated by the quadratic nonlinearity is not necessarily the same as the polarization of the source-frequency beam, and we are able to derive a general analytic solution for second-harmonic generation from a Gaussian source condition that gives explicitly the relationship between the polarization of the source-frequency beam and the polarization of the second harmonic. Finally, suggestions are made towards the possible experimental verification of the theory. [Work supported by the ARL:UT McKinney Fellowship in Acoustics.]

Effect of Nanostructuring on the Elastic Properties of Aluminum Alloy AMg6.V. Prokhorov^a, A. Korobov^b, A. Kokshaiskii^b, S. Perfilov^a and A. Volkov^b^aTISNCM, 7a, Centralnaya str., Moscow, Troitsk,, 142190 Troitsk, Russian Federation; ^bFaculty of Physics, M.V. Lomonosov Moscow State University, Leninskie gory 1, 119991 Moscow, Russian Federation
pvm@tisnum.ru

We experimentally investigated the nanostructuring effect on the elastic properties of aluminum alloy AMg6 (Al-Mg-Mn system). The n-AMg6 nanostructured samples were prepared from a commercial polycrystalline alloy by refinement and homogenization a mixture of small chips of the alloy with the addition of 0.3 wt.% of C60 fullerite in a planetary mill. The resulting product consists of 200-500-micron agglomerates of nanoparticles. The coherent scattering length (CSL) distribution in the powdered samples showed the mean nanoparticle size of $\sim 40-60$ nm. The process was conducted in a protected Ar-atmosphere; additional studies confirmed the absence of oxygen and the corresponding insertion of aluminum oxidation. Then, the milled nanopowder was pre-compacted in a cylindrical mold with a 180 mm diameter at a 250 °C temperature and a 200-300 MPa pressure. The resulting compact (preform) was subjected to extruding at a temperature of 300 °C with a reduction of cross-sectional area at least 4 times (in this case to a 90 mm diameter). The recrystallization process is hindered by grain boundary modification with a C60 fullerite; the latter plays the role of a compacted samples' stabilizer. For the experiments, 9 samples in a cuboid shape of 20'20'40 mm size were cut from the central and peripheral parts of the n-AMg6 ingot. Three samples of the same size were made of AMg6 billet alloy. The velocities of longitudinal VL and shear VT BAWs defined with high precision allowed, in the approximation of an isotropic solid, to compute the second-order elastic constants (SOEC) C_{ij} , the 2nd-order compliance modules S_{ij} , Young's modulus E , bulk modulus K , and Poisson's ratio σ in the samples [1]. Errors in the determination of these coefficients do not exceed 2%. To characterize the nonlinear elastic properties of solids, the third-order elastic constants (TOEC) are used. They determine the anharmonic properties of the crystal lattice, such as thermal expansion, ultrasound attenuation, and efficiency of the nonlinear interaction of elastic waves in solids. The TOECs were determined with a Thurston-Brugger method [2]. To do this, the relative changes in velocity of bulk waves depending on the applied uniaxial compression were experimentally measured in the test samples. Comparison of the determined SOECs in the AMg6 and n-AMg6 alloys showed that they are equal within the measurement errors. However, the values of TOECs vary considerably in these alloys. A similar behavior of TOEC and SOEC were previously found by us in aluminum alloy B95 and B95/Nanodiamond Composite [3]. This indicates that the TOEC is more sensitive to the composition, structure and stoichiometry of the material than the SOEC. The studies were supported by the Russian Science Foundation (project N° 14-22-00042) and by the Ministry of Education and Science of the Russian Federation (grant UI RFMEFI57714X0090). References 1. R. Truell, Ch. Elbaum, and B. Chik, *Ultrasonic Methods in Solid State Physics* (Academic, New York, 1969). 2. R. N. Thurston and K. Brugger, *Phys. Rev. [Sect.] A133*, 1604 (1964). 3. A. I. Korobov, V. M. Prokhorov, and D. M. Mekhedov. *Physics of the Solid State*. 55, 8 (2013).

Application of Weak Shock Theory to Transient Plane Shear Waves

J. Cormack and M. Hamilton

Applied Research Laboratories, University of Texas at Austin, 10000 Burnett Road, Austin, TX 78758, USA

jcormack@utexas.edu

The very low shear modulus in soft tissue results in shear wave speeds on the order of 1 m/s and facilitates generation of shear waves with large particle displacements. In experiments performed by Catheline et al. [Phys. Rev. Lett. **91**, 164301 (2003)], a fully developed periodic shock wave was measured 15 mm away from a source radiating a 100 Hz shear wave into a tissue-like phantom. The focus of the present work is on the propagation of transient shear waves containing shocks. An integral formulation of weak shock theory developed by Whitham for quadratic nonlinearity [J. Fluid Mech. **1**, 3 (1956)] is extended to cubic nonlinearity. Whereas Whitham's formulation predicts the well-known result that the head shock decays asymptotically as the reciprocal of the square root of distance, for cubic nonlinearity it is the reciprocal of the cube root of distance. Similarly, the position of the head shock in a coordinate system moving at the small-signal shear wave speed advances asymptotically as the cube root of distance for cubic nonlinearity, compared with the square root of distance for quadratic nonlinearity. Analytic results are presented for an N wave, thus recovering the result obtained by Lee-Bapty and Crighton [Phil. Trans. R. Soc. Lond. A **323**, 1570 (1987)], a shock followed initially by an exponential tail, and a waveform that is initially a single cycle of a sinusoid. The results are confirmed by comparison with numerical solutions of a Burgers equation augmented for cubic nonlinearity. Weak shock theory is also applied analytically to a shear wave with a step shock in a relaxing medium, as reported at the spring 2015 meeting of the Acoustical Society of America, extending the work of Polyakova, Soluyan, and Khokhlov for a compressional wave [Sov. Phys. Acoust. **8**, 78 (1962)]. [Work supported by the ARL:UT McKinney Fellowship in Acoustics.]

Histotripsy: Nonlinearities Essential for Therapeutic Lesion Formation

C. Cain

University of Michigan, 2200 Bonisteel Blvd, 2121 Gerstacker, Ann Arbor, MI 48109, USA
cain@umich.edu

Histotripsy produces non-thermal lesions by generating dense energetic bubble clouds with very short intense acoustic pulses. Repeated expanding/contracting bubble clouds mechanically fractionate tissue in the focus until only small cellular fragments are left. Because it is a highly nonlinear thresholding phenomenon, the bubble clouds, and the subsequent lesions, are highly localized with lesion boundaries often bisecting individual cells. Dense bubble clouds are only initiated when some part of the negative pressure waveform(s) in the focus exceeds the Intrinsic Threshold, around 28 MPa for most soft tissues. Negative pressures beyond the intrinsic threshold can be obtained by 2 approaches: shock scattering and direct excitation. With histotripsy pulses exceeding 3 cycles in length, but with P- values (from about 12 MPa to 25 MPa) less than the intrinsic threshold, positive shock fronts with peak pressures greater than 50 MPa are easily formed by nonlinear propagation. The lower pressure peak negative half-cycles cannot initiate dense bubble clouds directly, but do initiate sparsely distributed incidental bubbles in the focus. These bubbles produce little damage but invert the subsequent positive shock fronts at the pressure release bubble boundary. The inverted shock front can exceed the intrinsic threshold inducing a dense bubble cloud from the scattered negative pressure waveform. After 7 to 10 cycles, the bubble cloud exits the focus towards the transducer. If any negative pressure part of the primary pulse exceeds the intrinsic threshold, a dense bubble cloud is directly generated, even with a single negative half cycle. No shock front is necessary. This thresholding phenomenon has a number of very useful consequences. For short primary pulses less than 2 cycles, a single principal negative cycle can exceed the intrinsic threshold directly generating a dense lesion producing bubble cloud. Moreover, by changing the intensity, a variable fraction of the pulse can be made to exceed the threshold resulting in variable diameter bubble clouds. If the bubble cloud consists of very few bubbles, when only the tip of the waveform (P-) exceeds the intrinsic threshold, very small lesions, much less than the diffraction limit in size, can be generated. This is called Microtripsy. Moreover, beam side lobes from distorting aberrations can be "thresholded out" if the main lobe intensity exceeds any side lobe (often the case even with severe aberrations). Thus, if the main lobe is still extant, and exceeds the intrinsic threshold, a clean bubble cloud and lesion is formed thus conferring significant immunity to aberrations. This allows clean lesions through ribs, skull, and other highly aberrating and attenuating structures. If a high frequency probe waveform (could be an imaging pulse) intersects a low frequency pump waveform in the focus, the compounded waveform can momentarily exceed the intrinsic threshold, thus producing a lesion with the probe (imaging) transducer. Multi-beam histotripsy can allow precise lesions to be formed with higher frequency imaging transducers with the "heavy lifting" being accomplished with a low frequency pump transducer. Frequency compounding can also be used to create nearly monopolar acoustic pulses useful in imaging and histotripsy.

Use of Shock-Wave Heating for Faster and Safer Ablation of Tissue Volumes in High Intensity Focused Ultrasound Therapy

V. Khokhlova^a, P. Yuldashev^a, I. Sinilshchikov^a, A. Partanen^b, T. Khokhlova^c, N. Farr^c, W. Kreider^c, A. Maxwell^c and O. Sapozhnikov^{a,c}

^aPhysics Faculty, Moscow State University, Leninskie Gory, 119991 Moscow, Russian Federation; ^bClinical Science MR Therapy, Philips Healthcare, Andover, MA 01810, USA; ^cCenter for Industrial and Medical Ultrasound, Applied Physics Laboratory, University of Washington, 1013 NE 40th Street, Seattle, WA 98105, USA
vera@acs366.phys.msu.ru

In high intensity focused ultrasound (HIFU) applications, reported *in situ* intensities can reach several thousand or even tens of thousands of W/cm². In such fields, nonlinear acoustic effects result in the formation of high-amplitude shock fronts in focal waveforms, with amplitudes that can exceed 100 MPa. The presence of such shocks can lead to tissue heating and boiling in just a few milliseconds. Even though this enhanced heating is very strong, shock fronts are highly focused and produce extreme heating effects in a very small focal volume. For single, fixed lesions, nonlinear heating thus can be utilized for rapid tissue ablation only within very small volumes before boiling occurs to limit the process. However, if the focus is steered, this localized enhancement of heating combined with thermal diffusion can be used effectively to accelerate thermal treatments over large volumes. In addition, recent experimental studies have shown that a method termed boiling histotripsy can be used to mechanically disintegrate tissue volumes with varying thermal effects by changing shock-wave parameters in the exposure. In this work, numerical simulations were performed to evaluate the efficacy of using nonlinear effects to accelerate the thermal ablation of tissue volumes and, at the same time, to provide safer exposure conditions for intervening tissues. Acoustic modeling based on the Westervelt equation was combined with temperature modeling using a bioheat equation and calculations of thermal dose in tissue. The Westervelt equation was solved using a previously developed finite-difference algorithm. The bioheat equation was solved in the spatial-frequency domain; the numerical scheme was optimized using superposition of temperature fields produced by individual sonication foci. Simulations followed experimental conditions of recent studies done for a multi-element 1.2 MHz HIFU phased array (Sonalleve V1 3.0T, Philips Healthcare, Vantaa, Finland) to generate volumetric lesions in *ex vivo* bovine tissue. A pulsing scheme was combined with discrete electronic steering of the array focus. Sonications were performed at a tissue depth of 2 cm with millisecond-long pulses of different durations, different pulse repetition rates, and *in situ* shock amplitudes of 65 MPa and 100 MPa. Various steering trajectories of sonications were tested to thermally ablate tissue volumes of either cylindrical or cubical shape. Simulation results were compared to the experimental data obtained in *ex vivo* bovine liver with the same sonication parameters. It was shown that with the same time-average power, the use of pulsing schemes with high amplitude shocks compared to harmonic wave sonications results in several clinical advantages: faster ablation of the desired volume and lesser damage to the surrounding tissues caused by heat diffusion. In addition, a relative decrease of the nearfield heating occurs, because nonlinear enhancement of heating is localized at the focus. Work supported by the Russian Science Foundation 14-12-00974 and NIH NIBIB EB007643.

Nonlinear effects in ultrasound fields of diagnostic-type transducers used for kidney stone propulsion: characterization in water and derating to clinically relevant depth in tissue

M. Karzova^{a,b}, B. Cunitz^c, P. Yuldashev^b, Y. Andriyakhina^b, W. Kreider^c, O. Sapozhnikov^{b,c}, M. Bailey^c and V. Khokhlova^b

^aLaboratoire de Mécanique des Fluides et d'Acoustique, Ecole Centrale de Lyon, 36 Avenue Guy de Collongue, 69134 Ecully, France; ^bPhysics Faculty, Moscow State University, Leninskie Gory, 119991 Moscow, Russian Federation; ^cCenter for Industrial and Medical Ultrasound, Applied Physics Laboratory, University of Washington, 1013 NE 40th Street, Seattle, WA 98105, USA

masha@acs366.phys.msu.ru

Newer imaging and therapeutic ultrasound technologies require higher *in situ* pressure levels compared to conventional diagnostic values. One example is the recently developed use of focused ultrasonic radiation force to move kidney stones and residual fragments out of the urinary collecting system. A commercial diagnostic 2.3 MHz C5-2 array probe is used to deliver the acoustic pushing pulses. The probe is a curve-linear array comprised of 128 elements (0.37 mm by 12.5 mm) equally spaced along the 55 mm convex cylindrical surface with 41.2 mm radius of curvature. Steering of the focus is performed electronically in the azimuthal plane and by a cylindrical acoustic lens for the elevation plane. It has been shown that nonlinear propagation, and even saturation effects, are strongly pronounced at the power levels used in the current preclinical and clinical studies of stone propulsion for measurements performed in water. Accurate characterization of the nonlinear ultrasound fields generated in water and development of derating approaches to determine *in situ* pressures are therefore important for treatment planning and further optimisation of the technology. Accurate characterization of nonlinear ultrasound fields have recently been performed using a combined measurement and modeling approach for various high intensity focused ultrasound transducers. This included axially symmetric single sources or multi-element arrays with approximate axial symmetry. A novel derating approach based on scaling the source pressure, not the focal pressure, has been proposed and validated; the technique uses only a look-up table of focal measurements in water. However, few results are available for the highly nonlinear fields created by rectangular-shaped diagnostic transducers. In this work nonlinear propagation effects were analyzed for the C5-2 transducer using a combination of measurements and modeling. 3D numerical simulations were based on the Westervelt equation and performed for nonlinear propagation both in water and in tissue. The boundary condition for the numerical model was set by matching the Rayleigh integral linear solution for acoustic pressure to the low power measurements on the axis and in the focal plane of the beam. Focal waveforms simulated for several output power levels and for 16, 32, 40, 64, and 128 active elements are compared to fiber-optic hydrophone measurements in water. The experimental data were found to be in good agreement with the modeling results. To evaluate the accuracy of the previously developed derating method for nonlinear focused fields and compare it to the conventional derating procedure of scaling the focal pressures, the derated focal waveforms are compared to the results of direct simulations in tissue. It was shown that the method of scaling the source amplitude provided better accuracy than the conventional derating method of scaling the focal pressure. Work supported by NIH NIBIB EB007643, NIH NIDDK P01 DK43881, Russian Science Foundation 14-12-00974, and NSBRI through NASA NCC 9-58.

Quantitative Assessment of Reactive Oxygen Species Generation by Cavitation Incepted Efficiently Using Nonlinear Propagation EffectY. Jun^a, S. Yoshizawa^a and S.-I. Umemura^b^aTohoku Univ. Department of Communications Engineering, Aoba 6-6-05, Aramaki, Aoba-ku, 980-8579 Sendai, Japan;^bTohoku Univ. Medical Bio Engineering, Aoba 6-6-05, Aramaki, Aoba-ku, 980-8579 Sendai, Japan

j_yasuda@ecei.tohoku.ac.jp

Ultrasonic cavitation bubbles can produce sonochemical bioeffect of HIFU (high-intensity focused ultrasound) in combination with a sonosensitizer. It is activated through the collapse of cavitation and, when activated, it generates reactive oxygen species (ROS) which can induce irreversible changes to the tissue. A treatment method using such a sonosensitizer is called sonodynamic treatment. Rose Bengal (RB) is a kind of sonosensitizers. In sonodynamic treatment, high generation efficiency of ROS is an important key and triggered HIFU sequence has been proposed for it. This sequence consists of an extremely high intensity short pulse (trigger pulse) for cavitation cloud inception immediately followed by a moderate intensity long burst (sustaining waves) for sustaining bubbles by volume oscillation. There are two factors that may define the amount of ROS generation; the amount of cavitation cloud generated by triggered pulse and cavitation bubbles remained by sustaining waves. Originally, it is hard to obtain cavitation bubbles efficiently because positive pressure is emphasized around the focal area of HIFU, and, in contrast, negative pressure is decreased by nonlinear propagation and focusing. But, it has been already proved that extremely highly positive pressure generated by such effect of nonlinear propagation is an important factor in formation of cavitation cloud. Therefore, triggered pulse can generate cavitation cloud efficiently. Additionally, it is expected that such volume oscillation may be useful for efficient generation of ROS. In this study, the behavior of cavitation bubbles in RB solution was observed using high-speed camera and ROS generated by triggered HIFU sequence were quantified in order to investigate the factor that define the amount of generated ROS. A focused ultrasound transducer and a sealed chamber were placed in a water tank. The solution sealed in the chamber contained either 0, 1.0, 5.0, or 10 mg /L of RB and 500 g/ L of potassium iodide (KI). Cavitation bubbles were generated in the chamber. Triggered HIFU sequence was employed and the intensity and exposure duration of the trigger pulse were 40 kW/cm² and 100 μs, while those of the sustaining waves were 500 W/cm² and 1 ms, respectively. The ultrasound frequency was 1.2 MHz. The high-speed camera captured the cavitation cloud generated by trigger pulse and remained cavitation bubbles during sustaining waves exposure for estimating the amount of them. The amount of ROS was quantified using KI. When cavitation bubbles are generated in a solution containing KI, triiodide ion is generated. Triiodide ion has a peak absorbance at 355 nm. Therefore, the amount of it can be quantified by comparing the absorbance at 355 nm before and after ultrasound exposure. As a result, it is found that RB concentration did not affect on the amount of generated cavitation cloud but affect on the amount of remained cavitation bubbles by sustaining waves. Additionally, correlation between RB concentration and generated ROS was observed. It indicates that RB affect on the lifetime of cavitation bubbles during sustain waves exposure and it is the primary factor of the amount of ROS generation.

Nonlinear Diffusion-Wave Equation for a Gas in a Regenerator Subject to Temperature Gradient

N. Sugimoto

Kansai University, Faculty of Engineering Science, Suita, 564-8680 Osaka, Japan

sugimoto@me.es.osaka-u.ac.jp

This paper derives an approximate equation of nonlinear thermoacoustic waves for a gas in a regenerator subject to temperature gradient. By the regenerator is meant usually a thermal device acting as a heat exchanger, in which a transverse length of flow passages for a gas is much smaller than a thermal diffusion layer so that the gas is in perfect thermal contact with solid walls locally. Such an ideal picture occurs in the limit of infinitesimally small transverse length and infinitesimally small pressure disturbance. As the transverse length and the pressure disturbance tend to be large, however, their finite effects will come into play to change the above picture. To understand them, a simple equation but derived on the basis of fluid dynamics is useful. Analysis of the equation is expected to illuminate physical mechanisms occurring in the regenerator.

The problem is formulated for the simplest case of two-dimensional channels or circular pores without tortuous passages usually found in a random stack of fine meshes. The wall is subject to temperature gradient axially but, for the sake of simplicity, no temporal change is assumed in the wall temperature. In developing the theory, use is made of the narrow-tube approximation in a sense that a typical axial length associated with temperature gradient or an axial length of the regenerator is much longer than the transverse length. Outcome of this approximation suggests that the pressure may be regarded as being uniform transversely. Making use of this assumption and taking account of small but finite magnitude of pressure disturbances, the systematic asymptotic theory is developed to derive the approximate equation with quadratic nonlinear terms inclusive.

In the linear regime, the diffusion-wave equation has already been derived from the thermoacoustic-wave equation in time and space domain, when the transverse length is infinitesimal. The temperature gradient gives rise to wave propagation in the positive sense of the gradient. The axial velocity distribution is given by Poiseuille flow driven by the axial pressure gradient, and its mean value over the cross-section of flow passage is then consistent with the one by Darcy's law. On the other hand, the gas temperature is equal to the wall temperature so that the gas is subject to isothermal process locally. As the flow passage tends to be wide, there appears a phase lag in the axial velocity and also transverse variations both in velocity and gas temperature.

In the nonlinear regime, the advective terms in the equation of motion give rise to nonlinear velocity terms, which is responsible for harmonic generation and acoustic streaming. In the energy equation, the advective term of the pressure and the stress power due to the shear stress dominate to change the temperature distribution transversely. It is revealed that the approximate equation for the excess pressure is then governed by the diffusion-wave equation with nonlinear terms, where the nonlinear velocity terms are of higher order. Influence of temperature dependence of the viscosity and heat conductivity remains small in the equation.

Magnetoacoustic Nonlinear Waves in a Heat-Releasing PlasmaD. Ryashchikov^a, N. Molevich^b and D. Zavershinskiy^a^aSamara State Aerospace University, 34 Moskovskoe sh., 443086 Samara, Russian Federation; ^bLebedev Physical Institute, 221 NovoSadovaya str, 443011 Samara, Russian Federation

ryashchikovd@gmail.com

The evolution of weak magnetoacoustic waves in a heat-releasing completely ionized plasma medium with a thermal instability is investigated. The nonlinear magnetoacoustic equations describing the evolution of fast and slow magnetoacoustic waves are obtained. The correlation between the obtained nonlinear magnetoacoustic equations and the nonlinear acoustical equation of nonequilibrium medium with exponential relaxation law is shown. The dispersion properties of the wave modes existing in the plasma medium are discussed. The acoustic amplification and damping conditions are defined by solving the dispersion relation. The influence of the thermal conduction and finite electrical conductivity on the process of nonlinear acoustical structure formation is discussed. The shape and parameters of the magnetoacoustic pulse that is an automodel solution of this equation under conditions of magnetoacoustic thermal instability have been determined analytically. Results of the numerical simulation of the full one-dimensional system of magneto-hydrodynamics equations are compared with the solutions of the nonlinear magnetoacoustic equation obtained for these unstable regions. The disintegration of any initial weak perturbation of compression into sequence of self-sustained magnetoacoustic pulses is shown numerically.

Lagrangian description of energy conversion in the Taconis oscillationsK. Ishii^a, S. Adachi^b, H. Hayashi^a and I. Menshov^c^aITC, Nagoya University, Furo-cho, Chikusa-ku, 464-8601 Nagoya, Japan; ^bTokyo International University, Matobakita, 350-1197 Kawagoe, Japan; ^cKeldysh Institute of Applied Mathematics, 4 Miusskaya Sq., 125047 Moscow, Russian Federation

ishii@nagoya-u.jp

Energy conversion in the Taconis oscillations is studied from the Lagrangian point of view. Numerical simulations are performed for the spontaneous thermoacoustic oscillations of helium gas which are observed in a tube when a strong temperature gradient along the tube axis is imposed on the tube wall. Flow fields in a closed straight cylindrical tube are obtained by solving the axisymmetric compressible Navier-Stokes equations. Temporal evolution of thermodynamic quantities of fluid particles is calculated from the obtained flow fields. The wall temperature of both end parts of the tube is maintained at room temperature $T_H = 300\text{K}$ and that of the central region at $T_C = 20\text{K}$. The ratio of the length of the hot part to that of the cold part ξ is changed. Steady oscillations in a closed tube are observed at ξ between 0.26 and 4.4. Three oscillation modes are observed: a second mode in which pressures at both ends oscillate in phase, a shock-wave mode and a fundamental mode in which pressures at both tube ends oscillate π out of phase. The amount of work done by each fluid particle during one period is estimated for the fundamental mode as well as the second mode. If the fluid particle performs a positive amount of work, it serves as a prime mover. On the other hand it performs a negative amount of work, it serves as a heat pump. In the second mode at $\xi = 0.4$, the pressure amplitude is smaller than other cases, and the radial variation of the temperature is small. Fluid particles move in the vicinity of the starting point. Fluid particles in the region of finite temperature gradient serve as prime movers, and those near the tube end walls serve as heat pumps. Almost no work is done by fluid particles in the region of the tube center. In the fundamental mode at $\xi = 1.0$, the radial variation of the flow field is large and the oscillation of the temperature in the tube is large. Displacement of fluid particles during one period is large. Both in the region of finite temperature gradient and in the region of the tube center, fluid particles near the tube wall serve as heat pumps and those near the tube axis serve as prime movers. Fluid particles near the tube end wall serve as heat pumps. It is presented that the whole region in the tube is concerned with energy conversion in this oscillation mode with larger amplitudes.

Experiments on the acoustic solitary wave generated thermoacoustically in a looped tubeD. Shimizu^a and N. Sugimoto^b^aFukui University of Technology, Faculty of Engineering, 3-6-1, Gakuen, 910-8505 Fukui, Japan; ^bKansai University, Faculty of Engineering Science, Suita, 564-8680 Osaka, Japan
shimizu@fukui-ut.ac.jp

Emergence of an acoustic solitary wave is studied experimentally in a gas-filled, looped tube with an array of Helmholtz resonators connected. The solitary wave is generated thermoacoustically by a pair of stacks subject to temperature gradient and positioned diametrically on exactly the opposite side of the loop. The temperature gradient is imposed on both stacks in the same sense along the tube. The stacks made of ceramics and of many squared pores are sandwiched by hot and cold heat exchangers.

When the temperature gradient is beyond a critical value of instability, acoustic disturbances are generated spontaneously and propagated along the tube. As their magnitude is increased, the profile of pressure waves is distorted due to nonlinearity to form a shock so that many harmonics are observed to be involved. However, by connecting an array of Helmholtz resonators with equal spacing along the tube, and choosing the natural frequency of the resonator to be higher than the frequency of acoustic disturbances, it is observed that many higher harmonics are suppressed because of weakly dispersive effects due to the array. Then the acoustic solitary wave emerges. Its pressure profile shows a good agreement with the theoretical profile (N. Sugimoto, *J. Acoust. Soc. Am.*, 1996).

The solitary waves generated appear to be propagated in both directions and reflected by the stacks. Although the two stacks have the same porosity of 0.49, the cold end of the stack acts like a fixed end because the acoustic impedance is higher there. It is seen that the peak of the solitary wave propagated from the hot end of one stack to the cold end of the other stack is larger than that in the opposite direction. When the solitary wave propagates along the loop, delay in the period compared with that of the shock with no resonators is observed. Thus it is confirmed that the solitary wave is propagated with a subsonic speed slower than the sound speed. This is one of the features of the acoustic solitary wave in comparison with the supersonic shock wave.

Acoustic Agglomeration of Fine Particles Based on a High Intensity Acoustical Resonator

Y. Zhao, X. Zeng and Z. Tian

National University of Defense Technology, No.137, Yanwachi Street, 410073 Changsha, China

zhaoyun@nudt.edu.cn

Acoustic agglomeration (AA) is considered to be a promising method for reducing the air pollution caused by fine aerosol particles. Removal efficiency and energy consuming are primary parameters for the industry applications. It was proved that removal efficiency is increased with sound intensity and optimal frequency is presented for certain polydisperse aerosol. As a result, a high efficiency and low energy cost removal system was constructed using acoustical resonance. High intensity standing wave is generated by a tube system with abrupt section driven by four loudspeakers. Strong nonlinearity is avoided by the dissonant characteristic. Extensive tests were carried out to investigate the acoustic field in the agglomeration chamber. Removal efficiency of fine particle was tested by mass comparison of the filter paper at different operating conditions including sound pressure level, frequency and mass loading. Numerical model of the nonlinear acoustic was built based on finite element method and Westervelt equation. The experimental study has demonstrated that agglomeration increases with sound pressure level and the optimal frequency is around 1.6kHz for aerosol generated by graphitic powder. Sound pressure level in the agglomeration chamber is between 145 dB and 165 dB from 500 Hz to 2 kHz. The resonance frequency can be predicted with the quarter tube theory. Sound pressure level gain of more than 10 dB is gained at resonance frequency. Higher resonance frequencies are not the integral multiplies of the first one and shock wave is not found in the testing results. The mechanism and testing system can be used effectively in industrial processes.

Tu. 11:00 Amphi 2

Plenary lecture 2: Vincent Tournat

Nonlinear acoustic wave processes in granular media

V. Tournat

LAUM UMR-CNRS 6613, Université du Maine, Av. O. Messiaen, 72085 Le Mans, France

vincent.tournat@univ-lemans.fr

Unconsolidated granular media are known to exhibit strong elastic wave nonlinearities of various types (quadratic, Hertzian, hysteretic, etc.) due to the contacts between grains. Depending on the specific granular medium configuration (ordered / disordered, compressed or not, etc.) peculiar scattering, dissipative and dispersive properties coexist with these nonlinearities. Consequently, various specific nonlinear wave processes can be observed in these media, relevant for applications in geophysics, phononic crystals, metamaterials and wave control, vibration control, fundamental physics or non destructive testing. After a general introduction, we go through several examples of “ historical ” research results of nonlinear wave effects observed in granular media. Then, starting from the properties of a single contact between two beads, and going to collective effects encountered in ordered and disordered packings, a review of specific nonlinear processes is presented with the associated theoretical interpretations. Finally, some research perspectives in the nonlinear acoustics of granular media are proposed.

Three dimensional full-wave nonlinear acoustic simulations: applications to ultrasound imaging

G. Pinton

University of North Carolina & North Carolina State University, 348 Taylor Hall, Chapel Hill, NC 27599, USA
gfp@unc.edu

Characterization of acoustic waves that propagate nonlinearly in an inhomogeneous medium has significant applications to diagnostic and therapeutic ultrasound. The generation of an ultrasound image of human tissue is based on the complex physics of acoustic wave propagation: diffraction, reflection, scattering, frequency dependent attenuation, and nonlinearity. The nonlinearity of wave propagation is used to the advantage of diagnostic scanners that use the harmonic components of the ultrasonic signal to improve the resolution and penetration of clinical scanners. One approach to simulating ultrasound images is to make approximations that can reduce the physics to systems that have a low computational cost. Here a maximalist approach is taken and the full three dimensional wave physics is simulated with finite differences.

The objective of this paper is to present finite difference simulations for the nonlinear acoustic wave equation that we have developed and to demonstrate how they can be used to generate physically realistic two and three dimensional ultrasound images anywhere in the body. To achieve this goal a three dimensional representation of the human body is converted into acoustical maps. These maps are based on the National Library of Medicine's Visible Human data set which provides high resolution registered optical, MRI, and CT (but not ultrasound) scans of the entire male and female bodies. The fullwave nonlinear acoustic simulation tool is used to propagate ultrasound with 1D and 2D ultrasound arrays with an arbitrary emission (pulse shape, duration), transducer geometry (linear, curved), and transducer acoustical properties (lens, backing impedance). The backscattered signal is recorded in the simulations at the transducer surface and it is used to generate the first simulated 3D ultrasound images of the human body based on nonlinear propagation physics.

Once the propagation simulations have been established we analyze a specific intercostal liver imaging scenario for two cases: with the ribs in place, and with the ribs removed. This configuration provides an imaging scenario that cannot be performed in vivo but that can test the influence of the ribs on image quality. Several imaging properties are studied, in particular the beamplots, the spatial coherence at the transducer surface, the distributed phase aberration, and the lesion detectability for imaging at the fundamental and harmonic frequencies.

The results indicate, counterintuitively, that at the fundamental frequency the beamplot improves due to the apodization effect of the ribs but at the same time there is more degradation from reverberation clutter. At the harmonic frequency there is significantly less improvement in the beamplot and also significantly less degradation from reverberation. Therefore, under these imaging conditions, reverberation clutter plays a much weaker role in the degradation of image quality at the harmonic frequency. It is shown that even though simulating the full propagation physics is computationally challenging it is necessary to quantify ultrasound image quality and its sources of degradation.

Tu. 9:20 Amphi 1 bis

Computational methods in Nonlinear Acoustics 1

Numerical Modelling of Nonlinear Full-Wave Acoustic Propagation

P.L. Rendón and R. Velasco

CCADET, Universidad Nacional Autónoma de México, Ciudad Universitaria, 04510 Mexico, Mexico

pablo.rendon@ccadet.unam.mx

The various model equations of nonlinear acoustics are arrived at by making assumptions which permit the observation of the interaction with propagation of either single or joint effects. We present here a form of the conservation equations of fluid dynamics which are deduced using slightly less restrictive hypothesis than those necessary to obtain the well known Westervelt equation. This formulation accounts for full wave diffraction, nonlinearity, and thermoviscous dissipative effects. A two-dimensional, finite-volume method using Roe's linearization has been implemented to obtain numerically the solution of the proposed equations. This code, which has been written for parallel execution on a GPU, can be used to describe moderate nonlinear phenomena, at low Mach numbers, in domains as large as 100 wave lengths. Applications range from models of diagnostic and therapeutic HIFU, to parametric acoustic arrays and nonlinear propagation in acoustic waveguides. Examples related to these applications are shown and discussed.

Tu. 9:40 Amphi 1 bis

Computational methods in Nonlinear Acoustics 1

GPU Simulation of Nonlinear Propagation of Dual Band Ultrasound Pulse ComplexesJ. Kvam^a, B. Angelsen^a and A. Elster^b^aNTNU, Department of Circulation and Medical Imaging, 7491 Trondheim, Norway; ^bNTNU, Department of Computer and Information Science, 7491 Trondheim, Norway

johannes.kvam@ntnu.no

In a new method of ultrasound imaging, called SURF imaging, dual band pulse complexes composed of overlapping low frequency (LF) and high frequency (HF) pulses are transmitted, where the frequency ratio LF:HF \sim 1:20, and the relative bandwidth of both pulses are \sim 50 -70%. The LF pulse length is hence \sim 20 times the HF pulse length. The LF pulse is used to nonlinearly manipulate the material elasticity observed by the co-propagating HF pulse. This produces a manipulation of both the propagation velocity and the scattering observed by the HF pulse. The manipulation of the propagation velocity introduces a LF pulse dependent nonlinear propagation delay, and as the LF pulse has some variation along the HF pulse, it also produces a nonlinear pulse form distortion of the HF pulse.

Due to the large difference in frequency and pulse length between the LF and the HF pulses, we have developed a dual level smulation where the LF pulse propagatipn is first simulated independent of the HF pulse, using a temporal sampling frequency matched to the LF pulse. A separate equation for the HF pulse is developed, where the the pre-simulated LF pulse modifies the propagation velocity. The equations are adapted to parallel processing in a GPU, where nonlinear simulations of a typical HF beam of 10 MHz down to 40 mm is done in \sim 2 secs in a standard GPU. This simulation is hence very useful for studying the manipulation effect of the LF pulse on the HF pulse.

Tu. 10:00 Amphi 1 bis

Computational methods in Nonlinear Acoustics 1

Simulation of Nonlinear Ultrasound Wave Propagation in Fourier DomainF. Varray^a, O. Basset^b and C. Cachard^b^aCreatis, 7 av Jean capelle, 69621 Villeurbanne, France; ^bCREATIS, 7, avenue Jean Capelle, 69100 Villeurbanne, France

francois.varray@creatis.insa-lyon.fr

In medical ultrasound (US), the harmonic images, with or without contrast agents, offer new opportunities in terms of resolution, contrast and diagnosis. The harmonic image is a consequence of the nonlinear propagation of the US wave in the medium and the wave distortion creates harmonics. This distortion can be modeled with the Westervelt equation which takes into account the diffraction of the transducer, the nonlinearity of the medium and the attenuation. Few simulation tools, including the modeling of the nonlinear propagation have been implemented. In this paper, we propose to solve the Westervelt equation directly in the Fourier domain in order to decrease the derivative order of the equation.

To solve the US wave propagation equation, two different methods are proposed. Both of them are based on the expression in the Fourier domain of the propagation in the axial direction. Indeed, the derivative order of the equation is reduced using the Fourier transform. Then, a quasi-linear approximation is used to compute separately the fundamental and each harmonic component. This approximation is valid only when the amplitudes of the successive harmonic components are clearly different (harmonic $n+1$ is weaker than harmonic n) [Varray *et al.*, TUFFC, 2011]. This assumption may not be valid when the nonlinearity of the medium is high, which is the case in contrast agent for example. A second strategy is to use a slowly varying envelope approximation (SVEA) with allow to compute the entire spectrum [Marti *et al.*, IEEE ICASSP, 2014]. With this second method, the spectrum is updated and distorted at each propagation step. This method suffers from a shorter discretization in the axial direction but compute the entire spectrum without any limitations on the number of harmonics. Both strategies can consider medium having an inhomogeneous nonlinear coefficient. Moreover, a GPU implementation is proposed to allow fast computation, even with finer axial steps.

The pressure fields are simulated for both strategies in the same conditions, using the parameters of a real ultrasound transducer. The maximal differences obtained for the fundamental and the second-harmonic components in the axial direction are 0.7dB and 2dB, respectively. The second strategy computes the entire spectrum when the first one is limited to the 2nd harmonic. A careful attention has to be taken concerning the dimension of the axial steps. In term of computation time, both cases lead to similar values (less than 10s for classical geometry). Indeed, the elementary step of the SVEA is faster but more steps are required to ensure the slowly variation envelope approximation.

Finally, the two Fourier spectrum methods proposed offer similar advantages and allow the simulation of nonlinear ultrasound radio-frequency images, as proposed in Creanuis software. Different methods to compute the harmonic RF image will then be included in the package. Future work will consist in experimental measurement using the Ula-Op scanner in order to compare the simulated spectrum with measured one. The proposed developments are freely available to the US community thanks to the Creanuis package.

Tu. 9:00 Amphi 2

Therapeutic applications 2

Enhancement of Cavitation Inception by Second-harmonic Superimposition for Focused Ultrasound TreatmentS.-I. Umemura^a, S. Yoshizawa^b, R. Takagi^c and J. Yasuda^c^aTohoku Univ. Medical Bio Engineering, Aoba 6-6-05, Aramaki, Aoba-ku, 980-8579 Sendai, Japan; ^bTohoku Univ. Department of Communications Engineering, Aoba 6-6-05, Aramaki, Aoba-ku, 980-8579 Sendai, Japan; ^cTohoku University, Aoba 6-6-05, Aramaki, Aoba-ku, 980-8579 Sendai, Japan

sumemura@ecei.tohoku.ac.jp

Microbubbles, whether administered or ultrasonically generated, are known to accelerate the thermal as well as mechanical effects of ultrasound. Furthermore, they are essential for the sonochemical effects. We have proposed an efficient cavitation-enhanced high-intensity focused treatment, in which cavitation microbubbles are generated by an extremely-high-intensity short trigger pulse in prior to a moderately-high-intensity ultrasound burst maintaining the microbubbles. Therapeutic reaction such as microbubble enhanced ultrasonic heating and microbubble mediated sonochemical reaction should take place during the ultrasound burst.

We have also proposed superimposing the second harmonic to the fundamental to enhance the cavitation inception efficiency of the trigger pulse. Either the peak negative or positive acoustic pressure can be enhanced by the second-harmonic superimposition. The peak negative pressure is essential to initiate cavitation in a scattered form, and the peak positive pressure is essential to grow it to a thick cavitation cloud through the process in which the wave is reflected by the cavitation microbubbles and its phase is inverted. Based on this consideration, we have proposed the sequence consisting of the peak-negative-pressure enhanced wave immediately followed by the peak-positive-pressure enhanced wave.

The peak positive and negative pressure of high-intensity focused ultrasound tends to be respectively enhanced and suppressed by the nonlinear propagation followed by the focal phase shift. Therefore, the efficacy of the second-harmonic superimposition to enhance the peak negative pressure is especially noteworthy.

The efficient cavitation inception by the proposed sequence was demonstrated first in water and then in an optically transparent gel. The result of an ex-vivo test of the proposed sequence will also be showed in the presentation.

Numerical Study of a Confocal Ultrasonic Setup for Creation of Cavitation

M. Lafond, F. Chavrier, F. Prieur, J.-L. Mestas and C. Lafon

LabTAU - INSERM U1032, 151, cours Albert Thomas, 69424 Lyon, France

maxime.lafond@inserm.fr

Acoustic cavitation is used for various therapeutic applications such as local enhancement of drug delivery, histotripsy or hyperthermia. One of the utmost important parameter for cavitation creation is the rarefaction pressure (p_-). The typical magnitude of p_- to initiate cavitation from gas dissolved in tissue is beyond the range of the megapascal. Nonlinear effects need therefore to be taken into account. A numerical simulator based on the Westervelt equation was used to study the acoustic field generated by our setup consisting of two high intensity focused ultrasound mounted confocally. Simulations with both transducers from the confocal setup and only one transducer showed that the distortion of the pressure signal due to the combined effects of nonlinearity and diffraction is less pronounced when both confocal transducers are used. Consequently, at constant acoustic power, the confocal setup generates a greater p_- at focus which is favorable for cavitation initiation. Comparing the confocal setup with a single transducer with the same total emitting surface as the entire confocal setup puts in evidence the role of the spatial separation of the two beams. Furthermore, it has been shown that the location of the maximum p_- created by a single transducer shifts from focus towards the transducers in the presence of nonlinear effects. . The simulator was used to study the case of transducers positioned so that their acoustical axes intersect at the location of the peak negative pressure instead of the geometrical focus. For a representative confocal setup, namely moderate nonlinear effects, the intersection of the beams on their peak negative pressure resulted in a 2% increase of p_- and 8% decrease of the peak positive pressure. These differences tend to increase by increasing nonlinear effects. Moreover, while the location of the peak p_- for a single transducer can shift by a few millimeters in strong nonlinear regime, the focal point of a confocal device is independent of the power. This point is particularly important for therapeutic applications, frequently requiring high spatial accuracy.

Tu. 10:00 Amphi 2

Therapeutic applications 2

Enhanced focus steering abilities of multi-element therapeutic arrays operating in nonlinear regimesP. Yuldashev^a, S. Ilyin^a, L. Gavrilov^b, O. Sapozhnikov^{a,c}, W. Kreider^c and V. Khokhlova^a

^aPhysics Faculty, Moscow State University, Leninskie Gory, 119991 Moscow, Russian Federation; ^bAndreyev Acoustics Institute, 4 Schvernika Str., 117036 Moscow, Russian Federation; ^cCenter for Industrial and Medical Ultrasound, Applied Physics Laboratory, University of Washington, 1013 NE 40th Street, Seattle, WA 98105, USA
petr@acs366.phys.msu.ru

Multi-element phased arrays are used in many modern high intensity focused ultrasound (HIFU) surgical systems. Such arrays enable complex beamforming to avoid overheating of obstacles, for example ribs, and phase and amplitude corrections to improve focusing through inhomogeneities in soft tissues and skull bones. Electronic steering of the focus is also used to sonicate tissue volumes without mechanical movement of the transducer. Focal steering can be performed only within certain limits due to generation of secondary grating lobes, which can result in unintentional damage of intervening tissues. The steering range is a key metric for arrays with regard to their safety and efficacy in surgical applications. Enlarging the safe steering volume in tissue is important clinically; in particular, the importance of this problem has been widely discussed for HIFU applications in brain. Nonlinear propagation effects have been shown to provide various advantages for HIFU applications. For example, tissue is heated much more effectively when shock fronts are formed at the focus. The heat deposition rate for waveforms with a shock front is about one order greater than that for a linear wave of the same pressure amplitude. Since shock formation in the focal region of the beam requires intensities that exceed a certain amplitude threshold, this effect can be used to diminish thermal effects in grating lobes where the intensity remains below the threshold. In this work, the steering abilities of a typical array operated in linear and nonlinear regimes were compared. The array included 256 elements of 1 MHz frequency and 7 mm diameter distributed in a quasi-random pattern over a spherical shell with a 170 mm aperture. The shell had a 40 mm diameter hole in the middle and a focal length of 130 mm. In the case of linear focusing, thermal effects are proportional to the intensity levels and the criterion for safe array operation is that the intensity in the grating lobes should be less than 10% of the intensity in the main focus. In the case of nonlinear focusing, the heating effect is no longer proportional to intensity; therefore the heat deposition rate was chosen as the relevant metric, using the same 10% threshold for the secondary lobe in comparison with the focal maximum. When steering the focus, the same linearly predicted intensity level at the focal maximum was maintained by increasing the array power. Numerical simulations of the acoustic field were based on the 3D Westervelt equation and performed for nonlinear propagation both in water and in tissue. It was shown that for shock forming conditions in the main focus, the steering range of safe electronic focusing is considerably larger than that for linear propagation conditions. Nonlinear sonication regimes therefore can be used to enlarge tissue volumes that can be sonicated using electronic steering of the focus of HIFU arrays. Work supported by NIH EB007643, RFBR 14-02-31878 and 15-02-00523 grants.

Analogy between the One-dimensional Acoustic Waveguide and the Electrical Transmission Line in the Cases of Nonlinearity and Relaxation

D. Yang, H. Zhang, S. Shi, J. Shi, D. Li and B. Hu

Harbin Engineering University, 145 Nantong Str. Nangang Dist. Harbin Heilongjiang, 150001 Harbin, China

zhanghaoyangjohn@163.com

The propagation of plane acoustic waves can be investigated by taking advantage of the electro-acoustical analogy between the one-dimensional acoustic waveguide and the electrical transmission line, because they share the same type of equation. This paper follows the previous studies and expands the analogy into the cases of quadratic nonlinearity and dispersion produced by relaxation process. From the basic equations relating acoustic pressure, density fluctuation and velocity, which are valid for the nonlinear and relaxing medium, the equivalent travelling-wave circuits of one-dimensional acoustic waveguide with the consideration of nonlinearity and relaxation processes are obtained. Furthermore, we also discuss the analogical relationships of parameters which exist in the acoustical and electrical systems.

Suppression of Oscillations in a Coupled Thermoacoustic Oscillators

T. Biwa

Tohoku University, 6-6-04 Aramaki, Aoba-ku, 980-8579 Sendai, Japan

biwa@amsd.mech.tohoku.ac.jp

Thermoacoustic oscillations, unstable acoustic oscillations of a gas column maintained by heat, are also referred to as thermo-acoustic oscillations, seemingly depending on whether one wants to create intense oscillations as high as possible, or one wants to suppress them. The former aims at producing a new kind of heat engines by using sound waves in place of mechanical pistons, and the latter tries to achieve safety operation of gas-turbine engines and cryogenics systems. Although the goals are different, these research groups have a common ancestor, Lord Rayleigh. He gave a detailed explanation on thermoacoustic oscillations of Sondhauss tube, Rijke tube, and singing flame together with various topics on acoustics and vibrations. The phenomenon of amplitude death is one of them. He described as "*when two organ-pipes of the same pitch stand side by side, ... the pipes may almost reduce one another to silence.*" In this study, we experimentally demonstrate amplitude death by coupling two thermoacoustic oscillators to propose it as a new suppression method of unwanted thermoacoustic oscillations. The test thermoacoustic oscillators were built by using air-filled cylindrical tubes of 720 mm in length and 24 mm in internal diameter. Each oscillator contained a differentially heated stack made of a ceramic catalyst support. Acoustic oscillations of the fundamental mode were observed to start in the test oscillators when the temperature difference along the stack exceeded 270 K. We first tested a needle valve to couple two oscillators and controlled the coupling strength and frequency detuning by changing a valve opening and a resonator length, respectively. Acoustic pressures at the antinode were measured in two oscillators by using small pressure transducers and a spectrum analyzer. When the valve was closed, steady oscillation states were achieved. But by opening the valve, three different states were observed in the coupled thermoacoustic system; phase drift, synchronization, and oscillation death. We present the bifurcation diagram on the plane of valve opening and frequency detuning, and describe the necessary conditions to stop the oscillations completely.

Theoretical Study of a Thermo-acousto-electric Engine equipped with an Electroacoustic Feedback Loop

C. Olivier, G. Penelet, G. Poignand and P. Lotton

Laboratoire d'Acoustique de l'Université du Maine, Av.Olivier Messiaen, 72085 Le Mans Cedex9, France
come.olivier@univ-lemans.fr

The behavior of thermoacoustic wave-generators beyond the onset threshold of the self-sustained oscillations is governed by nonlinear phenomena. By dissipating acoustic power and perturbing the temperature field in the thermoacoustic core, these nonlinear effects reduce the overall efficiency of thermal-to-acoustic conversion. However, software tools for the design and optimization of thermoacoustic engines (TAEs) are mostly based on the linear theory of thermoacoustics, leading to overestimated performance compared to experimental one. That is the reason why semi-empirical technics (flow straighteners, tapered tubes, membranes or jet pumps) are generally used to limit the influence of nonlinear effects such as acoustic streaming or aerodynamical processes dissipating acoustic power at the end of the stack and heat exchangers.

Recently, the use of an electroacoustic feedback loop has been proposed to control the global efficiency of a TAE. An acoustical source, powered by the amplified signal from a reference pressure measurement on the engine itself, is used to control the self-sustained thermoacoustic oscillations. By tuning the properties of this feedback (in terms of amplification gain and phase-shift relative to the reference signal), the efficiency of the transducer can either be reduced down to the death of the auto-oscillation, or increased, thus generating a greater output power for the same heat input [Olivier et al., *J. Appl. Phys.*, 115 (2014)]. However, at the present time, the multiplicity of the involved nonlinear effects and their complexity do not allow to fully understand how and why the mechanisms at stake in this process of "active control" allow this increase of efficiency.

The present work proposes a simplified model of a thermo-acousto-electric generator to interpret the experimental observations. This reduced-order model is based on a lumped element approach for the description of the acoustic propagation, coupled with a resolution of unsteady heat transfer within the thermoacoustic core based on a finite difference scheme. Such a description allows the rendering of both transient and steady-state operation of the TAE under the influence of an external forcing. The study of various phenomena such as the coupling of the auxiliary electrodynamic source with the engine or the influence of the feedback on both the acoustic field and on the distribution of the temperature field within the thermoacoustic core is made possible by gradually increasing the degree of complexity of the model. This simplified description of a forced thermoacoustic transducer will help to get a better understanding of the phenomena responsible for the complex behaviors induced by the electroacoustic feedback loop on an actual prototype: death of oscillations, efficiency improvement accompanied by a temperature gradient reduction and hysteretic behavior during the processes of gradual heat input increase followed by a gradual decrease.

Tu. 10:00 Amphi 3

Thermoacoustics 2

Evolution equation of subcritical Hopf bifurcation in thermoacoustic oscillations

H. Hyodo and T. Biwa

Tohoku University, 6-6-04 Aramaki, Aoba-ku, 980-8579 Sendai, Japan

hyodo@amsd.mech.tohoku.ac.jp

Hopf bifurcation, a bifurcation to a limit cycle from a fixed point, is observed in various systems such as electrical system, chemical system and thermoacoustic system and so on. There are two different types of Hopf bifurcation. One is the supercritical bifurcation. In phase space, a stable fixed point changes into an unstable one and a stable limit cycle appears around it when the bifurcation parameter goes beyond a critical value. Another is the subcritical Hopf bifurcation. The difference from the supercritical bifurcation is the emergence of an unstable limit cycle between a stable fixed point and a stable limit cycle in phase space. Since all the states near the unstable limit cycle go away from it, the unstable limit cycle in principle cannot be observed in real systems unless the time evolution is reversed in numerical calculations.

Recently, the method to obtain the evolution equation of bifurcation system has been proposed. By using this method, the unstable state of the subcritical Hopf bifurcation system may be pinpointed as one of steady states.

In this study, we determine the evolution equation of a thermoacoustic system to identify the unstable limit cycle. The thermoacoustic oscillator with a straight resonance tube filled with atmospheric air was used. A honeycomb ceramic, which is called stack, was inserted in the resonance tube and a temperature difference between both ends of it was created by two heat exchangers. The evolution equation was determined based on energy conservation law expressed by using the acoustic energy stored in the system and the supplied external acoustic power. In order to supply the power, an acoustic driver was placed at the bottom of the resonance tube, which consisted of the loudspeaker and dynamic bellows. The acoustic energy and the acoustic power supply were determined with the two sensor method measuring acoustic pressures in the resonator.

The evolution equations were obtained for different temperature difference. For small temperature difference, the equation had no fixed point except for the origin. For large temperature difference, a stable fixed point at certain energy appeared. And for the middle temperature difference in the hysteresis region, the equation had unstable equilibrium point. The unstable equilibrium point can be observed in the subcritical Hopf bifurcation system by evolution equation.

Tu. 13:40 Amphi 1 bis

General nonlinear acoustics 2

Fatigue Crack Detection based on Change of Linear Ultrasonic Features caused by Structural Nonlinearity

H.J. Lim and H. Sohn

KAIST, 291 Daehak-ro, Yuseong-Gu, 305-701 Daejeon, Republic of Korea

limhj87@gmail.com

This paper presents a fatigue crack detection technique using changes of linear ultrasonic features caused by structural nonlinearity. We theoretically and experimentally demonstrate that a nonlinear mechanism produced by a fatigue crack not only generates nonlinear modulations or harmonics, but also reduces the amplitude of the linear responses because the energy in the linear responses is partially transmitted to the harmonic or modulation components. The experimental results show that the amplitude reduction of the linear responses is more sensitive to a fatigue crack than the amplitude increase of the harmonics and modulation components. In addition, a baseline-free fatigue crack detection technique is proposed considering the additional amplitude reduction of the linear components due to nonlinear ultrasonic modulation.

Tu. 14:00 Amphi 1 bis

General nonlinear acoustics 2

Finite Element Modeling of the Non Collinear Mixing Method for Detection and Characterization of Closed CracksA. Meziane^a and P. Blanloeuil^b^aUniv. Bordeaux, I2M, UMR 5295,, 351, cours de la libération, 33405 Talence, France; ^bSchool of Mechanical & Mining Engineering,, St Lucia QLD, 4072 Brisbane, Australia
anissa.meziane@u-bordeaux.fr

The non-collinear mixing technique is applied for detection and characterization of closed cracks. The method is based on the nonlinear interaction of two shear waves generated with an oblique incidence. This interaction leads to the scattering of a longitudinal wave. A Finite Element model is used to demonstrate its application to a closed crack. Contact acoustic nonlinearity is the nonlinear effect considered here and is modeled using unilateral contact law with Coulomb's friction. Directivity pattern are computed using a two-step procedure. The Finite Element (FE) model provides the near-field solution on a circular boundary surrounding the closed crack. The solution in the far-field is then determined assuming that the material has a linear behavior. Directivity patterns will be used to analyze the direction of propagation of longitudinal wave(s) scattered from the closed crack. Numerical results show that the method is effective and promising when applied to a closed crack. Scattering of the longitudinal wave also enables us to image the crack, giving position and size indications. Finally, the method offers the possibility to distinguish classical nonlinearity from contact acoustic nonlinearity.

Tu. 14:20 Amphi 1 bis

General nonlinear acoustics 2

Numerical and Experimental Analysis of harmonic generation method for detection of closed cracksA. Saidoun^a, A. Meziane^b, M. Rénier^a, F. Zhang^c and H. Walaszek^c^aI2M Institut de Mécanique et d'Ingénierie, 351 cours de la Libération, 33405 Talence, France; ^bUniv. Bordeaux, I2M, UMR 5295, 351, cours de la libération, 33405 Talence, France; ^cCETIM Fondation, CETIM/EPI, 52 avenue Félix Louat, 60300 Senlis, France

abdelkrim.saidoun@u-bordeaux.fr

Early detection and characterization of damages in materials are an important key to control the durability and reliability of parts and materials in service. Although linear ultrasonic methods are sensitive for detecting and sizing open cracks, they failed to detect closed cracks. An alternative to linear ultrasonic methods is to use nonlinear methods, which have shown to be effective for this kind of defects. Nowadays, there are several nonlinear acoustic techniques used in non-destructive evaluation. In this study the harmonic generation technique is considered. A numerical study based on a one-dimensional model describing the linear propagation of a plane longitudinal acoustic wave and its reflection on a rigid plan shows the appearance of new frequency components in the reflected wave spectrum due to unilateral contact law applied at the rigid plane. This numerical model is used to study the evolution of harmonic amplitudes depending on prestress. The evolution of the second harmonic as a function of the ratio of the static stress and the incident wave amplitude has an optimal value, which is analyzed using an analytical model. The influence of experimental parameters on the harmonics amplitudes is studied in order to optimize these parameters in view to experiments. Measurements on an artificial crack, carried out by bringing two solids in contact with a prestress are presented in order to validate numerical results. This work is a first step for optimizing the method in view to detect fatigue closed cracks.

Tu. 14:40 Amphi 1 bis

General nonlinear acoustics 2

Nonlinear Ultrasonic Imaging of Thermal Fatigue Cracks of Several Tens nm Gap in Glass PlatesM. Hertl^a, K. Kawashima^b, K. Sekino^c, H. Yasui^d and T. Aida^a

^aInsight kk, 2-6-7 Hyakunin-cho, Shinjuku-ku, 169-0073 Tokyo, Japan; ^bUltrasonic Materials Diagnosis Laboratory, 4 Hazamacho, Showa-ku, Nagoya, 466-0062 Aichi, Japan; ^cKanto Gakuin University, 1-50-1 Mitsuura-Higashi, Kanazawa-ku, Yokohama, 236-8501 Kanagawa, Japan; ^dToyota Motor Corporation, 1 Toyota-cho, Toyota, 471-8571 Aichi, Japan

michael-hertl@insightkk.co.jp

Very narrow gaps of several tens nm could exist in bonded wafers. If such disbonds or weakly bonded spots are included within the bonded interface, IC tips could be damaged by dicing. Therefore, nondestructive evaluation of these disbonds is required. However, the detection of the disbonds by conventional ultrasonic technique is very difficult due to quite small difference in acoustic impedance ΔZ . On the contrary, the nonlinear ultrasonic technique, which detects higher harmonics of the wave scattered at defects of very narrow gaps by transmitting sinusoidal waves of large amplitude, has high sensitivity.

In this study, we apply this technique for imaging thermal fatigue cracks, which have gap distances of several tens nm, in a glass plate. Thermal fatigue cracks were generated in glass plates of thickness, width and length of 15 mm, 100 mm and 150 mm, respectively. Through thickness cracks are extended by cyclic heating and cooling. The gap distance is approximately 30 nm as determined by SEM observation.

A sinusoidal tone-burst wave pulser, RITEC RPR-4000, was used for transmission and reception of ultrasonic waves in water immersion. A focused transducer with a diameter, central frequency and focal length of 9.6 mm, 5 MHz, 51 mm, respectively, was used. Sinusoidal burst wave of 4.5 MHz was transmitted and higher harmonics were extracted by an analog high-pass filter of 6 MHz. For through transmission mode, tone-burst wave of 5.49 MHz, which is a resonant frequency of the plate thickness, was transmitted and the seventh harmonic wave received by a high pass filter.

Some parts of the thermal fatigue crack of some tens nm gap in a glass plate is clearly imaged by the immersion higher harmonic imaging technique. Cracked face near the crack tip is not imaged due to high residual compressive stress. If spatial resolution will reach to a few micron meter, the technique could be applied for detection of disbonds in bonded wafers.

Tu. 13:40 Amphi 2

Radiation force in biology and medicine

Nonlinear Aspects of Acoustic Radiation Force in Biomedical ApplicationsL. Ostrovsky^a and A. Sarvazyan^b^aNOAA ESRL/PSD, 325 Broadway, R/PSD99, Boulder, AK 80305, USA; ^bArtann Laboratories, 1459 Lower Ferry Road, Trenton, AK 08618, USA

lev.a.ostrovsky@noaa.gov

In the past decade acoustic radiation force became a powerful tool in numerous biomedical applications. Radiation force from a focused ultrasound beam acts as a virtual "finger" for remote probing of internal anatomical structures and obtaining diagnostic information. This presentation deals with generation of shear waves and acoustic streaming by nonlinear focused beams. Albeit the radiation force has intrinsically nonlinear origin, in most cases the primary ultrasonic wave and the motions it generates were considered in the linear approximation. In this presentation, after a brief historical outline, we consider the effects of nonlinearly distorted beams on generation of shear waves, as well as nonlinearity in acoustic flows generated by such beams. Along with theoretical modeling, the relevant experimental data are presented. This study was partly supported by the NIH grant R21AR065024

Tu. 14:00 Amphi 2

Radiation force in biology and medicine

Effect of particle-particle interactions on the acoustic radiation force in an ultrasonic standing waveB. Lipkens^a, Y. Ilinskii^b and E. Zabolotskaya^b^aWestern New England University, 1215 Wilbraham Road, Box S-5024, Springfield, Massachusetts, AK 01119, USA;^bApplied Research Laboratories, University of Texas at Austin, 10000 Burnett Road, Austin, TX 78758, USA

b lipkens@wne.edu

Ultrasonic standing waves are widely used for separation applications. In MEMS applications, a half wavelength standing wave field is generated perpendicular to a laminar flow. The acoustic radiation force exerted on the particle drives the particle to the center of the MEMS channel, where concentrated particles are harvested. In macro-scale applications, the ultrasonic standing wave spans multiple wavelengths. Examples of such applications are oil/water emulsion splitting [1], and blood/lipid separation [2]. In macro-scale applications, particles are typically trapped in the standing wave, resulting in clumping or coalescence of particles/droplets. Subsequent gravitational settling results in separation of the secondary phase. An often used expression for the radiation force on a particle is that derived by Gor'kov [3]. The assumptions are that the particle size is small relative to the wavelength, and therefore, only monopole and dipole scattering contributions are used to calculate the radiation force. This framework seems satisfactory for MEMS scale applications where each particle is treated separately by the standing wave, and concentrations are typically low. In macro-scale applications, particle concentration is high, and particle clumping or droplet coalescence results in particle sizes not necessarily small relative to the wavelength. Ilinskii et al. developed a framework for calculation of the acoustic radiation force valid for any size particle.[4] However, this model does not take into account particle to particle effects, which can become important as particle concentration increases. It is known that an acoustic radiation force on a particle or a droplet is determined by the local field. An acoustic radiation force expression is developed that includes the effect of particle to particle interaction. The case of two neighboring particles is considered. The approach is based on sound scattering by the particles. The acoustic field at the location of one particle then consists of two components, the incident sound wave and the scattered field generated by the neighboring particle. The radiation force calculation then includes the contributions of these two fields and incorporates the mutual particle influence. In this investigation the droplet/particle influence on each other has been analyzed theoretically by using the method developed by Gor'kov and modified by Ilinskii et al.

1) J. Dionne, B. McCarthy, B. Ross-Johnsrud, L. Masi and B. Lipkens, "Large volume flow rate acoustophoretic phase separator for oil water emulsion splitting," Proceedings of Meetings on Acoustics, Vol. 19, 045003 (2013) 2) B. Dutra, M. Rust, D. Kennedy, L. Masi and B. Lipkens, "Macro-scale acoustophoretic separation of lipid particles from red blood cells," Proceedings of Meetings on Acoustics, Vol. 19, 045017 (2013) 3) L. P. Gor'kov, "On the forces acting on a small particle in an acoustical field in an ideal fluid," Sov. Phys. Dokl. 6, 773-775 (1962). 4) Y. A. Ilinskii, E. A. Zabolotskaya and M. F. Hamilton, "Acoustic radiation force on a sphere without restriction to axisymmetric fields," POMA 19, 045004 (2013)

Tu. 14:20 Amphi 2

Radiation force in biology and medicine

Acoustic Radiation Force due to Arbitrary Incident Fields on Spherical Particles in Soft Tissue

B. Treweek, Y. Ilinskii, E. Zabolotskaya and M. Hamilton

Applied Research Laboratories, University of Texas at Austin, 10000 Burnett Road, Austin, TX 78758, USA

btreweek@utexas.edu

Acoustic radiation force is of interest in biomedical applications that range from measuring elastic moduli of soft tissue to pushing kidney stone fragments toward locations that facilitate their exit from the kidney. At ISNA 19 a theory was reported for the radiation force on a sphere embedded in a soft elastic medium with a shear modulus several orders of magnitude smaller than its bulk modulus [Ilinskii et al., AIP Conf. Proc. 1474, 255-258 (2012)]. Subsequent work extended the theory to accommodate nonaxisymmetric incident fields described via spherical harmonic expansion [Ilinskii et al., Proc. Meet. Acoust. **19**, 045004 (2013)]. The present contribution addresses the effects of various fields incident on spherical scatterers. This is accomplished via angular spectrum decomposition of the incident field, spherical wave expansions of the resulting plane waves about the center of the scatterer, Wigner D-matrix transformations to express these spherical waves in a coordinate system with the polar axis aligned with the desired radiation force component, and finally integration over solid angle to obtain spherical wave amplitudes as required in the theory. Computations are performed for diffracting sound beams and compared with results for traveling plane waves, and various standing wave fields are also examined. Scatterers with different sizes and mechanical properties are considered, including both gas bubbles and elastic spheres, and scatterer position within the incident field is varied as well. The model predicts a change in direction of the axial or the transverse component of the radiation force depending on properties of the particle and the host medium. Finally, comparisons are made with liquid as the shear modulus of the host medium spans the range of values encountered in soft tissue. [Work supported by the ARL:UT McKinney Fellowship in Acoustics.]

Tu. 14:40 Amphi 2

Radiation force in biology and medicine

Experimental Study of Acoustic Radiation Force of an Ultrasound Beam on Absorbing and Scattering ObjectsA. Nikolaeva^a, M. Kryzhanovskiy^a, S. Tsysar^a, W. Kreider^b and O. Sapozhnikov^{c,b}^aPhysics Faculty, Moscow State University, Leninskie gory, 119991 Moscow, Russian Federation; ^bCenter for Industrial and Medical Ultrasound, Applied Physics Laboratory, University of Washington, 1013 NE 40th Street, Seattle, WA 98105, USA; ^cPhysics Faculty, Moscow State University, Leninskie Gory, 119991 Moscow, Russian Federation
niko200707@mail.ru

Acoustic radiation force is a nonlinear acoustic effect due to wave momentum transfer to absorbing or scattering objects. This phenomenon is exploited in modern ultrasound metrology for measurement of the acoustic power radiated by a source and is used for both therapeutic and diagnostic sources in medical applications. The relationship between acoustic power and radiation force on a target is the basis of the radiation force balance method. Although this relationship is fairly simple for plane waves interacting with absorbing or reflecting targets, real sources radiate beams rather than plane waves. To help relate power and radiation force under these conditions, a method of acoustic holography can be used to describe these fields at any point in space. The true field of the ultrasound beam can be recorded by measuring both the amplitude and phase of the acoustic wave along a two-dimensional region perpendicular to the axis of beam propagation. The obtained two-dimensional record (a hologram) enables calculation of the radiation stress tensor on the surface of a scattering or absorbing target. As an alternative to direct calculation of the stress tensor, the hologram can also be used to calculate radiation force using previously derived analytical expressions based on the angular spectrum of the measured field. The results of an experimental investigation of radiation forces in two different cases are presented in this paper. In one case, the radiation force of an obliquely incident ultrasound beam on a large absorber (which completely absorbs the beam) is considered. The second case concerns measurement of the radiation force on a spherical target that is small compared to the beam diameter. In both cases an ultrasound transducer was used with a diameter of 100 mm, operated in a continuous wave mode at a frequency of 1 MHz. The radiation force measurements on a distributed absorber were carried out by weighing the absorber on a precision scale with and without the incident ultrasound beam. In the case of small spherical scatterers, the radiation force was determined based on measurements of target displacement, either when suspended as a pendulum or attached to elastic rubber threads. In both cases, radiation force measurements from the targets were compared with forces calculated from beam holograms. Comparison of theoretical and experimental results permits both characterization of beams radiated by real sources and calibration of the hydrophone used for holography measurements. The work was supported by the RSF grant N°14-15-00665 and NIH R21EB016118.

Tu. 13:40 Amphi 3

Thermoacoustics 3

Oscillating viscous boundary layer at high Reynolds number : Experiments and numerical calculationsI. Reyt^a, H. Bailliet^a, E. Foucault^b and J.-C. Valière^a^aInstitut Pprime, CNRS, Université de Poitiers, ENSMA, Bât B17, 6 rue Marcel Doré, 86073 Poitiers Cedex 9, France;^bInstitut Pprime, CNRS, Université de Poitiers, ENSMA, Bât B17, 6 rue Marcel Doré, 86022 Poitiers Cedex, France
helene.bailliet@univ-poitiers.fr

The transition to turbulence for an acoustically oscillating flow (without any mean motion) in a resonant wave guide is considered. Departure from the laminar behaviour of the Stokes boundary layer formed in the near wall region is studied both experimentally and numerically for increasing acoustic levels.

In the experimental study, the oscillating flow is generated by the coupling of two acoustic sources and a cylindrical wave guide filled with air at atmospheric pressure. The resonance of this system yields high acoustic level. Laser Doppler Velocimetry is used to measure oscillating particle velocity in the near wall region for increasing Reynolds number $Re_{\delta_\nu} = U_0\delta_\nu/\nu$, with U_0 the amplitude of velocity oscillations in the core of the guide, δ_ν the acoustic boundary layer thickness and ν the fluid kinematic viscosity. The time resolved Laser technique synchronized with the loudspeaker source signal permits to obtain velocity profiles at different phases of the acoustic cycle. The distortion of the measured velocity profile from laminar Stokes boundary layer can thus be investigated and the critical value of Re_{δ_ν} for transition can be estimated.

On the other hand, the oscillating boundary layer is investigated numerically with a one dimensional scheme for comparison with experimental results. The effective viscosity that models the transition to turbulence is included and the velocity profile is integrated along the radial coordinate in the near wall region.

The experimental profile distortion is interpreted as the consequence of the development of a turbulent boundary layer. The eddy viscosities associated respectively with experiments and calculations are compared.

Tu. 14:00 Amphi 3

Thermoacoustics 3

Measurements of acoustic minor loss in a tube with geometrical irregularities

Y. Ueda, S. Yonemitsu and T. Saito

Tokyo University of Agriculture and Te, 2-24-16 Nakacho, Koganei, Tokyo 184-8588, Japan, 1848588 Tokyo, Japan
uedayuki@cc.tuat.ac.jp

When fluid flows in tubes with geometrical irregularities, the two types of the energy loss occur. One is caused due to a length of tubes. The other is due to the geometrical irregularities and is referred to as minor loss. To evaluate the losses are important to design and improve fluid machines.

In the case that fluid flow is unidirectional, both the type losses have been studied and are covered in many of textbooks on fluid dynamics. However, only a few investigations has been addressed the minor loss for the oscillatory flow, namely the acoustic minor loss, though the energy loss due to a tube length has been well understood.

In this study, we have measured the acoustic minor loss generated in tubes with two types of geometrical irregularities. One is abrupt area change and the other is bend. For the case of abrupt area change, the acoustic minor loss factor was evaluated as a function of the tube cross-sectional area ratio. For the case of bended tube, it was evaluated as a function of the ratio of the tube radius and the bend radius. The obtained values of the acoustic minor loss factor for both cases were compared with the minor loss factor for unidirectional flow.

Tu. 14:20 Amphi 3

Thermoacoustics 3

LDV measurements of Rayleigh streaming in narrow channels

R. Bessis, H. Bailliet, I. Reyt and J.-C. Valière

Institut Pprime, CNRS, Université de Poitiers, ENSMA, Bât B17, 6 rue Marcel Doré, 86073 Poitiers Cedex 9, France
remi.bessis@univ-poitiers.fr

Rayleigh streaming, suspected to hamper the efficiency of thermoacoustic devices, has been the subject of numerous theoretical and experimental studies in the last decades. However, analytical and numerical prediction of Rayleigh streaming within narrow channels have never been confronted to measurements due to the experimental challenge such measurements represent. Theories show that the inner and outer vortices that form Rayleigh streaming share the channel section, the proportion of inner vortex in the section increasing as the channel gets narrower. For very narrow channels only one vortex is expected. We propose to present results of Laser Doppler Velocimetry measurements in a rectangular channel for different height of the channel from large to narrow channels. The axial second order particle velocity is estimated from velocity measurements. Axial acoustic and streaming velocity evolution along both the axial and the two transverse axes are considered for different channel heights. We found it also interesting to address the limit of validity of the usual 2D channel hypothesis when considering a rectangular enclosure. [The research leading to these results has been performed under the collaborative framework OpenLab Peugeot Citroën Automobiles - Institut Pprime (UPR CNRS 3346, Poitiers).]

Tu. 14:40 Amphi 3

Thermoacoustics 3

New Method to Increase the Energy Conversion Efficiency of Thermoacoustic Engine.A. Kido^a, S.-I. Sakamoto^b, K. Taga^a and Y. Watanabe^a^aDoshisha University, Miyakodani 1-3, Tatara, Kyotanabe-shi, 610-0321 Kyoto, Japan; ^bUniversity of Shiga Prefecture, Hassakacho 2500, Hikone-shi, 522-0057 Shiga, Japan
dmo1015@mail4.doshisha.ac.jp

Many researches have been reported to improve an energy conversion efficiency of thermoacoustic engine. As the one of the method of improvement way, we proposed a Phase Adjuster (PA) or an Expanding Phase Adjuster (EPA) devices those have partially reduced or expanded inner-diameter path. When the PA or EPA set on the thermoacoustic system, it acts as the amplifier and stabilizer of the system oscillation. As the results, the efficiency of energy conversion improved steeply, and the stabilized resonant oscillation are also observed. However, there are some problems for these devices. Because of the solidified device and located in the thermoacoustic tube, it is difficult to tune and move them to the best setting position under the system is running. Therefore, it is necessary to find more easy method to be able to get the same effects of PA or EPA. In this report, as an easy method to realize the improvement of efficiency and the stable oscillation, we propose the local heating method. Experiments are carried out using the loop-tube-type thermoacoustic system. The total length of the system is 3.3 m and inner diameter is 42 mm. The thickness of prime mover (PM) stack is 50 mm and channel radius is 0.45 mm (900 cells/inch²). Two electric heaters are set on the system, one is for the PM stack and the other is for the proposed heater H2. PM stack is driven by 330 W electric input power and H2 is also heated by 160 W. The setting position of the heater H2 is easily changed, then the heater is moved to the various positions from the PM stack along the system. The sound pressure fluctuation in the system is measured by the pressure sensors (PCB Piezotronics Inc.). The acoustic power intensity is calculated by substituting the measured sound pressures into the wave equation while applying Rott's acoustic approximation. The temperatures of the stack ends and inner working fluid are measured using K-type thermocouples. Resonant mode has been changed depending on the setting position of H2. The single wavelength resonant mode is observed when the H2 is set within 0.4 to 0.65 m and 2.0 to 2.3 m from PM on the other hand, the double wavelength resonant mode is observed at both 1.0 and 2.65 m, and the triple wavelength resonant mode is observed within 1.3 to 1.8 m and at 2.85 m. As the result of the change of resonant mode, energy conversion efficiency is also changed. Especially the resonant is realized in the single wavelength mode, it is confirmed that, the energy conversion efficiency in substantially increased compare with the system without the heater H2. These observed phenomena are similar to the behavior of EPA. Therefore, the presented method can be performed as the easy method to realize the higher efficiency and stable oscillation.

Tu. 15:00

Poster session

Velocity Measurement Method to Control the Coagulation Enzymatic

M. Derra, A. Amghar and H. Sahсах

Faculté des sciences université ibn zohr, Laboratoire de métrologie et traitement de l'infomation, 80000 Agadir, Morocco

younes.derra@hotmail.fr

The coagulation time is often used as a reference to determine the time of cutting the gel, in order to expel whey trapped in the pores of the gel. Cutting time means that the gel has reached a certain firmness allowing passage from the enzymatic phase to the physico-chemical phase of the cheese making process. Therefore, cutting the gel earlier or later will have negative effects on the quality of the final product. So, optimal evaluation of the coagulation time is necessary to maximize qualitative and quantitative cheese yields. In this work a non-destructive ultrasonic technique is developed to monitor in real time the coagulation process of renneted milk in order to determine the coagulation time. The latter is determined with high precision by exploiting changes of the ultrasonic velocity in the coagulating milk. We have developed a non-invasive technique that uses a single transducer, what is very important in the food industry.

Tu. 15:00

Poster session

Acoustic field distribution of sawtooth wave with nonlinear SBE modelX. Liu^a, L. Zhang^b, X. Wang^b and X. Gong^b^aKey Laboratory of Modern Acoustics, Institute of Acoustics, Hankou Road 22, Nanjing University, 210093 Nanjing, China; ^bKey Laboratory of Modern Acoustics, Institute of Acoustics, Hankou Road 22, Nanjing Univ, 210093 Nanjing, China

xzliu@nju.edu.cn

For precise prediction of the acoustic field distribution of extracorporeal shock wave lithotripsy with an ellipsoid transducer, the nonlinear spheroidal beam equations (SBE) are employed to model acoustic wave propagation in medium. To solve the SBE model with frequency domain algorithm, boundary conditions are obtained for monochromatic and sawtooth waves based on the phase compensation. In numerical analysis, the influence of sinusoidal wave and sawtooth wave on axial pressure distributions is investigated. According to the numerical results, with same fundamental frequency and initial pressure, for sawtooth wave, the focal gain of harmonics is higher and its impact and cavitation effect is better than the sinusoidal wave in the crush of calculi. Besides, the total focal gain of sawtooth wave can be improved by increasing the initial pressure.

Tu. 15:00

Poster session

Acoustic analysis of voices from students with speech disorders

B. Sabir

Faculty of science Ben M'Sik, Bd Commandant Driss Harti Casa, 20450 Casablanca, Morocco

sabir.brahim@hotmail.com

Abstract

Objective

Psycho-Communication disorders negatively affect the academic curriculum for students in higher education. Acoustic analysis is an objective leading tool to describe these disorders; however the amount of the acoustic parameters makes differentiating pathological voices among healthy ones not an easy task. The purpose of the present paper was to present the relevant acoustic parameters that differentiate objectively pathological voices among healthy ones.

Methods

Pathological and normal voices samples of /a/, /i/ and /u/ utterances, of 400 students were recorded and analyzed acoustically with PRAAT software, then a feature of acoustic parameters were extracted. A statistical analysis was performed in order to reduce the extracted parameters to main relevant ones in order to build a model that will be the basis for the objective diagnostic.

Results

Mean amplitude, jitter local absolute, second bandwidth of the second formant and Harmonic-to-Noise Ratio (HNR)); are relevant acoustic parameters that characterize pathological voices among healthy ones, for the utterances of vowels /a/, /i/ and /u/ Thresholds of the acoustic parameters of pathological /a/, /i/, and /u/ were calculated. A training model was built and simulated on Matlab, and a comparison between HMM (Hidden Markov Model) and KNN (K-Nearest Neighbors) classification methods were done (HMM had a rate of recognition of 95% and KNN within the reduced acoustic parameters reached a recognition rate of 97%)

Conclusion

Through the identified parameters, we can objectively detect pathological voices among healthy ones for diagnostic purposes. As a future work, the present approach is an attempt toward identifying acoustic parameters that characterize each voice disorder. Keywords: Psycho-Communication disorders, acoustic analysis, PRAAT, Classification methods.

Tu. 15:00

Poster session

Cavitation Activity Enhancement by Nanoparticles in Sonodynamic Therapy of Melanoma B16A. Nikolaev^a, A. Gopin^b, N. Andronova^b, N. Dezhkunov^c and E. Treshalina^a^aMoscow State University, Moscow, Russian, Leninskie gory 1, 119991 Moscow, Russian Federation; ^bMoscow State University, Leninskie gory 1, 119991 Moscow, Russian Federation; ^cBSUIR, P.Brovka st.6, 220013 Minsk, Belarus dnv@bsuir.by

In this paper the results of the study of solid inclusions in biological structures as "concentrators" of acoustic energy for ultrasound treatment of cancer (solid-phase sonosensitization) are presented. Particular attention is drawn to the possibility of synthesis of these inclusions directly in the tumor. The validity of the hypothesis of solid-phase sonosensitization is confirmed in experiments on model systems and animals. In these studies, we used unfocused ultrasound with a frequency of 0.88 MHz and an intensity of 2 W/cm². Cavitation properties of gels containing impurities and without them were comparatively estimated using an ICA-3MHF Cavitometer (BSUIR, Minsk). It was shown on model biological systems (*Enterococcus* spp. bacteria) that cavitation activity and the destructive effect of ultrasound are enhanced in the presence of nanoparticles. As a result of ultrasonic treatment some of the bacteria exposed to destruction apparently accompanied by the leakage of cytoplasm. However, most of the cells keep normal form. Bacteria pretreated with Theraphthal show a change in the shape and the destruction of the membranes that cover almost all the treated cells. This is confirmed by data on the survival of bacteria. Enhancing of effect of ultrasound treatment of cells is associated with the formation of calcium salts of Theraphthal solid phase on the membranes, thereby reducing the mechanical strength of membranes and enhancing the local cavitation effects. In vivo experiments melanoma B16 was inoculated intramuscularly into BDF1 mice in the right paw according to the standard procedure. The initial tumor volume at 8th day after inoculation was $V_0=1.1\pm 0.1$ cm³. Sonosensitizers were injected intravenously 1 hour prior to ultrasonic treatment. Ultrasonic treatment of inoculated tumors was performed simultaneously with two frequencies (0.88 MHz 1 W/cm² and 2.64 MHz 2 W/cm²) for 10 minutes at 40°C. The dynamics of tumor growth was assessed by the change in its volume. Preclinical trials of the method of solid-phase sonosensitization were carried out at N.N.Blokhin Russian Research Oncological Center. The experiments included estimation of the therapeutic efficiency, harmlessness, and the effect on metastatic disease. These studies showed a high therapeutic efficiency of the method, i.e., tumor regression by 75-80% on average with an increase in the animal lifetime by a factor to 2, good exposure tolerance, and the absence of the effect on metastatic disease. Currently, the method of ultrasonic therapy with solid-phase sonosensitizers is in clinical trials.

Tu. 15:00

Poster session

Axial acoustic radiation force on a sphere in a Gaussian beam

R. Wu, X. Liu and X. Gong

Key Laboratory of Modern Acoustics, Institute of Acoustics, Hankou Road 22, Nanjing University, 210093 Nanjing, China

wurongrong1988@live.cn

The Gaussian beam is expressed in terms of spherical wave functions based on the finite series method, and a weighting parameter, describing the beam shape and its location relative to the particle. The acoustical radiation force resulting from a Gaussian beam incident on a spherical object is investigated analytically. The radiation force function vs. ka curve is discussed for different beam widths compared with the plane wave. Also, we validate the method by computing the acoustical radiation force of liquid spheres and elastic spheres for different beam waist when the position of the sphere is deviated from the Gaussian beam center axially. Results have been presented for Gaussian beams with different waist sizes and wavelengths and it has been shown that the interaction of a Gaussian beam with a sphere can result in attractive axial force under specific operational conditions. The results provided here may provide a theoretical basis for development of single-beam acoustical tweezers.

Tu. 15:00

Poster session

Sound beam manipulation based on temperature gradientsF. Qian^{a,b}, L. Quan^a, X. Liu^a and X. Gong^a

^aKey Laboratory of Modern Acoustics, Institute of Acoustics, Hankou Road 22, Nanjing University, 210093 Nanjing, China; ^bSchool of Physics & Electronic Engineering, Changshu Institute of Technology Donghu Campus, 215500 Changshu, China

frozenmaple@126.com

Previous research with temperature gradients has shown the feasibility of controlling airborne sound propagation. Here, we present two temperature gradients based airborne sound manipulation schemes: a cylindrical acoustic omnidirectional absorber (AOA) and a curved sound propagation. The proposed AOA has high absorption performance which can almost completely absorb the incident wave. Geometric acoustics is used to obtain the refractive index distributions with different radii, which is then utilized to deduce the desired temperature gradients. For the curved sound propagating beam scheme, we optimize the locations and the temperatures of heat sources to find the desired temperature gradients, which is used to manipulate the acoustic directional deflection. Since neither of two methods requires resonant units, their working bandwidths are expected to be broad ones. Both schemes are temperature-tuned and easy to realize, which is of potential interest to fields such as noise control or acoustic cloaking.

Tu. 15:00

Poster session

Acoustic Characteristics of the Medium with Gradient Change of Impedance

B. Hu, D. Yang, Y. Sun, J. Shi, S. Shi and H. Zhang

Harbin Engineering University, 145 Nantong Str. Nangang Dist. Harbin Heilongjiang, 150001 Harbin, China

kidd1105@sina.com

The medium with gradient change of acoustic impedance is a new acoustic structure which developed from multiple layer structures. In this paper, the inclusion is introduced and a new set of equations is developed. It can obtain better acoustic properties based on the medium with gradient change of acoustic impedance. Theoretical formulation has been systematically addressed which demonstrates how the idea of utilizing this method. The sound reflection and absorption coefficients were obtained. At last, the validity and the correctness of this method are assessed by simulations. The results show that appropriate design of parameters of the medium can improve underwater acoustic properties.

Tu. 15:00

Poster session

Elastic Waves in a Wedge of Aluminum Alloy with Permanent Residual Deformations

A. Korobov, M. Izosimova and A. Kokshaiskii

Faculty of Physics, M.V. Lomonosov Moscow State University, Leninskie gory 1, 119991 Moscow, Russian Federation
aikor42@mail.ru

The paper presents results of experimental investigations of flexural elastic V-waves (EVW) in metallic wedges of isotropic aluminum alloy D16. For the experiments, several wedges with angle apertures of 32 degrees and 60 degrees have been prepared and investigated. Two wedge samples are made of alloy D16, where strong mechanical residual stresses were previously created. For excitation and reception of EVW the piezoelectric transducers are used. EVW recording are also carried out using the POLYTEC laser vibrometer. Ultrasonic measurements are performed using automated ultrasonic complex RITEC RPR-5000. In the frequency range of (0.25 - 3) MHz EVW velocities are measured. Velocity dispersion is found in this frequency range within the experimental errors. In a wedge with angle of 60 degrees at 250 kHz, EVW localization was investigated in the wedge rib using a laser vibrometer. An exponential decrease in the amplitude of the vibrational wave velocity V , depending on the distance from the edge of the wedge, is indicated. Studies of EVW amplitude dependence of its velocity and EVW second harmonic generation have been conducted. In isotropic wedges without permanent deformation, expectedly, amplitude dependence of EVW velocity and EVW second harmonic generation are not observed. (In isotropic solids, second harmonic generation of flexural EVW is impossible due the conditions of symmetry). In samples of wedges with residual strains, at excess of a certain level of amplitude of the probe signal on the EVW transmitter, EVW velocity decreasing linear in amplitude is detected. Besides, generation of the second harmonic of elastic EVW is observed in the wedges with residual stress. The dependence of amplitude of the second harmonic on EVW amplitude of the fundamental frequency is linear. Threshold and linear decrease of EVW velocity at EVW amplitude increase, as well as second harmonic generation of EVW can not be explained with classical elastic nonlinearity associated with the anharmonicity of the crystal lattice. Such behavior of the nonlinear properties of the EVW and second-harmonic generation is typical for media with non-classical (structural) nonlinearity and due to the residual strains made in the sample. A discussion of the experimental results is presented. This work was supported by grants RFBR 14-02-00288a

Tu. 15:00

Poster session

Influence of a low flow rate on an acoustic cavitation bubble cloudA. Seck^a, C. Inserra^b, S. Ollivier^a, J.-C. Béra^b and P. Blanc-Benon^a^aLaboratoire de Mécanique des Fluides et d'Acoustique, Ecole Centrale de Lyon, 36 Avenue Guy de Collongue, 69134 Ecully, France; ^bUniversité Claude Bernard Lyon 1, INSERM U1032, 151, cours Albert Thomas, 69424 Lyon, France
ababacar.seck@doctorant.ec-lyon.fr

When looking for technological improvements of the therapeutic effects of ultrasound cavitation, it is necessary to understand the critical processes of bubble inception and nucleation as well as bubble nonlinear dynamics and their effects on the onset of cavitation activity. Usually, such phenomena are studied in well-controlled cavitation conditions in which bubbles can be laser-nucleated, and are commonly considered in a static infinite fluid. Such approach does not take into account the interaction and possible coupling between cavitating bubbles and the surrounding moving fluid. Particularly, when looking at specific applications such as sonoporation, i.e. the weakening and poration of cell membrane by acoustic bubbles, the spatial control of these bubble-cells interaction could be highly influenced by the interaction between bubbles and the fluid flow in terms of perturbation of both the bubble cloud cavitation activity and the flow. In this study, an initially spatially-controlled bubble cloud is submitted to a preset flow rate and the impact of the flow on the cavitation activity and spatial distribution of the bubble cloud is characterized.

An annular piezoelectric transducer of 28 mm diameter driven at the frequency 550 kHz is used to generate an ultrasonic acoustic field. The acoustic field of the annular transducer is investigated experimentally at low acoustic level using optic-fiber hydrophones. The resulting radial pressure field takes the form of a Bessel mode as expected numerically. For higher acoustic level, a bubble cloud is generated, and optical measurements show that bubbles larger than the resonant bubble size aggregate into rings patterns that are located at the nodes of the acoustic pressure field. In order to study the influence of a low flow rate on a bubble cloud, the transducer is inserted between tubes with a mean flow velocity ranging from 0 to 12 mm/s. The extension of the bubble cloud is observed using a high speed camera. It is shown that increasing flow rate results in the narrowing of the bubble cloud extension.

To analyze the relative influence of flow on the spatial distribution of bubbles, the equilibrium location of bubbles submitted to both hydrodynamic and acoustic radiation forces are studied analytically and numerically resolved. Without flow, a good agreement with literature is observed: bubbles move towards pressure nodes or antinodes according to their sizes in comparison with the resonant size. With flow, equilibrium locations differ from their previous locations in static fluid condition. It is shown that the competition between hydrodynamic and acoustic forces could turn into selecting bubble location according to their sizes, i.e. a bubble sorter.

Tu. 15:00

Poster session

Flow Velocity Measurement with the Nonlinear Acoustic Wave ScatteringI. Didenkulov^a and N. Pronchatov-Rubtsov^b

^aInstitute of Applied Physics, 46 Ulyanov str., Nizhny Novgorod, 603950, Russia, 603950 Nizhny Novgorod, Russian Federation; ^bState University of Nizhny Novgorod, 23 Gagarin ave., 603950 Nizhny Novgorod, Russian Federation
diniap@mail.ru

A problem of noninvasive measurement of liquid flow velocity arises in many practical applications. To this end the most often approach is the use of the linear Doppler technique. The Doppler frequency shift of signal scattered from the inhomogeneities distributed in a liquid relatively to the emitted frequency is proportional to the sound frequency and velocities of inhomogeneities. In the case of very slow flow one needs to use very high frequency sound. This approach fails in media with strong sound attenuation because acoustic wave attenuation increases with frequency and there is limit in increasing sound intensity, i.e. the cavitation threshold. Another approach which is considered in this paper is based on the method using the difference frequency Doppler Effect for flows with bubbles. This method is based on simultaneous action of two high-frequency primary acoustic waves with closed frequencies on bubbles and registration of the scattered by bubbles acoustic field at the difference frequency. The use of this method is interesting since the scattered difference frequency wave has much lower attenuation in a liquid. The theoretical consideration of the method is given in the paper. The experimental examples confirming the theoretical equations, as well as the ability of the method to be applied in medical diagnostics and in technical applications on measurement of flow velocities in liquids with strong sound attenuation is described. It is shown that the Doppler spectrum form depends on bubble concentration velocity distribution in the primary acoustic beams crossing zone that allows one to measure the flow velocity distribution. The work is supported by the Russian Science Foundation (Grant 14-12-00882).

Tu. 15:00

Poster session

Experimental Nonlinearity in Soft Crystals

N. Vilchinska

LAA-Latvian acoustics association, 3,Kurzemes prospekts, LV1067 Riga, Latvia
vilcinska@hotmail.com

The only source of quartz sand is the broken quartz crystal. Recent field experiments and researches showed process of formation crystalline trace of completely water-saturated small quartz sand at seepage of water from the saturated massif. The crystal pattern is observed also at wash out the old dense sandy massif formed under water. Magic properties of a quartz crystal are known. It is now possible to broaden the sphere of their influence on the undisturbed pure beaches consisting of the quartz sand sediment under the influence of sea waves. . A number of experiments in massifs of the sea sand formed by sedimentation are carried out. Propagation velocity and spectra of a propagated ultrasonic impulse depending on basis and humidity in the presence of the strengthened filtration and without it is studied in-situ. Dynamic experiments in-situ show response spectra and wave propagation velocity depending from energy in source (shock, blast). Formation of soft crystals for laboratory research from sand is known. Tests on GDS (Geotechnical Digital System) show repeated dilatance by sample loading with constant velocity; the result shows that the dilatance changes the sign in moment achievements of some density which is called critical density. It is clear, that some properties of nonlinearity observed in works with sea quartz sand (soft crystals) will be similar in other granulated materials corresponding to classification soft crystals

Tu. 15:00

Poster session

Nonlinear Interaction of Air Bubbles and Ultrasonic Field: an Analysis of some Physical AspectsC. Vanhille^a and C. Campos-Pozuelo^b^aUniversidad Rey Juan Carlos, Tulipán s/n, 28933 Móstoles, Madrid, Spain; ^bConsejo Superior de Investigaciones Científicas, Serrano 144, 28006 Madrid, Spain

christian.vanhille@urjc.es

This paper deals with the propagation of finite-amplitude ultrasonic signals in bubbly liquids. A deeper understanding of the nonlinear interaction of ultrasonic waves and bubble oscillations is a theoretical challenge. Moreover, this knowledge may be useful for some industrial and medical applications for which this nonlinear interaction plays a fundamental role. Some physical aspects are addressed here via numerical simulations: multi-dimensional simulations, focused waves, Primary Bjerknes forces, frequency mixing, cavitation, diode, and switch. An experimental demonstration of inertial cavitation at high frequency is presented as well. This work is part of the research project DPI2012-34613 funded by the Ministry of Economy and Competitiveness of Spain.

Tu. 15:00

Poster session

Laser velocimetry for non-linear acoustics : an overview over two decades of research

J.-C. Valière and H. Bailliet

Institut Pprime, CNRS, Université de Poitiers, ENSMA, Bât B17, 6 rue Marcel Doré, 86073 Poitiers Cedex 9, France
jean.christophe.valiere@univ-poitiers.fr

Since two decades, progresses in Laser velocimetry technics have allowed the latter to become competitive for the investigation of complex acoustic fields [1]. These technics are of particular interest in situations where pressure measurements are not sufficient to entirely describe the acoustic fields, as is the case in nonlinear acoustics. The two main technics, the Laser Doppler Velocimetry (LDV) and the Particle Image Velocimetry (PIV), have been initially developed in the context of fluid mechanics. Their adaptation to acoustic particle velocity measurement has lead to several difficulties.

Firstly the dynamic of measurement is limited by the low magnitude of velocities and displacements in many acoustical applications. In a quiet medium, LDV lower limit is about 90 dB SPL at 1000 Hz in controlled conditions (pipes, cavities), i.e. an acoustic velocity of about 1 mm/s (equivalent free-field). PIV limit is 3 order of magnitude larger [1]. That is, in classical PIV, at 1000Hz, measurements cannot be performed for levels lower than 130 dB SPL (for a measurement window about $5 \times 5\text{cm}$).

Secondly, the frequency range validated for the use of these technics is small compared to the audible range. Indeed, the performances of LDV and PIV are linked to the particle displacement detection which is inversely proportional to the working frequency. It is why most of actual Laser velocimetry measurements performed to this date do not exceed 3000 Hz.

These are the reasons why the use of LDV and PIV for acoustics is appropriate for high levels/low frequencies situations often encountered in non linear acoustics such as measurements of flows induced around discontinuities as in musical acoustics [2] or thermoacoustic devices [3].

In this talk, performances of LDV and PIV will be presented with regards to acoustic velocities and displacements. Results available in the literature and expected improvements in performances will also be discussed.

In a second part, the benefit of these technics for a better understanding of certain nonlinear phenomena will be presented, especially the induced flows and vortices at discontinuities and acoustic streaming, based on a literature analysis. Through the previous exemples, the complementary of the two technics will be underscored: PIV permits a better global understanding and LDV allows a larger dynamic range, a larger frequency range and a better spatial precision.

References

- [1] J.-C. Valiere, Acoustic Particle Velocimetry using lasers, Principles, Signal Processing and Applications, Focus, Waves series, ISTE, John Wiley & Sons, 2014.
- [2] J. M. Buick, M. Atig, D. J. Skulina, D. M. Campbell, J.-P. Dalmont, J. Gilbert, Investigation of non-linear acoustic losses at the open end of a tube, *J. Acoust. Soc. Am.*, 129 (3), March 2011
- [3] X. Mao, Z. Yu, A. J. Jaworski, D. Marx, PIV studies of coherent structures generated at the end of a stack of parallel plates in a standing wave acoustic field, *Experiments in Fluids*, 45(5), pp. 833-846, 2008

Tu. 16:00 Amphi 1 bis

General nonlinear acoustics 3

Acoustic Streaming Jets: a Scaling and Dimensional Analysis.V. Botton^a, B. Moudjed^b, D. Henry^a, S. Millet^a, H. Ben Hadid^a and J.-P. Garandet^b^aLMFA, UMR CNRS 5509, Université de Lyon, ECL/INSA Lyon/U, 36 avenue guy de Collongue, 69134 Ecully, France; ^bLIEFT, CEA Saclay, DEN/DANS/DM2S/STMF/LIEFT, F-91191 Gif-Sur-Yvette, France
valery.botton@insa-lyon.fr

We present our work on acoustic streaming free jets driven by ultrasonic beams in liquids. These jets are steady flows generated far from walls by progressive acoustic waves. The approach combines an experimental characterization of both the acoustic pressure field (hydrophone) and the obtained acoustic streaming velocity field (PIV visualization) in water, with CFD using an incompressible Navier-Stokes solver on the other hand. It is shown that good comparisons between experimental and numerical results can be obtained with a theoretical model based on a linear acoustic propagation model accounting for diffraction coupled to a hydrodynamic model including inertia effects. The coupling is obtained by the introduction in the hydrodynamic model of the momentum source term formerly proposed by Lighthill and by Nyborg; this acoustic streaming force fac is such that $fac = 2\alpha Iac/c$, where α is the sound absorbing coefficient, Iac , the acoustic intensity and c , the sound celerity in the fluid. The shape of the flow is thus found to be directly affected by both the overall shape of the acoustic beam and the local variations in acoustic intensity. An order of magnitude analysis of the problem leads to three scaling laws for the streaming velocity level depending on the considered region along the jet. This analysis makes it possible to plot our data and former data by other teams in a consistent picture. A dimensional analysis is also performed and shows, when applied to liquid metals, that small acoustic powers can yield relatively high Reynolds numbers and velocity levels in melts like sodium or silicon; this could be a benefit for crystal growth applications but a drawback for ultrasonic velocimetry, frequently used in such opaque liquids.

Inertial effects on non linear acoustic streamingV. Daru^a, D. Baltean-Carlès^b and C. Weisman^b^aENSAM- DynFluid Lab., 151, boulevard de l'hôpital, 75013 Paris, France; ^bLIMSI - UPMC, Rue John Von Neumann, 91403 Orsay, France

virginie.daru@ensam.eu

Acoustic streaming is generated inside a cylindrical resonator filled with a compressible viscous fluid, as a consequence of the interaction between a plane standing wave and the solid boundaries. The streaming behavior in the nonlinear regime was previously analyzed in [Daru, Baltean-Carlès, Weisman, Debesse and Gandikota, *Wave Motion* 50 (2013)], [Reyt, Daru, Bailliet, Moreau, Valière, Baltean-Carlès and Weisman, *JASA* 134 (3) (2013)]. The object of this paper is to investigate numerically the sole effect of inertia on nonlinear streaming. In order to exclude thermal effects, the flow is considered to be isentropic, and the imposed standing wave is mono-frequency (with no harmonic content). Two codes are used to this effect: A code solving the full Navier-Stokes compressible equations provides the acoustic streaming generated by standing waves inside a cylindrical resonator filled with a compressible viscous fluid, with the assumption of isentropic flow. The standing wave is excited by imposing a sinusoidal vibration of all resonator walls along the main axis, at frequency corresponding to the lowest resonant acoustic mode of the waveguide. This code is used mainly to obtain the linear acoustic flow field established in the saturated regime (obtained for a small value of the nonlinear Reynolds number). A second code was developed to solve the time-averaged Navier-Stokes compressible equations, where the linear acoustic flow field is used as a source term. This code is used to evaluate the effect of increasing the amplitude of the linear acoustic flow field on the streaming flow. This numerical approach is used here to investigate nonlinear Reynolds number $Renl$ values ranging from 0.1 up to 60. As $Renl$ increases, the outer streaming cells (characteristic of the linear regime) are deformed with their center being displaced towards the maximum acoustic velocity amplitude locations (resonator center). Results agree with the asymptotic model of [L. Menguy and J. Gilbert, *Acustica, Acta Acustica* 86, 2000] for nonlinear Reynolds number $Renl$ values up to about 4. These results give rise to several questions: In previously reported experiments and numerical simulations [Reyt, Daru, Bailliet, Moreau, Valière, Baltean-Carlès, Weisman, *JASA* 134 (3) (2013)], the distortion of the outer streaming cells is different and yields the formation of new streaming cells for large $Renl$ values. In the experiments, the acoustic flow field seems to be linear (at least on the cylinder's axis), with no or very small harmonic content. Temperature variations are small therefore the isentropic flow model seems relevant. However, we show in the present study that the sole effect of inertia cannot be responsible for the behavior observed for large $Renl$ values.

Tu. 16:40 Amphi 1 bis

General nonlinear acoustics 3

Control of droplet temperature on disposable digital microfluidic system based on acoustic streaming

J. Kondoh and N. Ohashi

Shizuoka University, 3-5-1 Johoku, Naka-ku, 432-8561 Hamamatsu-Shi, Japan

kondoh.jun@shizuoka.ac.jp

Digital microfluidic system (DMFS) is proposed. The DMFS consists of sensor plate/water thin layer/piezoelectric substrate. An interdigital transducer (IDT) is fabricated on the piezoelectric substrate to generate a surface acoustic wave (SAW). The SAW radiates longitudinal waves. Thin water layer is a wave guide for the longitudinal wave. When the longitudinal wave reflects at the interface between the sensor plate and water layer, bulk acoustic wave (BAW) is generated into the sensor plate. On the sensor plate, droplets are manipulated and mixed by the BAW, and measured using a sensor, which is fabricated on the sensor plate. Also, the temperature of droplets are controlled. Mechanisms of droplet manipulation, uniform mixture, and temperature control is based on an acoustic streaming in liquid. We have been developing blood coagulation monitoring system using the DMFS. For the purpose, droplet temperature must be maintained at 37 deg. C. When a droplet is placed on a BAW propagating surface, longitudinal wave is also radiated into the droplet and an acoustic streaming is observed. As the longitudinal wave radiated attenuates in the droplet, the droplet temperature increases. The droplet temperature is strongly influenced an applied electrical signal. In other words, the temperature can be controlled by the electrical signal. In this study, power and duty ratio of the electrical signal applied to the IDT were varied. Droplet volume was fixed at 15 μ l. Linear relationships between temperature and power was obtained. Also, linear relationships between temperature and duty ratio was obtained. When the power and duty ratio were fixed at 1.5 W and 80 %, respectively, droplet temperature was maintained at 37 deg. C. Then an electrochemical sensor was fabricated on the sensor plate and monitored the blood coagulation reaction. As the droplet temperature was maintained at constant, reproducible results of impedance changed due to the coagulation reactions were obtained.

Tu. 17:00 Amphi 1 bis

General nonlinear acoustics 3

Tunable Optical Lens Array Using Viscoelastic Material and Acoustic Radiation ForceD. Koyama^a, Y. Kashihara^a, M. Hatanaka^a, K. Nakamura^b and M. Matsukawa^a^aDoshisha University, 1-3, Tataramiyakodani, Kyotanabe, 610-0321 Kyoto, Japan; ^bTokyo Institute of Technology, 4259-R2-26, Nagatsuta-cho, Midoriku, 226-8503 Yokohama, Japan

dkoyama@mail.doshisha.ac.jp

A tunable optical lens array that uses acoustic radiation force was investigated. The lens array consists of a transparent glass plate ($120 \times 4 \times 1$ mm³), a 300- μ m-thick viscoelastic transparent silicone gel, and two bimorph flexural transducers made from piezoelectric lead zirconate titanate ($30 \times 4 \times 1$ mm³). The configuration of the glass plate and the transducers was determined based on the finite element analysis results to obtain a large vibrational amplitude for the glass plate. When the two transducers were excited in phase at 113 kHz, the 5th flexural vibration mode was generated on the bimorph transducers, and a flexural vibration was generated along the glass plate in the length direction. Acoustic radiation force generated by the flexural vibration acts on the surface of the gel film and the gel surface can be statically deformed; the cylindrical convex lens array was fabricated on the gel surface. The average lens height under excitation by a peak-to-peak voltage of 70 V was 143 μ m. The lens pitch was approximately 9.3 mm, which corresponds to half the wavelength of the flexural vibration of the glass plate. Higher input voltages give greater lens heights, although the relationship between input voltage and lens height is not linear, because the acoustic radiation is a function of the square of the sound pressure amplitude.

The light paths through a lens were calculated by ray tracing. The focal length decreased with increasing input voltage because the lens displacement amplitude increased, and the focal point could be controlled by the input voltage. Larger standard deviations were obtained with smaller input voltages because the radius of curvature of the lens changed dramatically when the lens displacement amplitude was small. When the transducers were excited with a two-phase drive, the flexural vibration distribution could be changed using the driving phase difference between the two transducers. The position of the lens array shifted in the length direction with the change in phase difference, and the distance moved was 4.6 mm when the phase difference changed from 0 to 360°, which corresponds to half the wavelength of the flexural vibration of the glass plate. The lens positions could be controlled using the phase difference between two transducers.

The translation property of the lens array was applied in an optical scanner. If a light beam passes through the lens array in the thickness direction and the driving phase difference between the two transducers is varied, the light is then refracted at the lens surface, and the transmitted light can be swept because the angle of refraction varies with the phase difference. The refraction angle is correlated with the lens height and the maximum angle of refraction was 4.9° at the phase difference of 0°.

Tu. 17:20 Amphi 1 bis

General nonlinear acoustics 3

Pitch Glide Effect Induced by a Nonlinear String-Barrier InteractionD. Kartofelev^a, A. Stulov^a and V. Välimäki^b^aInstitute of Cybernetics at TUT, Akadeemia Rd. 21, 12618 Tallinn, Estonia; ^bAalto University, Otakaari 5A, 02150 Espoo, Finland
dima@ioc.ee

Interactions of a vibrating string with its supports and other spatially distributed barriers play a significant role in the physics of many stringed musical instruments. It is well known that the tone of the string vibrations is strictly determined by the string supports, and that the boundary conditions of the string termination may cause a short-lasting initial fundamental frequency gliding or shifting. Generally, this phenomenon is associated with the nonlinear modulation of the stiff string tension. The aim of this paper is to study the initial frequency glide phenomenon that is induced only by the string-barrier interaction, apart from other possible physical causes, and without the interfering effects of dissipation and dispersion. From a numerical simulation perspective, this highly nonlinear problem may present various difficulties, not the least of which is the risk of numerical instability. We propose a numerically stable and a purely kinematic model of the string-barrier interaction, which is based on the travelling wave solution of the ideal string vibration. This model is capable of reproducing the motion of the vibrating string exhibiting the initial fundamental frequency glide, which is caused solely by the complex nonlinear interaction of the string with its termination. The results presented in this paper can expand our knowledge and understanding of the timbre evolution and the physical principles of sound generation of numerous stringed instruments, such as lutes called the tambura, sitar, and biwa.

Implications of Superharmonic Ultrasound Contrast Agent Imaging

M. Verweij^a, D. Peruzzini^b, P. Tortoli^c, N. De Jong^b and H. Vos^b

^aAcoustical Wavefield Imaging, ImPhys, Delft U Technology, van der Waalsweg 8, 2628 CH Delft, Netherlands;

^bErasmus MC, 's-Gravendijkwal 230, Faculty Building, Ee 2302, 3015 CE Rotterdam, Netherlands; ^cMSD lab, Department of Information Engineering, Univ of Florence, Via S.Marta, 3, 50139 Firenze, Italy

h.vos@erasmusmc.nl

Ultrasound contrast agent (UCA) imaging that is based on the detection of the second harmonic suffers from the signal that is caused by nonlinear wave propagation in tissue. It has been reported that UCA imaging that is based on the third or higher harmonics, so-called superharmonic imaging [Bouakaz et al., *Ultrasound Med Biol.* 28(1)2002] or acoustic angiography [Lindsey et al., *IEEE TUFFC* 61(10)2014], show better contrast. However, using the superharmonics decreases contrast signal level. This study experimentally investigates the contrast-to-tissue ratio (CTR) and signal-to-noise ratio (SNR) of superharmonic UCA scattering in a tissue/vessel mimicking phantom with a custom dual-frequency cardiac phased array probe.

We used a dual-frequency phased array probe that was originally developed for cardiac tissue superharmonic imaging. It has interleaved low-frequency transmit elements ($N=44$, $f_c=1$ MHz) and high-frequency receive elements ($N=44$, $f_c = 3.5$ MHz). All elements were addressed individually through a custom-programmed commercial ultrasound machine (SonixTOUCH, Ultrasonix) in a sector scanning mode. Real-time images were produced during the measurements while beam formed RF data was stored for further offline processing. A tissue mimicking phantom with a UCA-filled cavity of 1 cm diameter was designed to produce realistic tissue and contrast scattering. BR14 (Bracco, Geneva) contrast agent was diluted in a 1:2000 ratio to mimic clinical concentration. The pressure level in the cavity of the phantom was 110 kPa ($MI = 0.11$) ensuring non-destructivity of UCA. Based on single frames captured with the high-frequency elements, the RF data were temporally filtered around the second, third and fourth harmonic, respectively, with 1-MHz wide band pass filters. To quantify the signal level, RMS levels from UCA and tissue areas are obtained from the data. To quantify the noise, RMS levels were obtained from acquired data with disabled transmission.

The UCA-filled cavity could be clearly observed in the images, while tissue signals were around or below the noise floor, even after averaging of 140 consecutive frames. Because of this, only an estimation of lower CTR bounds could be obtained for the third and fourth harmonics. The CTR values were 36 dB, >38 dB, and >32 dB, for second, third, and fourth harmonic respectively. These values are similar to those reported earlier for preliminary contrast superharmonic imaging that involve in-vitro and in-vivo measurements [Bouakaz et al., 2002]. The values show the improved CTR achieved by superharmonic imaging compared to second harmonic imaging. The single frame SNR values (in which 'signal' denotes the signal level from the UCA area) are 23 dB, 18 dB, and 11 dB, respectively. This indicates that noise, and not the tissue signal, is the limiting factor for the UCA detection when using the superharmonics in non-destructive mode. This finding is contrary to second harmonic UCA imaging in practice. As implication, increasing the SNR should be the main focus for optimising superharmonic ultrasound contrast imaging, similar to the work recently activated by Harput et al. for tissue superharmonic imaging [*IEEE tUFFC* 61(11)2014].

Cumulative Phase Delay Imaging - a new contrast enhanced ultrasound modality

L. Demi, R.J.G. Van Sloun, H. Wijkstra and M. Mischi

Eindhoven University of Technology, Den Dolech 2, 5612 AZ Eindhoven, Netherlands

l.demi@tue.nl

Recently, a new acoustic marker for ultrasound contrast agents (UCAs) has been introduced [1]. A cumulative phase delay (D) between the second harmonic and fundamental pressure wave field components is in fact observable for ultrasound propagating through UCAs. This phenomenon is absent in the case of tissue nonlinearity and is dependent on insonating pressure and frequency, UCA concentration, and propagation path length through UCAs. In this paper, ultrasound images based on this marker are presented.

The ULA-OP research platform [2], in combination with a LA332 linear array probe (Esaote, Firenze Italy), has been used to image a gelatin phantom containing a PVC plate (used as a reflector) and a cylindrical cavity measuring 7 mm in diameter (placed in between the observation point and the PVC plate).

The cavity contained a 240 $\mu\text{L/L}$ SonoVue® UCA concentration. Two insonating frequencies (3 MHz and 2.5 MHz) have been used to scan the gelatine phantom. A mechanical index $MI = 0.07$, measured in water at the cavity location with a HGL-0400 hydrophone (Onda, Sunnyvale, CA) was utilized.

The echoes obtained from the PVC plate were processed as described in [1] in order to obtain, for each line imaged, a measure of the cumulative phase delay $D=2\pi \Delta t f_0$, with Δt being the time delay between the second harmonic and the fundamental component and f_0 the transmitted frequency, respectively.

The axis of the cylindrical cavity was positioned at $(z,x)=(80 \text{ mm}, 0 \text{ mm})$, with z and x being the axial and lateral direction, respectively, and with the center of the linear array aperture coinciding with the center of the coordinate system.

Exploiting the employed linear array, D can thus be measured as a function of space in the lateral direction. For this particular in-vitro configuration, we can exploit the symmetry of the target and assume consecutive frames as if acquired from different observation angles. Consequently, a sinogram can be constructed, and an ultrasound image generated in a tomographic fashion using the filtered back-projection method [3].

As already observed in [1], significantly higher values of D are measured when imaging at a frequency of 2.5 MHz, as compared to imaging at 3 MHz. In conclusion, although a simple set-up was adopted, where the symmetry of the imaged target facilitated the image formation, these results confirm the applicability of the presented cumulative delay as an UCA marker for imaging. Comparison with standard contrast-enhanced ultrasound imaging modalities, together with the application of this imaging modality to flowing rather than static UCAs, will be the focus of future work.

[1] L. Demi, H. Wijkstra, and M. Mischi "Cumulative phase delay between second harmonic and fundamental components - A marker for ultrasound contrast agents", *JASA*, 136, pp. 2968-2975, 2014.

[2] E. Boni, L. Bassi, A. Dallai, F. Guidi, A. Ramalli, S. Ricci, R. Housden, and P. Tortoli, "A Reconfigurable and Programmable FPGA based System for non-standard Ultrasound Methods", *IEEE Transactions on Ultrasonics Ferroelectrics and Frequency Control*, 59, pp. 1378-1385, 2012.

[3] Paul Suetens. *Fundamentals of medical imaging*. Cambridge University Press, 2009.

Tu. 16:40 Amphi 2

Imaging and tissue characterization 1

Experimental Study of Transmission of a Pulsed Focused Beam through a Skull Phantom in Nonlinear RegimeS. Tsysar^a, A. Nikolaeva^a, V. Svet^b, V. Khokhlova^c, P. Yuldashev^c and O. Sapozhnikov^{c,d}

^aPhysics Faculty, Moscow State University, Leninskie gory, 119991 Moscow, Russian Federation; ^bAndreyev Acoustics Institute, 4, Shvernik Street, 117036 Moscow, Russian Federation; ^cPhysics Faculty, Moscow State University, Leninskie Gory, 119991 Moscow, Russian Federation; ^dCenter for Industrial and Medical Ultrasound, Applied Physics Laboratory, University of Washington, 1013 NE 40th Street, Seattle, WA 98105, USA
sergey@acs366.phys.msu.ru

The problem of ultrasound imaging of brain structures is complicated by the presence of a strongly inhomogeneous absorbing skull, which causes severe refraction and absorption artifacts. Recent advances in noninvasive transcranial focused ultrasound surgery are based on innovative solutions for acoustic aberration corrections using adaptive focusing of multi-element arrays in combination with computed tomography or magnetic resonance imaging. Contrary to focused ultrasound surgery, transcranial ultrasound imaging is still poorly developed despite the need to overcome the existing difficulties. In this paper, a pulse-echo imaging system is proposed, in which acoustic parameters of the skull are determined and corresponding aberration corrections are introduced based on measuring reflection of short high-frequency pulses; the imaging is then performed using lower frequency pulses. As the first step in this direction, an approach was suggested in which a single-element focused transducer was used to generate pulses that were nonlinearly distorted at the focus and thus contained both a signal of original frequency and its higher harmonics. The use of harmonic echoes allowed characterization of the skull bone with higher accuracy in comparison with processing the linear signal. In experiment, a focused piezoelectric transducer with 100 mm diameter, 100 mm focal distance, and 1 MHz central frequency was used. The transducer was positioned in front of the skull phantom at the distance of 100 mm, so that the focus of the beam was located at the front surface of the phantom. The transducer emitted short tone bursts containing 5-10 cycles of the fundamental frequency. The transducer voltage was adjusted to achieve nonlinear regime of propagation, so that several harmonics (up to 5) were present at the focus. The same transducer, which was sensitive to the odd harmonics, detected acoustic signals reflected from the phantom. To synthesize a 2D imaging array, the transducer was translated point-to-point along the skull phantom using a computer-controlled positioning system (VelmexUniSlide VP9000), so that the focus was always at the phantom surface. Using the reflected signal, the thickness of the phantom at each location was measured. It was shown that high-frequency components (3rd and 5th harmonics) of the signal provided higher accuracy in characterizing acoustic parameters of the phantom layer as compared to the fundamental frequency. In order to test the ability of the pulse-echo imaging, a strong scatterer (a Styrofoam sphere) was placed behind the skull phantom. Visualization of that target was based on the registration of the back-scattered pulse at the fundamental frequency that passed through the skull phantom, reflected from the target, passed through the skull phantom again, and propagated backward to the transducer. Amplitude and phase corrections obtained in characterization measurements were introduced in further processing of the signal. The quality of imaging was tested for the skull phantoms with various degrees of inhomogeneity and absorption. This work was supported by RSF 14-15-00665.

Tu. 17:00 Amphi 2

Imaging and tissue characterization 1

Simulation of nonlinear propagation of biomedical ultrasound using PZFlex and the KZK Texas code

S. Qiao, E. Jackson and R. Cleveland

Institute of Biomedical Engineering, Dep. of Engineering Science, University of Oxford, Old Road Campus Research Building, Headington, ox3 7dq Oxford, UK

shan.qiao@eng.ox.ac.uk

In biomedical ultrasound nonlinear acoustics can be important in both diagnostic and therapeutic applications and robust simulation tools are needed in the design process but also for day-to-day use such as treatment planning. For most biomedical applications the ultrasound sources generate focused sound beams of finite amplitude. The KZK equation is a common model as it accounts for nonlinearity, absorption and paraxial diffraction and there are a number of solvers available, primarily developed by research groups. We compare the predictions of the KZK Texas code (a finite-difference time-domain algorithm) to a FEM-based commercial software, PZFlex. PZFlex solves the continuity equation and momentum conservation equation with a correction for nonlinearity in the equation of state incorporated using an incrementally linear, 2nd order accurate, explicit algorithm in time domain. Nonlinear ultrasound beams from two transducers driven at 1 MHz and 3.3 MHz respectively were simulated by both the KZK Texas code and PZFlex, and the pressure field was also measured by a fibre-optic hydrophone. Further simulations (but no experiments) were carried out between these two frequencies. The comparisons showed good agreement for the fundamental frequency for PZFlex, the KZK Texas code and the experiments. For the harmonic components, the KZK Texas code was in good agreement with measurements but PZFlex underestimated the amplitude: 32% for the 2nd harmonic and 66% for the 3rd harmonic. The underestimation of harmonics by PZFlex was more significant when the fundamental frequency increased. Furthermore non-physical oscillations in the axial profile of harmonics occurred in the PZFlex results when the amplitudes were relatively low. These results suggest that careful benchmarking of nonlinear simulations is important.

Tu. 17:20 Amphi 2

Imaging and tissue characterization 1

Ultrasound Tissue Characterization: Comparison of Statistical Results using Fundamental and Harmonic Signals

F. Lin, A. Cristea, C. Cachard and O. Basset

CREATIS, 7, avenue Jean Capelle, 69100 Villeurbanne, France

anca.cristea@creatis.insa-lyon.fr

Quantitative ultrasound (QUS) imaging has been studied for decades to characterize biological tissue. The spectrum of backscattered RF signals or statistical results from signal envelopes can be used to obtain the QUS estimates. In the latter case, the distribution parameters of the signal envelope are estimated to distinguish tissue with different characteristics. Previous studies are mainly based on the whole backscattered signals analysis. However, the ultrasound propagation is a nonlinear process and the harmonic signals can therefore reveal the nonlinear nature of a biological medium. The present study investigates the statistical results of ultrasound harmonic signal envelopes and compares with the results from fundamental signal envelopes. The CREANUIS simulator was used to simulate ultrasound images. The transmitted frequency was 10MHz. Eight cell concentrations ranging from 2 to 30 scatterers per resolution cell and two different nonlinear coefficients β , 3.5 and 50 respectively, in the region of interest (ROI) were considered. For each concentration and each nonlinear coefficient, 50 images with randomly distributed scatterers were simulated. The Nakagami statistical model was adopted to analyze the backscattered fundamental and second-harmonic signal envelopes of each simulated image, because this model is mathematically simple and parameter estimation is robust and straightforward. The Nakagami model is defined by two parameters: μ is related to the scatterer density and ω is a measurement of the scattered energy. These parameters were estimated using a maximum-likelihood estimator. The Nakagami parameters versus scatterers concentration were drawn. The estimation results show that distributions exhibit a different behavior for fundamental and harmonic signals. For fundamental envelopes, curves corresponding to the two β are superposed. The Nakagami parameter μ increased from 0.57 to 0.75 with increasing concentration from 2 to 14 scatterers per resolution cell, and saturated around 0.75 for concentrations greater than 14. For second-harmonic envelopes, curves corresponding to the two β are separated. For the lower nonlinear coefficient ($\beta = 3.5$), μ increased from 0.6 to 0.72 with increasing concentration from 2 to 14 scatterers per resolution cell, and saturated around 0.72 for concentrations greater than 14. For the higher nonlinear coefficient ($\beta = 50$), μ increased from 0.4 to 0.46 with increasing concentration from 2 to 14 scatterers per resolution cell, and saturated around 0.46 for concentrations greater than 14. In conclusion, although the energy available in the second harmonic band is largely lower than in the fundamental, the statistical results using second-harmonic signal envelopes can provide tissue characterization capabilities from Nakagami parameters, similarly to the one obtained with the fundamental. In addition, it is shown that the parameters, known to be related to scatterer's behavior, are also related to the non-linear property of the investigated medium.

Tu. 16:00 Amphi 3

Computational methods in Nonlinear Acoustics 2

The development of a hybrid finite difference solution of the Westervelt equation using the Fast Nearfield Method as a boundary condition for focused sources

K. Bader and C. Holland

University of Cincinnati, 231 Albert Sabin Way, Cincinnati, OH 45267-0586, USA

kenneth.bader@uc.edu

Theoretical models of therapeutic ultrasound expand the understanding of the mechanisms of treatment, and expedite the development of regulatory standards. For focused ultrasound therapies that rely on thermal mechanisms to generate lesions, only modeling of the incident sound field needs is sufficient. Modeling of microbubble clouds formed through shock scattering for histotripsy requires computation of both the incident and scattered fields. The objective of this study was to utilize a finite-difference time-domain (FDTD) method to compute both fields. A fine computation grid is required to resolve the shocked field at the focus. In the nearfield, where nonlinearity is negligible, a fine resolution computation is unnecessary and adds significant computational time. A hybrid method model was developed that employs an analytic solution to compute the nearfield, and the FDTD method to compute the field at the focus. The Fast Nearfield Method (FNM) was used to compute the nearfield solution using Gaussian quadrature integration. A FDTD method was used to solve the Westervelt equation at the focus, using the FNM solution as the source boundary condition. Computed fields agree with previously reported 2-MHz insonations with peak pressures of 35-63 MPa when the FNM method calculation is set to half the focal distance. Thus, this hybrid technique allows reliable calculation of the focal pressure while reducing the FDTD computational domain by a factor of two. Implications of the model will be discussed, and the extension of the model to scattering of histotripsy pulses from spherical microbubbles will be presented.

Tu. 16:20 Amphi 3

Computational methods in Nonlinear Acoustics 2

A boundary condition to the Khokhlov-Zabolotskaya equation for modeling strongly focused nonlinear ultrasound fields

P. Rosnitskiy, P. Yuldashev and V. Khokhlova

Physics Faculty, Moscow State University, Leninskie Gory, 119991 Moscow, Russian Federation

pavrosni@yandex.ru

Nonlinear parabolic Khokhlov-Zabolotskaya (KZ) equation is a common model used for numerical modeling of high intensity focused fields generated by medical ultrasound transducers. Simulations in water, where calibration of field parameters of such transducers is usually performed, have become an important metrological tool. The equation itself includes parabolic approximation of the diffraction effects, which is valid for small angles of the beam focusing. In addition, the boundary condition to the KZ model is set in the initial plane whereas most therapeutic sources typically have the shape of a spherical shell. The model therefore can be applied with reasonable accuracy for modeling weakly focused fields of ultrasound imaging transducers, but there has been always a concern whether it can be used for strongly focused fields of the HIFU devices. Certain modifications to the equation have been proposed including its modification for spheroidal coordinates to account for the converging angle of the beam or a wide-angle parabolic approximation of the diffraction effects. Much less attention has been paid to the problem of an appropriate transfer of the boundary condition from the spherical surface of a real source to the plane for the KZ modeling. Up to date, in most numerical studies for single element focused transducers the boundary condition was set in a plane crossing the transducer center as a piston source with the aperture and the uniform pressure amplitude being the same as for the real transducer, and the parabolic phase distribution that follows its focusing angle. For strongly focused beams, this direct approach results in significant underestimation of the focal pressure values and distortion of the spatial beam structure even in the focal region of the beam comparing to the field measurements of a real source. However several recent studies have shown that the boundary condition in the form of an "equivalent piston source" with some larger aperture and amplitude can be set for the KZ model, so that the results of simulations match the field measurements in the focal lobe with high accuracy even for transducers with F -number=1, both for linear and nonlinear focusing conditions. In this work it is proposed that additional reposition of the plane, at which the "equivalent source" boundary condition is set, can further improve the agreement between the results of the full diffraction and the parabolic modeling. The aperture and the distance between the focus and the source center in the parabolic model were chosen based on the best match of the axial pressure amplitude and phase distributions of the Rayleigh integral solution (spherical transducer) and the linear parabolic approximation solution (equivalent source). It was shown that less than 0.5% difference between the axial solutions of these two models is achieved in at least several diffraction lobes around the focus by choosing the equivalent source aperture up to 10% larger and the distance from the source center to the focus up to 6% larger than the corresponding parameters of the spherical transducer. Work supported by Russian Science Foundation grant #14-12-00974.

Tu. 16:40 Amphi 3

Computational methods in Nonlinear Acoustics 2

Acoustic characterization of high intensity focused ultrasound fields generated from a transmitter with a large aperture

D. Zhang and T. Fan

Institute of Acoustics, Nanjing Univ, Institute of Acoustics, Nanjing Univ, 210093 Nanjing, China

dzhang@nju.edu.cn

Prediction and measurement of the acoustic field emitted from a high intensity focused ultrasound (HIFU) is essential for the accurate ultrasonic treatment. In this study, the acoustic field generated from a strongly focused HIFU transmitter was characterized by a combined experiment and simulation method. The spheroidal beam equation (SBE) was utilized to describe the nonlinear sound propagation. The curve of the source pressure amplitude versus voltage excitation was determined by fitting the measured ratio of the second harmonic to the fundamental component of the focal waveform to the simulation result; finally the acoustic pressure field generated by the strongly focused HIFU transmitter was predicted by using the SBE model. A commercial fiber optic probe hydrophone (FOPH) was utilized to measure the acoustic pressure field generated from a 1.1 MHz HIFU transmitter with a large half aperture angle of 30°. The maximum measured peak-to-peak pressure was up to 72 MPa. The validity of this combined approach was confirmed by the comparison between the measured results and the calculated ones. The results indicate that the current approach might be useful to describe the HIFU field. The results also suggest that this method is not valid for low excitations owing to low sensitivity of the second harmonic.

Tu. 17:00 Amphi 3

Computational methods in Nonlinear Acoustics 2

Experimental Validation of Computational Models for Large-scale Nonlinear Ultrasound Simulations in Heterogeneous, Absorbing Fluid MediaE. Martin^a, J. Jaros^b and B. Treeby^a^aUniversity College London, Wolfson House, 2-10 Stephenson Way, NW1 2HE London, UK; ^bFaculty of Information Technology, Brno University of Technology, DCSY FIT BUT, Božetěchova 2, 612 66 Brno, Czech Republic
elly.martin@ucl.ac.uk

In high intensity focused ultrasound (HIFU) treatments, a thermal dose is delivered to a target region to induce cell death. In order to deliver the required dose to the target volume effectively, particularly where there are different tissues such as bones located in the field, it is necessary to know how the sound propagates in the tissues of the body and where the focus of the acoustic field will be located. Aberrations of the acoustic field caused by the interaction of the sound with tissues of different acoustic properties in the body render simple propagation models ineffective for predicting the location of high intensity regions of the field. More complex numerical simulations that can predict ultrasound propagation in heterogeneous biologically relevant media are an essential requirement for planning of these treatments. The models used for this purpose must be validated to ensure the underlying assumptions are correct and to identify sources of uncertainty when the models are applied to individual patients. Due to the computational complexity of full wave simulations, many previous models used for this purpose have only accounted for the forward going wave, for a mono frequency field, or for a homogeneous medium. This work presents an experimental validation of the nonlinear model in the open source k-Wave MATLAB toolbox. This solves a generalised form of the Westervelt equation accounting for non-linearity, heterogeneities and power law absorption using a k-space pseudospectral method. A single element 1.1 MHz focused bowl transducer was used to generate the acoustic field. The heterogeneous propagation medium consisted of oil and air filled prisms and cylinders placed in a bath of degassed, deionised water. The sound speed and acoustic attenuation coefficient as a function of frequency for each fluid was measured using a through transmission substitution method. The acoustic pressure from the transducer over a pre-focal plane was measured under free field conditions in degassed, deionised water using a 0.1 mm PVDF needle hydrophone. The experimental configuration and material properties were used as inputs to k-Wave and a full 3D simulation with a domain size of 2048 x 2048 x 3072 grid points was run on a HPC cluster, modelling up to 20 harmonics with the measured source data as a Dirichlet boundary condition. Validation measurements were made on a plane beyond the heterogeneous medium. Line and point measurements of acoustic pressure were made between the objects, where possible, for further validation. There was good agreement between the simulated and measured time domain data at the plane positioned beyond the heterogeneous medium. The timing and magnitude of reflected waves at other measurement points agreed closely with simulations. The use of the k-Wave MATLAB toolbox has been validated for the non-linear, heterogeneous, absorbing fluid case. This is an essential step for these models to be incorporated into the planning and delivery of clinical HIFU treatments with increased accuracy and effectiveness.

Tu. 17:20 Amphi 3

Computational methods in Nonlinear Acoustics 2

A robust time-base transformation scheme for computing waveform deformation during nonlinear propagation of ultrasound

B. De Graaf, S.B. Raghunathan and M.D. Verweij

Delft University of Technology, Department Imaging Physics, Section Acoustical Wavefield Imaging, Lorentzweg 1, 2628CJ Delft, Netherlands

m.d.verweij@tudelft.nl

Nonlinear propagation plays an increasingly important role in many medical applications of ultrasound. In diagnostics, for example, the reflections from several higher harmonics in mildly nonlinear ultrasound waves have recently been used to improve the resolution and reduce the artifacts of echo images. For therapeutic purposes, current investigations involve the use of intense nonlinear ultrasound fields for heating up, ablating or emulsifying malignant tumor tissue, or vaporizing drug-loaded nano-droplets.

Simulation of nonlinear ultrasound waves may help in predicting the performance of novel procedures and devices and explaining experimental observations. Over the years, many nonlinear simulation methods have been developed. A large number of these methods are based on the forward stepping approach. This implies that the wave field in the transducer plane is marched out into space over a number of successive parallel planes. A mayor benefit of this approach is that the simulations are relatively fast because the distances between the computational planes may be large as compared to the wavelength of the fundamental, while the numerical errors remain low. A drawback of the forward stepping approach is that it is unsuitable for strongly inhomogeneous media because it excludes waves that propagate opposite to the stepping direction. Although the details may vary, the spatial steps are usually split into sub-steps that separately account for the diffraction, attenuation, and nonlinear deformation of the wave.

In virtually all methods that employ this split-step approach, including various solvers for the KZK-equation, the nonlinear sub-step is based on the implicit solution of the one-dimensional Burgers equation. This involves a pressure-dependent deformation of the time axis, followed by an interpolation procedure to get back at the original time grid. The traditional implementation of the deformation-interpolation procedure works well until reaching the shock wave regime. In that situation, the deformation of the time axis may result in the 'crossing over' of time points, which leads to a loss of causality and erroneous interpolations. For the given implementation the problem can only be avoided by decreasing the stepping distance, at the cost of an increase of computation time.

In this paper we first investigate the cause of the emerging difficulties. It turns out that the traditional time axis deformation shifts the time points corresponding to positive pressures backward in time. On a steep, positive slope of the wave, the shifted version of later time points may therefore appear before those of earlier time points. Next, we propose an alternative implementation of the deformation-interpolation procedure, in which the time points for increasingly high pressures are shifted forward in time. With this implementation, time points on a positive slope of the wave can no longer cross during the axis deformation. Finally, we will present numerical results that demonstrate that the spatial stepping distance can be chosen an order of magnitude larger as before, without causing a breakdown of the numerical procedure.

Tu. 17:40 Amphi 3

Computational methods in Nonlinear Acoustics 2

Efficient, Adaptive Mesh Distributions for Spectral Methods Applied to Nonlinear Acoustics

E. Wise, B. Cox and B. Treeby

University College London, Wolfson House, 2-10 Stephenson Way, NW1 2HE London, UK

elliott.wise.14@ucl.ac.uk

Large-scale nonlinear acoustics simulations play an important role in researching high intensity focussed ultrasound therapy, a technique which is used to destroy diseased biological tissue. Unfortunately, full-wave simulations can be very memory intensive, with terabytes of data needed to store acoustic fields and material properties. This is due to a combination of large simulation domains and short acoustic wavelengths (which require dense grids to accurately resolve). Computational tractability can be significantly improved by using an adaptive, nonuniform distribution of simulation nodes. For instance, it may be beneficial to cluster nodes around a travelling pulse, or across shock fronts and tissue boundaries. The goal of this clustering is to ensure that the numerical approximation to a wave equation's solution converges to the true solution as quickly as possible as more simulation nodes are added.

Adaptive moving meshes have a long history of use in finite difference methods. They use an error estimate, or monitor function, to determine the distribution of simulation nodes. Traditionally, they place nodes where the solution's gradient or curvature is high. This is because error bounds for finite difference methods exist that relate to the degree of interpolating polynomial, which is often low. For fixed nodes and smooth problems, spectral methods are known to generally require sparser meshes than finite difference methods. Recently, spectral moving mesh methods have been developed to extend this advantage to less smooth problems.

So far, spectral moving mesh methods have also used monitor functions based on solution gradients, however, this approach appears ad hoc. For spectral methods, error bounds (and convergence rates) for a function can be found by examining the region of analyticity of the function's continuation into the complex plane. Fast rates of convergence occur when the continued function has singularities far from the computational interval and slow rates of convergence occur when they're nearby. Tee, Hale and Trefethen have introduced an adaptive spectral method which aims to improve the convergence rate by mapping the approximated function such that it has a wider region of analyticity [SIAM J. Sci. Comput., 28(5), pp. 1798–1811, 2006; SIAM J. Sci. Comput., 31(4), pp. 3195–3215, 2009]. Their method has been applied to many models, however, this does not include any full-wave acoustics equation. Additionally, no explicit comparison has been made between their method and a spectral moving mesh method.

In this work, we compare a spectral moving mesh method with Tee, Hale and Trefethen's method by solving the one dimensional Westervelt and Burgers' equations. We find that Tee, Hale and Trefethen's method is much more effective, with basis function coefficients decaying at rates which are orders of magnitude faster than those found using the spectral moving mesh method. As coefficient decay rates correspond directly with convergence rates, this means their method requires far fewer nodes for a given level of accuracy. This method thus has the potential to reduce computational memory requirements drastically, increasing the accessibility of large-scale, nonlinear ultrasound simulations for research and clinical practice.

3D Numerical Simulation of the Long Range Propagation of Acoustical Shock Waves Through a Heterogeneous and Moving Medium.D. Luquet^a, F. Coulouvrat^b and R. Marchiano^c^aUniversité Pierre et Marie Curie, d'Alembert, boîte 162, 4 place Jussieu, 75005 Paris, France; ^bCNRS - Institut Jean Le Rond d'Alembert (UMR 7190), Université Pierre et Marie Curie, 4 place Jussieu, 75005 Paris, France; ^cInstitut Jean le Rond d'Alembert, 4, Place Jussieu, 75252 Paris Cedex 05, France

luquet@dalembert.upmc.fr

Many situations involve the propagation of acoustical shock waves through flows. Natural sources such as lightning, volcano explosions, or meteoroid atmospheric entries, emit loud, low frequency, and impulsive sound that is influenced by atmospheric wind and turbulence. The sonic boom produced by a supersonic aircraft and explosion noises are examples of intense anthropogenic sources in the atmosphere. The Buzz-Saw-Noise produced by turbo-engine fan blades rotating at supersonic speed also propagates in a fast flow within the engine nacelle. Simulating these situations is challenging, given the 3D nature of the problem, the long range propagation distances relative to the central wavelength, the strongly nonlinear behavior of shocks associated to a wide-band spectrum, and finally the key role of the flow motion. With this in view, the so-called FLHOWARD (acronym for FLOW and Heterogeneous One-Way Approximation for Resolution of Diffraction) method is presented with three-dimensional applications. A scalar nonlinear wave equation is established in the framework of atmospheric applications, assuming weak heterogeneities and a slow wind. It takes into account diffraction, absorption and relaxation properties of the atmosphere, quadratic nonlinearities including weak shock waves, heterogeneities of the medium in sound speed and density, and presence of a flow (assuming a mean stratified wind and 3D "turbulent" flow fluctuations of smaller amplitude). This equation is solved in the framework of the one-way method. A split-step technique allows the splitting of the non-linear wave equation into simpler equations, each corresponding to a physical effect. Each sub-equation is solved using an analytical method if possible, and finite-differences otherwise. Nonlinear effects are solved in the time domain, and others in the frequency domain. Homogeneous diffraction is handled by means of the angular spectrum method. Ground is assumed perfectly flat and rigid. Due to the 3D aspect, the code was massively parallelized using the single program, multiple data paradigm with the Message Passing Interfaces (MPI) for distributed memory architectures. This allows us to handle problems in the order of a thousand billion mesh points in the four dimensions (3 dimensions of space plus time). The validity of the method has been thoroughly evaluated on many cases with known solutions: linear piston, scattering of plane wave by a heterogeneous sphere, propagation in a waveguide with a shear flow, scattering by a finite amplitude vortex and nonlinear propagation in a thermoviscous medium. This validation process allows for a detailed assessment of the advantages and limitations of the method. Finally, applications to atmospheric propagation of shock waves will be presented. [Work performed within the European Union ATLLAS II Project - Grant 263913 ; D. Luquet benefits from a PhD grant co-funded by Direction Générale de l'Armement - France].

Modeling of strongly-nonlinear wave propagation using the extended Rankine-Hugoniot shock relationsJ.-W. Lee^a, W.-S. Ohm^a and W. Shim^b^aYonsei University, 50, Yonsei-ro, Seodaemun-gu, 120-749 Seoul, Republic of Korea; ^bAgency for Defense Development, 111, Sunam-dong, Yuseong-gu, 305-152 Daejeon, Republic of Korea
fantalex@yonsei.ac.kr

This paper presents a computational scheme solely based on the Rankine-Hugoniot shock relations to describe the propagation of strongly-nonlinear waves in fluids, the amplitude of which is so great that second-order approximations such as the weak shock theory and the Burgers equation do not apply. The Rankine-Hugoniot relations are three algebraic equations connecting the flow variables (pressure, density, and particle velocity) across a shock. What is not well known is that the Rankine-Hugoniot relations can be used to compute the nonlinear evolution of the continuous segment of a wave, if the continuous segment can be approximated by a succession of infinitesimal compression shocks [Ya. B. Zel'dovich and Yu. P. Raizer, *Physics of shock waves and high-temperature hydrodynamic phenomena* (Dover, New York, 2002), pp. 85-86]. We further extend this idea to the other continuous segment that can be discretized into a series of infinitesimal rarefaction shocks. Although rarefaction shocks in fluids are unstable, the unshocking of rarefaction shocks takes place over the time scale much greater than the shock rise time. Therefore the basic assumption (i.e., steady flow) of the Rankine-Hugoniot relations remains valid. The discretization of a waveform and the subsequent application of the Rankine-Hugoniot relations provide a unified computational approach that conveniently treats continuous segments and shocks in the same manner. The scheme is verified against the full Euler-equation solver for the case of strong blast waves.

Time-domain simulation of constitutive relations for nonlinear acoustics including relaxation for frequency power law attenuation media modellingN. Jimenez^a, F. Camarena^a, V. Sanchez-Morcillo^a, J. Redondo^a and E.E. Konofagou^b^aUniversitat Politècnica de València, C/Paraninf 1, 46730 Grao De Gandía, Spain; ^bColumbia University, 351 Engineering Terrace, mail code 8904, 1210 Amsterdam Avenue,, New York City, 10027, USA

nojigon@upv.es

We report a numerical method for solving the constitutive relations of nonlinear acoustics, where multiple relaxation processes are included in a generalized formulation that allows the time-domain numerical solution by an explicit finite differences scheme. Thus, the proposed physical model overcomes the limitations of the one-way Khokhlov-Zabolotskaya-Kuznetsov (KZK) type models and, due to the Lagrangian density is implicitly included in the calculation, the proposed method also overcomes the limitations of Westervelt equation in complex configurations for medical ultrasound. In order to model frequency power law attenuation and dispersion, such as observed in biological media, the relaxation parameters are fitted to both exact frequency power law attenuation/dispersion media and also empirically measured attenuation of a variety of tissues that does not fit an exact power law. Finally, a computational technique based on artificial relaxation is included to correct the non-negligible numerical dispersion of the finite difference scheme, and, on the other hand, improve stability through artificial attenuation when shock waves are present. This technique avoids the use of high-order finite-differences schemes leading to fast calculations. The present algorithm is especially suited for practical configuration where spatial discontinuities are present in the domain (e.g. axisymmetric domains or zero normal velocity boundary conditions in general). The accuracy of the method is discussed by comparing the proposed simulation solutions to one dimensional analytical and k-space numerical solutions.

Nonlinear Propagation and Decay of Intense Regular and Random Waves in Relaxing MediaS. Gurbatov^a, O. Rudenko^b and I. Demin^a^aLobachevsky State University of Nizhni Novgorod, Gagarin Aven 23, 603950 Nizhni Novgorod, Russian Federation;^bLomonosov Moscow State University, Leninskie Gory, 119991 Moscow, Russian Federation

gurb@rf.unn.ru

The evolution of nonlinear regular and random waves (high-intensity noise) in dissipative and dispersive media is studied. To describe wave processes, the mathematical model in the form of a nonlinear integrodifferential equation is used. An integrodifferential equation contains terms responsible for nonlinear absorption, visco-heat-conducting dissipation, and relaxation processes in a medium. A general integral expression is obtained for calculating energy losses of the wave with arbitrary characteristics-intensity, profile (frequency spectrum), and kernel describing the internal dynamics of the medium. It is shown that for weak waves, the general integral leads to well-known results of a linear approximation. Profiles of stationary solutions are constructed both for an exponential relaxation kernel and for other types of kernels. Energy losses at the front of weak shock waves are calculated. General integral formulas are obtained for energy losses of intense noise, which are determined by the form of the kernel, the structure of the noise correlation function, and the mean square of the derivative of realization of a random process. The nonlinear energy loss of broadband noise is considered in two limiting cases: (i) at the initial stage of propagation, when the wave profile contains a small number of shock fronts, and (ii) at the later stage when the wave reshapes to saw tooth-like one with randomly located shocks.

The study of intense waves in soft biological tissues is necessary both for diagnostics and therapeutic aims. Tissue represents an inherited medium with frequency dependent dissipative properties, in which waves are described by nonlinear integrodifferential equations. The equations for such waves are well known. Their group analysis has been performed, and a number of exact solutions have been found. However, statistical problems for nonlinear waves in tissues have hardly been studied. As well, for medical applications, both intense noise waves and waves with fluctuating parameters can be used. In addition, statistical solutions are simpler in structure than regular solutions; they are useful for understanding the physics of processes. Below a general approach is described for solving nonlinear statistical problems applied to the considered mathematical models of biological tissues. We have calculated the dependences of the intensities of the narrowband noise harmonics on distance. For wideband noise, we have calculated the dependence of the spectral integral intensity on distance. In all cases, wave attenuation is determined both by the specific dissipative properties of the tissue and the nonlinearity of the medium.

The work is supported by the Russian Science Foundation (Grant 14-12-00882).

Nonlinearity parameter B/A of biological tissue ultrasound imaging in echo modeM. Toulemonde^a, F. Varray^a, A. Bernard^a, O. Basset^b and C. Cachard^b^aCreatis, 7 av Jean capelle, 69621 Villeurbanne, France; ^bCREATIS, 7, avenue Jean Capelle, 69100 Villeurbanne, France

matthieu.toulemonde@creatis.insa-lyon.fr

The ultrasound imaging is a common diagnostic tool thanks to its non- invasive behavior and relatively cheap equipment. Nonlinear imaging mainly known by harmonic imaging, based on the harmonic frequencies generated by the nonlinear properties of the tissue, is largely used for clinical application because of the contrast improvement. The nonlinear property of tissue is characterized by the B/A nonlinearity parameter. The B/A varies for healthy or unhealthy tissues and the B/A estimation using an echographic approach would bring new modalities for imaging and diagnosis.

The extended comparative method (ECM) (F. Varray, UFFC 2011) is suitable for B/A estimation in clinical application and moreover in echo mode but has some limitations: the energy concentration due to the focalization prevents to obtain a homogeneous and accurate evaluation of the B/A parameter on the whole image. The ECM approach is based on the measurement of the second- harmonic pressure which not directly accessible in echo mode, on radio- frequency (RF) or envelope images. We made the assumption that the local pressure field can be derived from envelope image local amplitude if the speckle noise is smoothed. So, an alternative sequential filter (ASF) was used to reduce the speckle noise but it was not completely suppressed.

Previous work has demonstrated that the energy concentration could be overcome using the standard coherent plane wave compounding (CPWC) (G.Montaldo, UFFC 2009). The B/A evaluation and delimitation from pressure field and radio-frequency image approaches is improved (M.Toulemonde, ICASSP 2014). However the speckle noise still limits the B/A evaluation for RF images.

In this paper the multitaper coherent plane wave compounding (MCPWC) (M.Toulemonde, Ultrasonics 2015) and the ECM approach are combined in order to improve the nonlinearity parameter estimation in echo mode. The MCPWC method is based on the Thomson's multitaper approach (A.C. Jensen, UFFC 2012). Several orthogonal apodizations are used during the plane wave beamforming creating several RF images for each transmitted steering angles. The RF images built for the same DPSS tapers are averaged. After the envelope detection, the B-mode images obtained with different tapers are averaged to produce the final B-mode image.

The proposed method is evaluated in simulations and acquisitions in comparison to standard focalization and CPWC. In simulations, a phantom having an inhomogeneous scatterers' distribution and a nonlinearity map composed of a homogeneous B/A background and several elliptic inclusions with different B/A is used. In acquisitions, phantoms with several oil concentrations are made in order to have different second-harmonic generation.

In simulations, the Thomson's multitaper approach improves the localization of the different nonlinear areas. Using MCPWC, the delineation is improved and the approach is less sensible to the nonhomogeneous scatterer's distribution than the focalization approach. In addition, no depth is privileged in terms of energy with the plane wave transmission. In acquisitions, the proposed method allows to identify the phantom with different oil concentrations. However the aperture size of the probe is a strong limitation for plane wave transmission. A larger aperture probe may improve the B/A estimation.

Symmetry Analysis for Nonlinear Time Reversal methods applied to Nonlinear Acoustic ImagingS. Dos Santos^a and J. Chaline^b

^aINSA Centre Val de Loire, Inserm U930 'Imaging and Brain', 3, rue de la Chocolaterie, 41034 Blois, France; ^bInserm U930 'Imaging and Brain', 'Imaging and Ultrasound' group, 10 Boulevard Tonnellé, 37000 Tours, France
serge.dossantos@insa-cvl.fr

Recent ten years have seen considerable development of optimized signal processing methods for improving nonlinear NDT methods and harmonic imaging derived from Nonlinear Elastic Wave Spectroscopy (NEWS). Using symmetry invariance, nonlinear Time Reversal (TR) and reciprocity properties, the classical NEWS methods are supplemented and improved by new excitations having the intrinsic property of enlarging frequency analysis bandwidth and time domain scales, with now both medical acoustics and electromagnetic applications[1,2] The analysis of invariant quantities is a well-known tool which is often used in nonlinear acoustics in order to simplify complex equations. The most famous invariants in nonlinear acoustics are probably Riemann invariants which describe physical characteristics (local gauge symmetry) of the associate acoustic flow. Based on a fundamental physical principle known as symmetry analysis, this approach consists in finding judicious variables, intrinsically scale dependant, and able to describe all stages of behaviour on the same theoretical foundation. It postulates that we can always find a local region where the acoustical dynamics can be express by the formalism of the conventional acoustics, and nonlinear acoustics can be formulated as the interaction among these local dynamics[3]. Based on previously published results within the nonlinear acoustic areas[4], some practical implementation will be proposed as a new way to define TR-NEWS based methods applied to NDT and medical bubble based non-destructive imaging. This paper tends to show how symmetry analysis can help us to define new methodologies and new experimental set-up involving modern signal processing tools. Generalized TR based NEWS methods and their associate symmetry skeleton will be taken as an example with some new specific signal processing tools such as Pulse Inversion (PI), ESAM, DORT or SSM modern coding schemes. Some example of practical realizations will be proposed in the context of biomedical non-destructive imaging using Ultrasound Contrast Agents (ACUs) where symmetry and invariance properties allow us to define a microscopic scale-invariant experimental set-up describing intrinsic symmetries of the microscopic complex system[5].

[1] S. Dos Santos and Z. Prevorsevsky. *Imaging of human tooth using ultrasound based chirp-coded nonlinear time reversal acoustics*. Ultrasonics, **51** (6) :667-674, 2011.

[2] M. Frazier, B. Taddese, T. Antonsen, and S. M. Anlage, *Nonlinear time reversal in a wave chaotic system*. Phys. Rev. Letters, **110**, p. 063902, 2013.

[3] I.J.R. Aitchison and A.J.G. Hey, *Gauge Theories in Particle Physics*, IOP Publishing, Bristol and Philadelphia (1989)

[4] S. Dos Santos, M. Domenjoud, and C. Plag. *Symmetry analysis applied to nonlinear acoustics: Principle and application for acoustic signal processing*. In proc. of the 18th International Symposium on Nonlinear Acoustics ISNA, pages 46-49, Stockholm, Sweden, 2008.

[5] V. J. Sánchez-Morcillo, N. Jiménez, J. Chaline, A. Bouakaz and S. Dos Santos, *Spatio-Temporal Dynamics in a Ring of Coupled Pendula: Analogy with Bubbles*, chapter in Localized Excitations in Nonlinear Complex Systems Current State of the Art and Future Perspectives, edited by Ricardo Carretero-González et al, Nonlinear Systems and Complexity, Springer International Publishing Switzerland, ISBN 978-3-319-02056-3, Vol. 7, pp. 251-262 (2014)

Feasibility of Low-frequency Ultrasound Imaging Using Parametric Sound

H. Nomura, H. Adachi and T. Kamakura

University of Electro-Communications, 1-5-1, Chofugaoka, 182-8585 Chofu-Shi, Japan

h.nomura@uec.ac.jp

The penetration depth of high-frequency ultrasound is limited, since the ultrasound at high frequency is much attenuated by medium viscosity. In this study, to resolve this problem, we propose low-frequency ultrasound imaging using parametric sound sources as a low-frequency directive sound. In order to verify the proposed imaging method in water, a ring type transducer with the center hole was used to transmit modulated primary ultrasounds with center frequency of 2.8 MHz, and a hydrophone placed within the hole of transmitter was used to receive chirp-modulated parametric sound echoes with center frequency of 300 kHz and a bandwidth of 400 kHz. After receiving parametric sound echo signals from targets with dimensions of several centimeters, a pulse compression technique was applied to the signals in order to improve the range resolution and signal-to-noise ratio. The obtained B mode images reveal the feasibility of low-frequency ultrasound imaging using compressed parametric sounds.

Focused Shear Shock Waves in Soft Solids and the Brain: Simulations and ExperimentsB. Giammarinaro^a, F. Coulouvrat^b and G. Pinton^c^aUniversité Pierre et Marie Curie, Institut Jean Le Rond d'Alembert (UMR 7190), 4 place Jussieu, 75252 Paris Cedex 05, France; ^bCNRS - Institut Jean Le Rond d'Alembert (UMR 7190), Université Pierre et Marie Curie, 4 place Jussieu, 75005 Paris, France; ^cUniversity of North Carolina & North Carolina State University, 348 Taylor Hall, Chapel Hill, NC 27599, USA

giam@dalembert.upmc.fr

Soft solids like biological tissues are quasi-incompressible solids, with a bulk elastic modulus several orders of magnitude larger than the shear one (in practice about 5 orders). This leads to shear wave velocities equal to a few meters per second, compared to compression waves propagating close to the water speed of sound (1500 m/s). Wave nonlinear effects can be quantified in terms of Mach number, as the ratio of the velocity excitation to the wave speed. Given the low value of this last one, shear waves in soft solid may exhibit an extremely nonlinear behavior, with nonlinear properties three orders of magnitude larger than for classical solids. Consequently nonlinear shear waves can transition from a smooth to a shocked profile in less than one wavelength. Moreover, pure shear waves in isotropic media have a dominant nonlinear term that is cubic instead of quadratic. Cubic nonlinearities are characterized by the generation of odd harmonics of the input frequency. We hypothesize that traumatic brain injuries (TBI) could be caused by sharp gradients in shear shock waves. However shear shock waves are not currently modeled by simulations of TBI. Strong nonlinear effects may also be enhanced by the concave skull geometry inducing focusing effects.

The objective of the present study is therefore to investigate shear shock wave propagation and focusing from a theoretical and experimental point of view. A two-dimensional nonlinear paraxial equation with cubic nonlinearities and ad hoc absorption is used. We present numerical solutions based on a second-order operator splitting which allows the application of optimized numerical methods for each physical effect (diffraction, absorption, cubic nonlinearities). The diffraction is solved in the time domain by means of a standard Crank-Nicolson scheme, the absorption in the frequency domain using an empirical law. The nonlinear term is solved in the time domain by a shock capturing, mixed first/second order scheme coupled with a "minmod" flux limiter. The proposed numerical scheme is validated by several methods. In particular, the 2D nonlinear/diffraction part is validated by means of Guiraud's self-similarity law applied to cusp caustics. It generalizes a self-similar behavior observed for a nonlinear transonic equation modeling sonic boom focusing. The validated numerical scheme is then used to estimate injury criteria in a blunt trauma. A CT measurement of the human skull is used to determine the initial conditions, and shear shock wave simulations are presented to demonstrate the focusing effects of the skull geometry. In a second part, we present experiments of focused shear shock waves performed in a homogeneous gelatin phantom. Shear waves are excited by the impulsive displacement of a plate coupled to a shaker. Geometrical focusing is obtained by means of a curved plate. Medium displacements within the phantom are measured using an ultrafast ultrasound imaging. Medium linear and nonlinear propagation properties are determined by measurements for quasi plane wave excitation. Experiments for focused shock shear waves will be discussed and compared to numerical simulations.

Acoustic solitary waves in a lattice of Helmholtz resonatorsB. Lombard^a, J.-F. Mercier^b and O. Richoux^c^aLMA CNRS, 31 chemin Joseph Aiguier, 13402 Marseille, France; ^bPOEMS-CNRS, ENSTA ParisTech, 91762 Palaiseau, France; ^cLAUM, avenue Olivier Messiaen, 72085 Le Mans, France

lombard@lma.cnrs-mrs.fr

Solitons are nonlinear waves with large amplitude and constant profile, resulting from the competition between non-linearity and dispersion. They occur in many physical area, such as fluid mechanics (Korteweg-de Vries equations), electromagnetism and optics (Klein-Gordon equations). In acoustics, the intrinsic dispersion is too low compared to the nonlinearity to produce solitons. Thus additional geometric dispersion must be considered to observe acoustic solitons. It was the basis of a series of works of Sugimoto and coauthors [1], where the propagation of shock waves was investigated in a tube connected to an array of Helmholtz resonators. A mathematical model was proposed, as well as a theoretical analysis and a comparison with experimental data.

Sugimoto's work was extended in two means. In [2], a time-domain numerical model was proposed to incorporate efficiently the fractional derivatives modeling linear viscothermic losses. In [3], comparisons with experimental results were proposed. It was shown that nonlinear attenuation in the resonators has also to be incorporated for describing accurately the experiments.

An overview of this topics will be given in this presentation, as well as new numerical and theoretical results.

[1] N. Sugimoto, Propagation of nonlinear acoustic waves in a tunnel with an array of Helmholtz resonators, *J. Fluid. Mech.*, 244: 55-78, 1992.

[2] B. Lombard, J. F. Mercier, Numerical modeling of nonlinear acoustic waves in a tube with Helmholtz resonators, *J. Comput. Phys.*, 259: 421-443, 2014.

[3] O. Richoux, B. Lombard, J. F. Mercier, Generation of acoustic solitary waves in a lattice of Helmholtz resonators, submitted to *Wave Motion*, 2014. Available on <https://hal.archives-ouvertes.fr/hal-01069252/document>.

We. 10:00 Amphi 3

Non-linear propagation in heterogeneous media 1

Nonlinear ultrasonic testing by Rayleigh waves on control of concrete cover - Application in thermal damage evaluationQ.A. Vu^a, V. Garnier^a, C. Payan^b, J.-F. Chaix^a and M. Lott^a^aAix Marseille Université, LMA UPR CNRS 7051, 31 chemin Joseph Aiguier, 13042 Marseille Cedex 20, France; ^bAix Marseille Université, LMA UPR CNRS 7051, 13402 Marseille, France

quang-anh.vu@univ-amu.fr

This paper present the use of Rayleigh wave in Dynamic Acousto-Elasticity Testing for non-destructive evaluation of concrete cover. Dynamic anomalous nonlinear elastic behavior with primary manifestations like modulus decrease reached to conditioning state and slow dynamic process, has been observed in many variety of solids, also in concrete. In ideal, we hope the surface wave with its advantages for an on-site measurement, can show locally nonlinear properties of a cover concrete layer with depth predetermined. In the first step, we work in laboratory with a small size specimen series of concrete damaged thermally in different temperature. In this paper, only conditioning level is analyzed to be sensitive with thermally damage by Rayleigh waves. The variation trend is compared with NRUS method result on the first bending mode. This technique offers a real possibility of test by a single face of a structure which opens up possibilities for transposition on site.

We. 11:00 Amphi 2

Plenary lecture 3: Robert Mettin

Bubble dynamics in high-power ultrasonic fields

R. Mettin

Georg-August-University Göttingen, Drittes Physikalisches Institut, Friedrich-Hund-Platz 1, 37077 Göttingen, Germany

rmettin@gwdg.de

Intense sound in liquids can lead to acoustic cavitation: gas and vapor bubbles are generated and activated by the acoustic field to undergo partly extreme volume oscillations. In the presentation, several aspects of acoustic cavitation and bubble dynamics are discussed, including the following:

- The attenuation of the acoustic wave in the presence of cavitation bubbles increases significantly. This in turn causes strong acoustic streaming. For cavitation at 20 kHz in water, flow measurements are shown that allow for the deduction of an effective damping coefficient.
- Acoustic cavitation bubbles tend to form distinct structures in space due to their interaction with the sound wave and with each other. Furthermore, the structure formation appears to be involved in the phenomenon of subharmonic sound emission, which is a well-known characteristic of acoustic cavitation. It is shown that synchronization of bubble oscillations within a double layer structure contributes to the occurrence of the emission of half the driving frequency in an ultrasonic bath. In this framework, audible sound movies of cavitation bubbles are presented where the bubble dynamics and the according sound emissions are slowed down accordingly.
- Intense bubble collapses can cause shock wave emission, material erosion, heating of the bubble interior, chemical reactions, and light emission (sonoluminescence). Experimental results highlight the connection of liquid phase chemistry in the collapsing bubble with non-spherical bubble dynamics. Moreover, the extremely bright light emission in sonicated phosphoric acid is used in high-speed recordings to investigate details of active bubble distributions and their properties in acoustically cavitating systems.

Modeling elastic wave propagation in a solid with distributed damage and kissing bonds using the Discontinuous Galerkin Finite Element Method

O. Bou Matar, A. Trifonov and V. Aleshin

IEMN / Ecole Centrale de Lille, IEMN, LCI, Avenue Poincaré, Cité Scientifique, 59652 Villeneuve D'Ascq, France
olivier.boumatar@iemn.univ-lille1.fr

We present a high performance numerical tool based on the nodal Discontinuous Galerkin Finite Element Method (DG-FEM) for the simulation of elastic wave propagation in nonlinear heterogeneous media. DG-FEM, combining geometrical flexibility of the finite element approach and a high parallelization potential of the finite volume technique, is a perfect technique to reduce the number of cells to be used while maintaining a high degree of accuracy needed in nonlinear acoustics. We apply this method to solve the nonlinear elastic wave equation written in a conservative form on unstructured meshes, for the case of heterogeneous media, with an arbitrary order of accuracy in space. The code uses the open source software Hedge [A. Klöckner, T. Warburton, J. Bridge, and J. Hesthaven, "Nodal discontinuous Galerkin methods on graphics processors," *J. Comp. Phys.* 228, 850 7863- 7882 (2009)] and runs on a single CPU or on a multi CPU system, but its best performance (speedup of about 14-64 times) is achieved while running on a GPU with the CUDA interface. We implement in our numerical tool a wide variety of constitutive equations, such as classical quadratic and cubic nonlinearities, and hysteretic nonlinearities. To simulate semi-infinite or infinite media, new perfectly matched layers (PML), called CFS-NPML (Complex Frequency Shifted - Nearly Perfectly Matched Layers), well adapted to the DG-FEM formalism were introduced. The developed DG-FEM scheme was verified by means of a comparison with analytical solutions and numerical results already published in the literature for simple geometrical configurations: Lamb's problem and plane wave nonlinear propagation. We also extended the capability of the numerical tool by introducing in the scheme a second kind of nonlinearity called Contact Acoustic Nonlinearity (CAN) to simulate localized defects, such as cracks or delaminations. Indeed, in contrast to classical FEM, with the DG-FEM framework the solution can be discontinuous across the element interfaces, which allows incorporating boundary conditions corresponding to an internal contact or crack. This feature allowed us to use the method for simulating nonlinear ultrasound NDT experiments: The boundary conditions we applied in order to model cracks corresponded to the diode-like nonlinearity (hard compression, easy tension), to imperfect adhesive bounds (double-well potentials), and to cracks with friction (Coulomb friction). Examples of using the method for nonlinear imaging of defects in MEMS or composite plates with a Localized Defect Resonance are presented.

This work was supported by the EC FP7-AAT-2012-RTD-1 ALAMSA project.

Evolution of bulk strain solitons in cylindrical inhomogeneous shells

A. Shvartz, A. Samsonov, G. Dreiden and I. Semenova

The Ioffe Institute, 26, Polytekhnicheskaya st., 194021 St.Petersburg, Russian Federation

andrew.shvartz@mail.ioffe.ru

The study of nonlinear bulk wave propagation in a shell as in one of the standard structural elements attracts considerable interest in theory and applications to problems of stability of thin shells and non-destructive testing of them.

Recently a refined theory of longitudinal strain waves in thin-walled cylindrical shell has been developed, and an equation in the form of Doubly Dispersive Equation (DDE) for a strain component has been derived for a material governed by the 5-constant elasticity theory. This equation has, amongst others, a solution representing a solitary bulk wave, which was observed in our physical experiments in a duct-like shell. The strain soliton parameters have been estimated and it was shown that the soliton propagates at the distances ten times bigger than its wavelength without any significant losses in shape and amplitude.

To study possible application of the elastic strain solitons in the nondestructive testing, we consider the problem of the evolution of the bulk strain solitary waves in inhomogeneous shells. We considered the infinite cylindrical shell with variation of both geometric and elastic properties along the shell axis. Using the model described, we proposed the DDE with variable coefficients for the strain component.

To solve the Cauchy problem for DDE we used a conservative finite-difference scheme, which satisfies the integral conservation laws for "pseudo-mass" and "pseudo-energy" of the solitary wave. The numerical approach provides the opportunity to analyze the spatiotemporal evolution of the strain solitons caused by inhomogeneity of the waveguide. In numerical simulations, we considered both monotonic and abrupt variations of the geometric and elastic properties of the shell and studied the nonlinear wave propagation through the interfaces between different waveguides as well as through local defect areas of the shell.

We have shown that the change of the waveguide cross-section leads to remarkable variations of the soliton shape and velocity. However, the soliton is completely recovered after propagation through a local defect area, while the memory of the defect is stored as the phase shift from the reference soliton propagating in a homogeneous waveguide. We believe that the results of the numerical simulation are important for better understanding of both advantages and limitations for the NDT of lengthy shells using elastic bulk strain solitons.

Acknowledgement. The support of this study by the Russian Scientific Fund via grant no. 14-12-00342 is gratefully acknowledged.

Discontinuous Galerkin Method with Gaussian Artificial Viscosity on Graphical Processing Units for Nonlinear AcousticsB. Tripathi^a, B. Sambandam^b, F. Coulouvrat^c and R. Marchiano^d

^aInstitut Jean le Rond d'Alembert, Université Pierre et Marie Curie, 4, place Jussieu, 75252 Paris, France; ^bIndian Institute of Technology Bombay, Department of Mathematics, 400076 Mumbai, India; ^cCNRS - Institut Jean Le Rond d'Alembert (UMR 7190), Université Pierre et Marie Curie, 4 place Jussieu, 75005 Paris, France; ^dInstitut Jean le Rond d'Alembert, 4, Place Jussieu, 75252 Paris Cedex 05, France
bharat@dalembert.upmc.fr

Propagation of acoustical shock waves in complex geometry is a topic of interest in the field of nonlinear acoustics. For instance, simulation of Buzz Saw Noise requires the treatment of shock waves generated by the turbofan through the engines of aeroplanes with complex geometries and wall liners. Nevertheless, from a numerical point of view it remains a challenge. The two main hurdles are to take into account the complex geometry of the domain and to deal with the spurious oscillations (Gibbs phenomenon) near the discontinuities. In this work, first we derive the conservative hyperbolic system of nonlinear acoustics (up to quadratic nonlinear terms) using the fundamental equations of fluid dynamics. Then, we propose to adapt the classical nodal discontinuous Galerkin method to develop a high fidelity solver for nonlinear acoustics. The discontinuous Galerkin method is a hybrid of finite element and finite volume method and is very versatile to handle complex geometry. In order to obtain better performance, the method is parallelized on Graphical Processing Units. Like other numerical methods, discontinuous Galerkin method suffers with the problem of Gibbs phenomenon near the shock, which is a numerical artifact. Among the various ways to manage these spurious oscillations, we choose the method of parabolic regularization. Although, the introduction of artificial viscosity into the system is a popular way of managing shocks, we propose a new approach of introducing smooth artificial viscosity locally in each element, wherever needed. Firstly, a shock sensor using the linear coefficients of the spectral solution is used to locate the position of the discontinuities. Then, a viscosity coefficient depending on the shock sensor is introduced into the hyperbolic system of equations, only in the elements near the shock. The viscosity is applied as a two-dimensional Gaussian patch with its shape parameters depending on the element dimensions, referred here as *Gaussian Artificial Viscosity*. Using this numerical solver, various numerical experiments are presented for one and two-dimensional test cases in homogeneous and quiescent medium. This work is funded by CEFIPRA (Indo-French Centre for the Promotion of Advance Research) and partially aided by EGIDE (Campus France).

Simulation of the interaction between a bubble and a ultrasound wave by implementing a two-phase compressible solver adapted to low Mach number regime.G. Huber^a, S. Tanguy^a, J.-C. Béra^b and B. Gilles^b^aUniversité de Toulouse, IMFT, Allée du Professeur Camille Soula, 31400 Toulouse, France; ^bUniversité Claude Bernard Lyon 1, INSERM U1032, 151, cours Albert Thomas, 69424 Lyon, France

ghuber@imft.fr

This presentation is focused on the numerical simulation of the interaction of an ultrasound wave and an air bubble surrounded by water. Our interest is to develop a fully compressible solver in the two phases and to account for surface tension effects.

As the volume oscillation of the bubble occurs in a low Mach number regime (in particular in water), a specific care must be paid to the effectiveness of the numerical method which is chosen to solve the compressible Euler equations. Three different numerical methods, the explicit HLLC (Harten-Lax- van Leer-Contact) solver [3], a preconditioning explicit HLLC solver [1] and the compressible projection method [4] are implemented and confronted on a one dimensional spherical benchmark introduced in Ref.[2]. This preliminary test highlights that the projection method is the fastest method and the most accurate one.

Then, in a 2D cylindrical configuration, a basic implementation of the surface tension, though efficient for incompressible two-phases flow, leads to strong spurious currents and numerical instabilities. This is why, a specific velocity/pressure time splitting is proposed to overcome this issue. Numerical evidences of the efficiency of this new numerical scheme are provided with the numerical simulation of the interaction between a bubble and a spherical wavefront. Indeed, both the accuracy and the stability of the overall algorithm are enhanced using this new numerical method.

Finally, the numerical simulation of the interaction of a moving and deformable bubble with a plane wave is presented in order to bring out the ability of the new method in a more complex situation.

References

- [1] H. Guillard and C.Viozat. On the behaviour of upwind schemes in the low mach number limit. *Computers & Fluids* 28, pages 63-86, 1999.
- [2] S.J. Shaw and P.D.M. Spelt. Shock emission from collapsing bubbles. *Journal of Fluid Mechanics* 646, pages 363-373, 2010.
- [3] E. Toro, M. Spruce, and W. Speares. Restoration of the contact surface in the hll riemann solver. *Shock Waves* 4, pages 25-34, 1994.
- [4] T. Yabe and P.Y. Wang. Unified numerical procedure for compressible and incompressible fluid. *J. Phys. Soc. Japan* 60, page 2105-2108, 1991.
- [5] B. Yang and A. Prosperetti. A second-order boundary-fitted projection method for free-surface flow computations. *Journal of Computational Physics* 213, pages 574-590, 2006. </latex>

Numerical Investigation of Bubble Nonlinear Dynamics Characteristics

J. Shi, D. Yang, H. Zhang, S. Shi, B. Hu and S. Jin

Harbin Engineering University, 145 Nantong Str. Nangang Dist. Harbin Heilongjiang, 150001 Harbin, China

shijie@hrbeu.edu.cn

The complicated dynamical behaviors of bubble oscillation driven by acoustic wave can provide favorable conditions for many engineering applications. On the basis of Keller-Miksis model, the influences of control parameters, including acoustic frequency, acoustic pressure and radius of gas bubble, are discussed by utilizing various numerical analysis methods. Furthermore, the law of power spectral variation is studied. It is shown that chaotic state can occur only in the suitable threshold. The results illustrate that the occurrence of the chaotic state is the result of interaction and equilibrium between each parameter in this nonlinear system, and only if all of the control parameter are in the suitable range, the dynamics characteristics and power spectral variation can be enhanced.

A model for acoustic vaporization of encapsulated droplets

F. Coulouvrat and M. Guédra

CNRS - Institut Jean Le Rond d'Alembert (UMR 7190), Université Pierre et Marie Curie, 4 place Jussieu, 75005 Paris, France

matthieu.guedra@dalembert.upmc.fr

Acoustic Droplet Vaporization (ADV) refers to the phase change of liquid droplets induced by pressure oscillations (acoustic waves) in order to form vapor bubbles. This process is investigated for about ten years for clinical applications such as vascular imaging, targeted drug delivery, embolotherapy or thrombolysis. ADV in medicine is generally realized from perfluorocarbon (PFC) emulsions because of their low boiling temperature, close to the body temperature. Because of their small diameter (100 to 1000 nm) and surface tension effects, injected droplets do not vaporize spontaneously and remain in a superheated liquid state, even if their normal boiling point is below the physiological temperature of 37°C. Numerous experimental studies have shown the efficiency of the vaporization of encapsulated PFC droplets for such applications. However, few theoretical works have been performed in order to better understand the physical mechanisms responsible for the ADV of encapsulated droplets. The present work proposes an improvement of the existing models which often consider that the vapor bubble is in an infinite medium, or which use simplifications for heat transfer around the bubble. In this work, we thus propose a theoretical modelling of ADV which accounts for the shell around the droplet and the outer liquid. The radial motion of the particle is governed by a generalized Rayleigh-Plesset equation which accounts for the evaporation rate at liquid/vapor bubble surface, the surface tension between droplet and outer liquid, and the viscoelasticity of the shell. This equation is coupled to heat equations in the liquid media which rule the temperature field around the bubble and thus the mass flux through the surface. Numerical simulations reveal behaviors of the vapor nucleus which can be substantially different from the case of a vapor bubble in an infinite medium. For example, the evaporation process can be stopped by the rigidity of the shell, thus trapping the bubble around an equilibrium radius inside the droplet. A static analysis notably reveals the existence of such an equilibrium state which depends on the characteristics of the encapsulation. The acoustic pressure amplitude thresholds obtained from numerical results show good qualitative agreement with measurements of ADV thresholds in literature, and allow to quantify the effect of the added Laplace pressure applied by the outer liquid on the droplet. Above ADV threshold, it is shown that the growth of the vapor bubble is mainly affected by the surface tension and the density contrast between inner and outer liquids, as well as by the rigidity of the encapsulating shell [with the financial support of ITMO Cancer AVIESAN (Alliance Nationale pour les Sciences de la Vie et de la Santé) in the frame of Plan Cancer].

Nonlinear Dynamics of a Vapor Bubble Expanding in a Superheated Region of a Finite SizeE. Annenkova^a, W. Kreider^b and O. Sapozhnikov^{a,b}^aPhysics Faculty, Moscow State University, Leninskie Gory, 119991 Moscow, Russian Federation; ^bCenter for Industrial and Medical Ultrasound, Applied Physics Laboratory, University of Washington, 1013 NE 40th Street, Seattle, WA 98105, USA

a-a-annenkova@yandex.ru

A high-intensity focused ultrasound (HIFU) beam can superheat the propagation medium and initiate boiling. Such conditions occur in certain regimes of HIFU therapy such as thermal ablation and histotripsy. Heat deposition from the focused beam results in a localized hot spot of about a millimeter that coincides with the focal region of the beam. If the medium is superheated, i.e., its temperature exceeds boiling temperature, a vapor bubble can grow from an existing nucleus, reaching a millimeter in size within several milliseconds. Such rapid growth creates significant stresses around the bubble and may result in the radiation of audible sound sometimes called 'popcorn noise'. If characterized, these sounds may be useful in monitoring some treatments; moreover, millimeter-sized boiling bubbles may also provide useful targets for monitoring treatments with ultrasound imaging. The current paper is devoted to a theoretical study of vapor bubble dynamics under conditions of spherical symmetry. The theory is built from first principles, based on the conservation of mass, momentum and energy; the equation of state; and the laws of heat and mass transfer. Liquid that is pushed by the expanding bubble is supposed to behave as an incompressible medium. Under such an assumption, the equation of motion of liquid around the bubble is reduced to a Rayleigh-Plesset type equation for the radial dynamics. A classical approximation is to consider the gas content inside a bubble to be adiabatic during violent collapses and isothermal during slow radial motions. This approach permits calculation of temperature gradients in the gas phase without consideration of thermal effects in the liquid. However, such an approach is problematic for bubbles with a considerable amount of vapor, in which phase-change processes and the enthalpy of vaporization can significantly affect the balance of energy at the liquid- gas boundary. Accordingly, both the liquid and the gaseous phases have to be taken into account in modeling the heat transfer. The gas medium inside the bubble is thus considered as a mixture of incondensable gas and vapor, with the vapor dynamics described by the kinetic theory of gases. Mass transfer across the boundary is divided into streams of condensing and evaporating molecules, which are calculated separately using the kinetic theory, and then added up. The process of bubble growth in a region of superheated liquid is characterized by two regimes: rapid initial growth that is limited by the inertia of the surrounding liquid, and subsequent growth that is limited by heat transfer from the surrounding liquid to the liquid-vapor boundary. Acoustic pressure generated by the growing bubble, as well as other parameters characterizing the growth, are calculated from the system of equations that relate these parameters with each other. The work was supported by the RSF grant N°14-15-00665 and NIH R01EB007643.

Numerical Study on the Effective Heating due to Inertial Cavitation in Microbubble-enhanced HIFU TherapyK. Okita^a, K. Sugiyama^b, S. Takagi^c and Y. Matsumoto^d^aNihon University, 1-2-1 Izumi-cho, Narashino, 275-8575 Chiba, Japan; ^bOsaka University, 1-3, Machikaneyama-cho, Toyonaka, 560-8531 Osaka, Japan; ^cThe University of Tokyo, 7-3-1, Hongo, Bunkyo, 113-8656 Tokyo, Japan; ^dThe University of Tokyo, 7-3-1, Hongo, Bunkyo, 113-8656 Tokyo, Japan

okita.kohei@nihon-u.ac.jp

The development of High Intensity Focused Ultrasound (HIFU) therapy has been of interest for a noninvasive treatment for the deep cancer such as liver cancer and brain cancer. An issue with current HIFU techniques is the attenuation of ultrasound. The microbubbles used as ultrasonic contrast agents are a key of the problem. The injection of microbubbles into the target tissue enhances tissue heating in HIFU therapy, via inertial cavitation. Thus, the control of the inertial cavitation is required to achieve the efficient tissue ablation. However, the behavior of microbubbles in a focused ultrasound field is not well investigated due to the complex interactions between the oscillating bubbles and the ultrasound. In the present study, the effective heating due to inertial cavitation to obtain the temperature rise at a target in microbubble-enhanced HIFU therapy is investigated by a numerical simulation. The equations for conservation of mass, momentum and energy are solved for a microbubble-infused mixture, model HIFU therapy in the presence of microbubbles. A bubble dynamics equation based on the Qin-Ferrara model, which considers a spherical shell bubble in a soft tissue. The mixture phase and bubbles are coupled by Euler-Lagrange method to take into account the interaction between ultrasound and bubbles. The basic equations are developed on the basis of the FDTD method. A bubble dynamics equation based on the Qin-Ferrara model, which considers a spherical shell bubble in a soft tissue. The bubbles are coupled with the mixture using the Euler-Lagrange method. According to an experimental setup, we simulate the propagation of 4.8MHz ultrasound provided by a transducer through a polyacrylamide gel including microbubbles. The represent diameter of microbubble is $2.2\mu\text{m}$. The impacts of initial void fraction on the ultrasound field and the temperature distribution were examined. As the initial void fraction increased from 10^{-5} to 10^{-4} %, the temperature around the target increased because of microbubble oscillation. Microbubbles actually induced efficient heating; however, at 10^{-3} %, the ultrasound was too attenuated to heat the target, and then the heating region moved from the target to the transducer side. These results were in qualitative agreement with the experimental observation.

Simulation of blast wave propagation from source to long distance with topography and atmospheric effects

M. Nguyen-Dinh, O. Gainville and N. Lardjane

CEA, DAM, DIF, F-91297 ArpaJon, France

maxime.nguyen@cea.fr

The main purpose of this work is to quantify sound annoyance in both the near and far vicinity of a pyrotechnic quarry. In this quarry, blast waves are generated every day by the explosion of a half thousand kilograms of TNT in a canyon and eared up to ten kilometres. Once the wave is generated, it interacts with a complex topography. It is well known that blast wave characteristics are deeply affected by topography and atmospheric inhomogeneities. However, their relative importance and imbrication quantification remains a challenging task in complex environment. In this talk, we present new results for the blast wave propagation from strong shock regime to the weak shock limit (acoustics). We mainly focus on both topography and effective sound speed effects. For this purpose, we analyse the blast wave propagation using both Direct Numerical Simulation and acoustic asymptotic models. We also compare simulation results with measurements in both the near and far field from the ANR-Prolonge project. Direct Numerical Simulations are performed with a state of the art in house High Performance Computing code, using Adaptive Mesh Refinement to solve the Euler's equations. Such a simulation requires several billions of cells for high resolution of both the source and the propagation up to several hundred meters. In this code, we take into account local topography and vertical sound speed profile only at the moment. An acoustic weak shock model is used when the shock strength is low enough and topography scale is of the same order as the wavelength. The model is based on a wave equation parabolic approximation. This equation can be solved numerically with an affordable computational cost. Moreover this method allows to take into account topography and sound speed variation as well as wind. This approach allows a full numerical study of a realistic pyrotechnic site taking into account main physical effects. From comparison with terrain measurements, we will point out the pros and cons of this strategy. This study is part of the french ANR-Prolonge (ANR-12-ASTR-0026) project.

We. 14:00 Amphi 3

Non-linear propagation in heterogeneous media 1

Revisiting Geometrical Shock Dynamics for blast wave propagation in complex environmentJ. Ridoux^a, N. Lardjane^a, T. Gomez^b and F. Coulouvrat^c^aCEA, DAM, DIF, F-91297 Arpajon, France; ^bInstitut Jean Le Rond d'Alembert (UMR 7190), Université Pierre et Marie Curie, 4 place Jussieu, 75005 Paris, France; ^cCNRS - Institut Jean Le Rond d'Alembert (UMR 7190), Université Pierre et Marie Curie, 4 place Jussieu, 75005 Paris, France

julien.ridoux@cea.fr

Direct numerical simulation of blast waves, from source location to long distance, is a challenging task due to the wide range of spatial and temporal scales. Billions of cells are necessary for 3D codes. Taking into account topography, obstacles and variable atmospheric conditions is further restricting.

In this paper we present a simplified model for blast wave propagation in complex environment designed to obtain reasonably accurate results at low computational cost. This new model is an extension of Whitham's Geometrical Shock Dynamics (GSD) to blast waves, which gives the first arrival time and overpressure of the front.

It is well known that GSD works well for strong shocks, and surprisingly well for weaker ones, but post-shock effects are omitted. Rather than neglecting some terms during the mathematical derivation of GSD, we propose a closure, much simpler than Best's one, fitted on blast waves' experimental overpressure laws. Doing so, the hyperbolic nature of GSD is not affected: shock-shock are still present. Since blast waves rapidly evolve to acoustic waves, we will discuss the effect of the cross area section closure, also known as the A-M relation.

From the numerical point of view, the model is solved through an Eulerian level-set procedure. This choice prevents any difficult numerical treatment for front interactions in 3D, which is a severe default of Lagrangian algorithms. Assuming a single pass front, we adapt the fast-marching paradigm to solve the resulting non linear system. Another interest of the Eulerian formulation is the ability to mimic rigid wall effects through an immersed boundary method. Performance and validation of this algorithm will be presented.

Numerical Study of Heterogeneous Mean Temperature and Shock Wave in a Resonator

T. Yano

Osaka University, 2-1, Yamada-oka, 565-0871 Suita, Japan

yano@mech.eng.osaka-u.ac.jp

When a frequency of gas oscillation in an acoustic resonator is sufficiently close to one of resonant frequencies of the resonator, the amplitude of gas oscillation becomes large and hence the nonlinear effect manifests itself. Then, if the dissipation effects due to viscosity and thermal conductivity of the gas are sufficiently small, the gas oscillation may evolve into the acoustic shock wave, in the so-called consonant resonators. At the shock front, the kinetic energy of gas oscillation is converted into heat by the dissipation process inside the shock layer, and therefore the temperature of the gas in the resonator rises. Since the acoustic shock wave travels in the resonator repeatedly over and over again, the temperature rise and resulting increase in the speed of sound become noticeable in due course of time even if the shock wave is weak. That is, in the presence of shock wave, the steady oscillation state or the time-periodic oscillation state is not realized in the strict sense. We numerically study the gas oscillation with shock wave in a resonator of square cross section by solving the initial and boundary value problem of the system of three-dimensional Navier-Stokes equations with a finite difference method. In this case, the heat conduction across the boundary layer on the wall of resonator causes a spatially heterogeneous distribution of mean (time-averaged) gas temperature. Based on the results of numerical simulations, we discuss the temporal development of heterogeneous mean temperature and gas oscillation with shock wave.

We. 14:40 Amphi 3

Non-linear propagation in heterogeneous media 1

Nonlinear reflection of a spherically divergent N-wave from a plane surface: optical interferometry measurements in airP. Blanc-Benon^a, M. Karzova^{a,b}, S. Ollivier^a, V. Khokhlova^b and P. Yuldashev^b^aLaboratoire de Mécanique des Fluides et d'Acoustique, Ecole Centrale de Lyon, 36 Avenue Guy de Collongue, 69134 Ecully, France; ^bPhysics Faculty, Moscow State University, Leninskie Gory, 119991 Moscow, Russian Federation
philippe.blanc-benon@ec-lyon.fr

Nonlinear reflection of shock waves was first experimentally observed by Ernst Mach in 1878 and then theoretically investigated by von Neumann in 1943. However the three-shock theory of von Neumann conflicts with experimental results for weak shocks with values of acoustic Mach number less than 0.05, which is known as von Neumann paradox. Numerous studies have been undertaken to resolve von Neumann paradox, mainly in the framework of aerodynamics covering step shock waveforms for acoustic Mach number greater than 0.035. In nonlinear acoustics, shock waves have more complicated waveforms than step shocks and the values of acoustic Mach numbers are at least one order smaller than in aerodynamics. Results for nonlinear reflection of such very weak, but nonetheless strongly nonlinear acoustic waves has not been reported to the same extent. The goal of this work was to demonstrate experimentally how nonlinear reflection occurs in air for very weak spherically divergent acoustic spark-generated pulses resembling an *N*-wave. Measurements of reflection patterns were performed using a Mach-Zehnder interferometer. A thin laser beam with sub-millimeter cross-section was used to obtain the time resolution of 0.4 μ s, which is 6 times higher than the time resolution of the condenser microphones. Pressure waveforms were reconstructed using the inverse Abel transform applied to the phase of the signal measured by the interferometer. The Mach stem formation was observed experimentally as a result of collision of the incident and reflected shock pulses. It was shown that irregular reflection of the pulse occurred in a dynamic way and the length of the Mach stem increased linearly while the pulse propagated along the surface. Since the front shock of the spark-generated pulse was steeper than the rear shock, irregular type of reflection was observed only for the front shock of the pulse while the rear shock reflection occurred in a regular regime. Work supported by LabEx CeLyA ANR-10-LABX-60/ANR-11-IDEX-0007 and by the student stipend from the French Government.

Resonant Acoustic Nonlinearity for Sensitive Defect-Selective Imaging and NDT

I. Solodov

IKT, University of Stuttgart, 32 Pfaffenwaldring, 70659 Stuttgart, Germany

igor.solodov@ikt.uni-stuttgart.de

The nonlinear approach to ultrasonic nondestructive testing (NDT) of imperfect materials traces back to the first experiments by Vladimir Krasilnikov and Mack Breazeale in 1960s-1970s. It is concerned with nonlinear material response, which is inherently related to the frequency changes of the input signal. However, a long-term bottleneck problem identified on the way of applications of nonlinear NDT is a low efficiency of conversion from fundamental frequency to nonlinear frequency components. In this presentation, a possibility to enhance substantially nonlinear frequency conversion is demonstrated by combining the nonlinearity of defects with their inherent resonance (Local Defect Resonance (LDR)). The LDR concept naturally provides an efficient energy pumping from the wave directly to the defect, so that it manifests a profound nonlinearity (efficient higher harmonic generation and frequency mixing) even at moderate ultrasonic excitation level. A combined effect of LDR and nonlinearity also results in qualitatively new "nonclassical" features (subharmonics, hysteresis, instability) characteristic of nonlinear and parametric resonances. Multiple case studies will be given to illustrate efficient nonlinear NDT and sensitive imaging of defects in the materials relevant to automotive and aviation industries.

High Frequency calibration of MEMS microphones using spherical N-wavesS. Ollivier^a, C. Desjoux^b, P. Yuldashev^c, A. Koumela^d, E. Salze^b, L. Rufer^d and P. Blanc-Benon^b

^aUniversité Lyon 1, LMFA UMR CNRS 5509, Ecole Centrale de Lyon, 36, avenue Guy de Collongue, 69134 Ecully, France; ^bLaboratoire de Mécanique des Fluides et d'Acoustique, Ecole Centrale de Lyon, 36 Avenue Guy de Collongue, 69134 Ecully, France; ^cPhysics Faculty, Moscow State University, Leninskie Gory, 119991 Moscow, Russian Federation; ^dLaboratoire TIMA. CNRS-UJF-INPG, 46 Avenue Felix Viallet, 38031 Grenoble, France

sebastien.ollivier@univ-lyon1.fr

In the context of the scientific program “ SIMMIC ” supported by the French National Agency for Research (SIMI 9, ANR 2010 BLANC 0905 03), new wide band MEMS piezoresistive microphones have been designed and fabricated for weak shock wave measurements. The fabricated microphones have a high frequency resonance between 300 to 800 kHz depending on the membrane size. In order to characterize the frequency response of the fabricated sensors up to 1 MHz, new calibration methods based on an N-wave source were designed and tested. Short duration spherical N-waves can be generated by an electric spark source. To estimate a constant sensitivity coefficient, a known method is based on the estimation of the peak pressure from the lengthening of N-waves induced by non linear propagation. However, to obtain the sensitivity as a function of frequency, the output voltage must be compared to the incident pressure waveform, which must be accurately characterized. Taking advantage of recent works on the characterization of pressure N-waves generated by an electric spark source by means of optical methods, two calibration methods have been designed to obtain the frequency response. A method based on the comparison with pressure waveforms deduced from the analysis of schlieren images allowed to estimate the frequency response. A second method, based on a Mach-Zender optical interferometer, was found to be the best method to estimate the sensitivity of microphones up to 1 MHz. The methods were first tested by calibrating standard 1/8 inch condenser microphones. Then, frequency responses of different MEMS microphones prototypes were characterized to test different sensor designs. Results show that using a spark source and optical methods it is possible to calibrate sensors in the frequency range 10 kHz-1 MHz. The new calibration methods were used to improve the design of new high frequency MEMS pressure sensors.

Acoustic emission and magnification of atomic lines resolution for laser breakdown of salt water in ultrasound field

A. Bulanov

Pacific Oceanological Institute, 43, Baltic Str., 690041 Vladivostok, Russian Federation

a_bulanov@me.com

Researches of the acoustic effects accompanying optical breakdown in a water, generated by the focused laser radiation with power ultrasound have been carried out. Experiments were performed by using 532 nm pulses from Brilliant B Nd:YAG laser. Acoustic radiation was produced by acoustic focusing systems in the form hemisphere and ring by various resonance frequencies of 10.7 kHz and 60 kHz. The experimental results are obtained, that show the sharply strengthens effects of acoustic emission from a breakdown zone by the joint influence of a laser and ultrasonic irradiation. Essentially various thresholds of breakdown and character of acoustic emission in fresh and sea water are found out. The experimental result is established, testifying that acoustic emission of optical breakdown of sea water at presence and at absence of ultrasound essentially exceeds acoustic emission in fresh water. Atomic lines of some chemical elements like a Sodium, Magnesium and so on were investigated for laser breakdown of water with ultrasound field. The effect of magnification of this lines resolution for salt water in ultrasound field was obtained. It is shown, that the method of registration of acoustic emission from a breakdown zone allows to investigate thresholds and dynamics of laser breakdown which will be in accord with high-speed optical methods. The revealed possibility of application of acoustic emission for breakdown and course diagnostics cavitation in opaque environments is practically important.

Novel NWV Procedure for Characterizing Nonlinear Systems with Memory for Combating and Reducing the Curse of Dimensionality

A. Nuttall, R. Katz, D. Hughes and R. Koch

Naval Undersea Warfare Center Division, 1176 Howell Street, Newport RI, Newport, RI, AK 02841, USA
derke.hughes@navy.mil

A generalized model for characterizing nonlinear systems was initially proposed by Italian mathematician and physicist Vito Volterra (1860-1940), in which a translated version was published in 1959 [1], and further developed by American mathematician and MIT Professor Norbert Wiener (1894-1964) and published in 1958 [2]. More recently, Albert H. Nuttall, a coauthor on the present article working with the Navy, has made new inroads in applying the Wiener-Volterra model to real world problems by significantly reducing the computational workload for characterizing nonlinear systems with memory. In this presentation, we give a general description of a nonlinear system model to third order, which we term the Nuttall-Wiener-Volterra model (NWV) after its co-founders. In this formulation, two measurement waveforms on the system are required in order to characterize a specified nonlinear system under consideration: an excitation input, $x(t)$ (the transmitted signal) and a response output, $z(t)$ (the received signal). Given these two measurement waveforms for a given propagation channel, a kernel or channel response, $h = [h_0, h_1, h_2, h_3]$ between the two measurement points, is computed via a least squares approach that optimizes modeled kernel values by performing a best fit between measured response $z(t)$ and a modeled response $y(t)$. New procedures developed by A. Nuttall are invoked to significantly diminish the exponential growth of the computed number of kernel coefficients with respect to second and third order in order to combat and reasonably reduce the curse of dimensionality. These techniques, among others, include: maximally-sparse sampling of the kernels (first-, second-, and third-order), combatting ill-conditioning on its own terms, and realizing an exponential slowdown of the growth problem. Footnotes [1] Volterra, V., Theory of Functionals and Integral and Integro-Differential Equations, Dover Publications, New York, 1959. [2] Wiener, Norbert, Nonlinear Problems in Random Theory, Technology Press of Massachusetts Institute of Technology, 1958.

Hydrodynamic aspects of explosive volcanic eruptions

V. Kedrinskiy

Lavrentyev Institute of Hydrodynamics, SB RAS, Lavrentyev prospect 15, 630090 Novosibirsk, Russian Federation
kedr@hydro.nsc.ru

The states of compressed magmatic melt and of flow structure in a channel at explosive volcanic eruptions are numerically analyzed within the framework of the model of high-speed hydrodynamics of multi-phase processes. It's well known that the magmatic melt is saturated by gas and micro-crystallites and the dynamics of its state is characterized phase transitions, diffusive processes and bubbly cavitation development under a decompression wave formed in the result of volcanic channel depressurization. At that the magmatic melt viscosity turn out to be changed by the orders of magnitude. The structure dynamics of such kind flow is considered on the base of the multi-phase homogeneous-heterogeneous physic-mathematical model which includes the conservation laws for mean characteristics (pressure, mass velocity and density). The model is supplemented by the kinetics equations, which take into account the physical processes that occur in the compressed magma during its explosive decompression under a volcanic eruption. According to previous studies the micro-crystallites saturating the magma can become new cavitation nuclei and significantly increase their density per volume unit of melt under the decompression wave relatively to the data predicted by the homogeneous nucleation model. The paper presents one of the recent results concerning the cyclicity problem of ash cloud ejections at explosive eruption. Numerical investigations of the flow structure were carried out for a 1-km height of magmatic melt column compressed up to 170 MPa and saturated by a water (5.7 %, wt) in a volcano channel. It was shown that the nuclei density increase by one or two orders of magnitude leads to formation of zone with anomalously high parameters of flow. The latter exceeds the corresponding magnitudes outside this zone at least by an order. As follows from the calculations the saturation zone with anomalous parameters is located in the vicinity of the free surface of a cavitating magma column. Zone is formed by diffusive flows redistribution and by the change of distribution of main characteristics (such, for example, as mass velocity and volumetric gas concentration) in the abnormal zone from a gradual increase to the jump of gradients values of mentioned characteristics. In the result of the analysis the cyclic ejections model was developed. According to the model, the formation of the anomalous zone with an jump of mass velocity in the flow is finalized by instantaneous discontinuity on the level of the mass velocity jump and by a simultaneous "explosive" transformation of the anomalous zone to a gas-droplet system with a subsequent its ejection and by formation of a free surface on the discontinuity boundary. The calculations of the dynamics of the magma column state remaining in the channel showed that the typical structure of the flow and its anomalous zone with jumps of the main characteristics of flow is again recovered in the vicinity of new free surface. We have the base to conclude that the cyclicity mechanism is triggered and determined by the mere evolution of the cavitation process under specific features of the magmatic melt. The cyclic ejections regime developing under explosive volcanic eruption can be considered as self-sustained one.

Multimode Nonlinear Resonant Ultrasound Spectroscopy (NRUS): From the 1D to 3D Characterization of the Elastic NonlinearityM. Remillieux^a, T. Ulrich^a, C. Lake^a, C. Payan^b and P.-Y. Le Bas^a^aLos Alamos National Laboratory, Geophysics Group (EES-17), M/S: D446, Los Alamos, NM 87545, USA; ^bAix Marseille Université, LMA UPR CNRS 7051, 13402 Marseille, France

mcr1@lanl.gov

Nonlinear Resonant Ultrasound Spectroscopy (NRUS) has been used extensively over the last two decades to quantify, through the nonlinear parameter α , the hysteretic nonlinearity of materials for geophysical, biomedical, and civil engineering applications. This technique relies on the variations of the damping and frequency of a resonance mode with the amplitude of this mode. A typical NRUS experiment is conducted on a long bar using its first longitudinal mode. In some experiments, higher order modes have been used because the nonlinearity was more pronounced but the type of motion involved has not been characterized. The parameter α measured from these experiments is then used to calibrate a 1D model of the non-classical nonlinearity. As a first step towards extending this model from 1D to 3D, experiments were conducted on long bar samples (assumed to be macroscopically isotropic) where modes are excited selectively and the type of motion involved in each mode is well characterized. In this simple isotropic case, longitudinal and torsional motions are decoupled in order to find the α_{11} and α_{44} parameters that correspond to the compression (C_{11}) and shear (C_{44}) moduli, respectively. A first set of NRUS experiments is conducted using only the longitudinal modes of the sample to compute the α_{11} parameter. The value of α_{11} with respect to the order of the longitudinal mode selected for the analysis is also studied. A second set of NRUS experiments is conducted using only the torsional modes of the sample to compute the α_{44} parameter. Last, a discussion is given on the possibility to predict what value of the α parameter would be measured using a bending mode of the bar, since longitudinal and torsional motions coexist in such a mode.

Coda Wave Interferometry Technique for Nonlinear Defects' Localization in composite plates

A. Trifonov, O. Bou Matar, N. Smagin and V. Aleshin

IEMN / Ecole Centrale de Lille, IEMN, LCI, Avenue Poincaré, Cité Scientifique, 59652 Villeneuve D'Ascq, France
atrifonov90@mail.ru

We present an original method combining Coda Wave Interferometry (CWI), a sensitive ultrasound technique for detection of weak and local changes in complex inhomogeneous media, and Time Reversal (TR) acoustics for structural health monitoring of airplane constructions. In this technique, we measure small variations of the time delay and the envelope of the coda wave induced by its nonlinear interactions with a pump wave with increasing amplitude [Y. Zhang et al. "Nonlinear mixing of ultrasonic coda waves with lower frequency-swept pump waves for a global detection of defects in multiple scattering media," *J. Appl. Phys.* 113, 064905 (2013)]. The measured variations increase with the quantity and density of the nonlinear scatterers, i.e. the defects. In media that don't contain any nonlinear scatterers, i.e. in intact samples, no nonlinear interactions are observed. Moreover, Time Reversal gives a means to concentrate the pump wave in a given region, thus providing an opportunity to realize a localized Coda Wave Interferometry analysis, leading to a localization of the defect in the studied sample. We also introduce the possibility to delay the coda wave probing relatively to the pumping, enabling the study of slow dynamics effects. Indeed, it is shown in glass plates with a localized cracked zone that after switching the pump off, probe signal continues to undergo the influence of the pump. The dependencies of Coda Wave Interferometry parameters with different time delays of probe wave relative to the pump wave are measured. We observe a saturation level of the effect followed by a decay after switching the pump off that is linear in a log scale, a behavior typical of slow dynamics effects in cracked materials. Moreover, the use of a pump wave with a frequency corresponding to a Localized Defect Resonance [I. Solodov, J. Bai, and G. Busse, "Resonant ultrasound spectroscopy of defects: Case study of flat-bottomed holes," *J. Appl. Phys.* 113, 223512 (2013)] increases the sensitivity of the method. Results of the use of the developed technique on 30 x 30 cm composite plates of 2.7 mm thickness with localized 20 x 20 or 35 x 35 mm square defects is presented. This work was supported by the EC FP7-AAT-2012-RTD-1 ALAMSA project.

We. 17:20 Amphi 2

Non-destructive evaluation methods

DAET Monitoring Targeting Quality Control of Complex Industrial Products ManufacturingC. Trarieux^a, M. Defontaine^a, H. Moreschi^a and S. Callé^b^aRheawave, Bâtiment Vialle, 10 bd Tonnellé, 37032 Tours, France; ^bINSERM U930 - Université François Rabelais de Tours, Bâtiment Bretonneau, 10 bd Tonnellé, 37032 Tours, France

trarieux.chloe@gmail.com

Few tools have been developed for industrial quality control of textures using the viscoelastic properties assessment. The use of non-contact acoustic techniques offers a clear advantage in industries meeting health and safety standards such as cosmetics and food domains.

Dynamic Acousto-Elastic Testing (DAET) is a "pump-probe" method transmitting simultaneously a low-frequency compression/expansion pump wave and ultrasound longitudinal pulses. A related model has been developed to identify from the DAET measurement nonlinear elastic ($B/A, C/A$) and viscous ($\omega\eta_B/A, \omega\eta_C/A$) parameters, derived from the variations of the complex longitudinal modulus [1].

We propose to present nonlinear viscoelastic measurements obtained in three different time-dependent experiments: 1/ sol-gel transition in silicone polymerization, 2/ percolation threshold in glass beads, and 3/ compaction and creaming in plain and hollow glass beads. In the first experiment, the DAET sol-gel transition time (50 min) has been compared to standard rheology and linear acoustic measurements. In the second experiment, we observe a transition from classical to non-classical viscoelastic nonlinearities, as soon as the percolation threshold is reached (51 to 56 %). Finally, the third experiment shows a significant and reproducible monitoring of hollow glass beads creaming thanks to three orders of viscoelastic nonlinear parameters.

[1] C. Trarieux, S. Callé, H. Moreschi, G. Renaud, and M. Defontaine, Appl. Phys. Lett. 105, 264103, 2014.

Nonlinear Ultrasonic Phased Array Imaging of Closed Cracks Using Global Preheating and Local Cooling

Y. Ohara, K. Takahashi, Y. Ino and K. Yamanaka

Tohoku University, 6-6-02 Aoba, Aramaki-aza, Aoba-ku, 980-8579 Sendai, Japan

ohara@material.tohoku.ac.jp

Crack depth can be measured by ultrasound if cracks are open, since ultrasound is strongly scattered by the crack tip. However, if cracks are closed because of compressive residual stress and/or the oxide films generated between the crack faces, ultrasonic inspection causes the underestimation or nondetection of cracks since ultrasound penetrates through the closed crack. To measure closed crack depths, two nonlinear ultrasonic methods have been mainly developed. One is a method of using a large-amplitude incidence to induce the interaction of the incident wave with closed cracks. The other is a method of applying tensile stress to closed cracks to temporarily open them. As the latter method, we proposed a crack opening method (GPLC) [Y. Ohara, et al., APL 103(2013)031917] that combines global preheating (GP) and local cooling (LC). In GPLC, after GP of the specimen, the top surface of the specimen is locally cooled by a cooling spray, which can cool the specimen to 218 K. The vicinity of the top surface thermally contracts, and thereby, tensile thermal stress is applied to the closed crack by a principle similar to that of a three-point bending test. Here, the tensile thermal stress applied can be controlled by varying the GP temperature since the tensile thermal stress depends on the temperature difference between the top surface and the crack area. In this study, we combined GPLC with linear phased array (PA). As a result, a tightly closed fatigue crack was visualized in PA images by opening the crack with the tensile thermal stress induced by GPLC, although the conventional method of using only local cooling could not fully open the crack. In addition, we propose an estimation method of crack closure stress (CCS), which is an important parameter that affects crack propagation rate. Here, we assumed that the crack appears in PA images after the thermal stress induced by GPLC exceeds CCS. Therefore, we calculated the thermal stress induced by GPLC using an analytical solution and thereby estimated CCS. Then, to validate the CCS estimation method, we compared the temporal variation in crack depth observed in the PA images with that calculated based on the analytical solutions. As a result, we demonstrated that the experimental results agreed well with the analytical results. Furthermore, we applied GPLC to coarse grained stainless steel specimen with a closed fatigue crack. Before applying GPLC, the crack was not imaged by PA. This shows that the crack was tightly closed. Then, by applying GPLC, the crack was imaged by PA. However, it was difficult to identify the crack tip because the signal-to-noise ratio was not high due to the strong linear scattering at coarse grains. Therefore, we applied the load difference phased array (LDPA) [Y. Ohara, et al., Ultrasonics 51(2011)661], which is based on the subtraction between PA images at different loads. As a result, we succeeded in accurately measuring closed crack depths. Thus, we demonstrated that the combination of GPLC and PA is useful in accurately measuring closed cracks and in estimating CCS.

Numerical simulation of weakly nonlinear acoustic propagation in bubbly liquid

J.-B. Doc, J.-M. Conoir, R. Marchiano and D. Fuster

Institut Jean le Rond d'Alembert, 4, Place Jussieu, 75252 Paris Cedex 05, France

jbdoc@dalembert.upmc.fr

The weakly nonlinear propagation of acoustic waves in bubbly liquid is numerically investigated using a hydrodynamic model based on the averaged two-phase fluid equations, coupled to the Rayleigh-Plesset equation modelling the bubble dynamic response within a computational cell. A finite-difference scheme is used to solve the motion equations of the fluid phase. On each time step, the Rayleigh-Plesset equation is locally solved by a Runge-Kutta method with adaptive step. Perfectly matched layers are used to bound the numerical domain. To observe the wave dispersion, a one-dimensional Gaussian pressure pulse is sent in a bubbly liquid at rest.

The theoretical solution obtained in the linear regime is used to validate the simulation method of the coupled phase model. When the initial amplitude of the pressure disturbance is sufficiently small, the phase velocity and attenuation of the acoustic waves are computed and compared to the multiple scattering theory. A good agreement is observed for several bubble parameters. Two resonance frequencies are observed on the pressure, one related to the Minnaert frequency, the other to a minimum of the group velocity. The gap between these two resonances is shown to depend on the bubble concentration.

When the amplitude of the initial pressure disturbance becomes of the order of the static pressure, the generation of higher harmonics is observed not only for the Minnaert resonance but also for the resonance associated to the minimum of the group velocity. This result can be explained by a combined effect of two factors, the non-linearity and the multiple scattering.

Second-Harmonic Generation by a Single Layer of BubblesO. Lombard^a, C. Barriere^b and V. Leroy^a^aUniversité Paris Diderot, 10 rue Alice Domon et Leonie Duquet, 75013 Paris Cedex 13, France; ^bInstitut Langevin, 1 rue Jussieu, 75005 Paris, France

olivier.lombard@univ-paris-diderot.fr

In acoustics, bubbles are known for being strong nonlinear scatterers, with a well-documented Minnaert resonance. This property is actually used in medical ultrasound [1], and nonlinear phenomena, such as phase conjugation [2] or second-harmonic generation [3], had been reported in bubbly liquids. However, the parameters of the bubbly medium (gas concentration, bubble size) and its nonlinear properties have not been clearly related.

Using a perturbative approach, we have study the theoretical nonlinear response of a single layer of identical bubbles, impinged by a plane wave. This simple situation gives an insight on the subtle interplay between the nonlinear response of the bubbles and the multiple scattering of sound waves in the medium. In particular, our model shows that the amplitude of the second-harmonic signal generated by the layer is not proportional to the number of nonlinear sources: an optimal concentration of bubbles is predicted. Stable and well-characterized samples were obtained by injecting 70- μm radius bubbles in a yield-stress fluid [4]. Experiments were then performed on layers of bubbles with different concentrations, insonified at the Minnaert resonance frequency (45 kHz), to check the model prediction of an optimal concentration for the second-harmonic generation.

[1] J. Powers et al, *Medica Mundi* 44 (2000) [2] D.V. Vlasov et al, *Sov. Phys. Acoust.* 29 (1983) [3] J. Wu and Z. Zhu, *J. Acoust. Soc. Am.* 89 (1991) [4] Leroy et al, *J. Acoust. Soc. Am.* 123 (2008)

Cavitation inception by the backscattering of pressure waves from a bubble interface

H. Takahira, T. Ogasawara, N. Mori and M. Tanaka

Osaka Prefecture University, 1-1 Gakuen-cho, Naka-ku, 599-8531 Sakai, Japan

takahira@me.osakafu-u.ac.jp

When a focused ultrasound is emitted in water, acoustic cavitation is generated near the focus. Maxwell, et al. (2011) showed that secondary cavitation was generated successively near a primary cavitation bubble which was generated by the negative pressure part of the incident focused ultrasound. They suggested that the secondary cavitation was caused by the backscattering of the incident ultrasound wave from the primary cavitation bubble. Such secondary cavitation might be useful for the energy exchange due to bubble oscillations in High Intensity Focused Ultrasound (HIFU). Thus, the control of secondary cavitation inception was conducted experimentally by changing the waveform of the incident focused ultrasound (Yoshizawa, et al., 2012). However, the details of cavitation inception by backscattering of pressure waves are still open. In the present study, therefore, the cavitation inception by the backscattering from a bubble is investigated experimentally and numerically.

In the present experiment, a laser-induced bubble which is generated by a pulsed focused laser beam with high intensity is utilized for a primary cavitation bubble. After generating the bubble, a focused ultrasound is emitted to the bubble. The primary bubble volume when the wave front of ultrasound reaches the laser-induced bubble can be controlled by changing timings of the laser beam and ultrasound emissions. The typical bubble size is of the order of 1 mm and the frequency of the ultrasound is 1.1 MHz. The acoustic field and the bubble motion are optically observed with a high-speed video camera in the shadowgraph method. We first confirmed the ultrasound condition in which a primary cavitation bubble does not appear with moderate amplitude pressure when a laser-induced bubble is absent. Under the same ultrasound condition, however, the secondary cavitation is generated in the backscattering region due to the presence of the laser-induced bubble. The relationship between the primary bubble volume and the secondary cavitation area is investigated. Also, the growth of cavitation bubble cloud is analyzed with the image processing method.

The direct numerical simulations are also conducted for the backscattering of incident pressure waves from a bubble in order to evaluate quantitatively a pressure field near the bubble for a better understanding of the formation of secondary cavitation by using the ghost fluid method. It is shown that the ratio of a bubble collapse time t_0 to a characteristic time of wave propagation t_s , $\eta = t_0/t_s$, is an important determinant for generating negative pressure region by backscattering. When η is of the order of 10, high negative pressures are generated in a relatively smaller volume during shorter duration leading to cavitation inception. We also evaluate a negative pressure volume V and a duration of negative pressure τ by the backscattering. The results also show that the product of V and τ , which is an indicator of probability of cavitation inception in the classical homogeneous nucleation theory, takes the local maximum in terms of η .

The sessile liquid droplet as a geometrically self-reconstructed nonlinear acoustic resonatorA. Begar^a, V. Mozhaev^a and I. Nedospasov^b^aLomonosov Moscow State University, Faculty of Physics, Leninskie Gory, 119991 Moscow, Russian Federation;^bKotel'nikov Institute of Radio-engineering & Electronics of RAS, Mokhovaya 11-7, 125009 Moscow, Russian Federation

annazyr@mail.ru

The study of peculiarities of resonant acoustic vibrations in liquid microdroplets lying on the solid substrates is important to develop new microfluidic acoustoelectronic devices of the "labs-on-chips" type, and also to improve the acoustical methods for measuring microdroplet properties and parameters. The present work is devoted to the theoretical study of nonlinear effects in acoustic thickness resonances of a small droplet on the rigid substrate. The method of perturbation theory based on the application of the complex reciprocity relation (Auld, 1973) is used to take into account the nonlinearity, the ultrasonic absorption in the droplet due to liquid viscosity and other fine effects. To find an initial linear approximation to the solution of the nonlinear problem, the droplet on the substrate is considered as an acoustic analog of laser resonators. This allows the parabolic-equation formalism popular in the theory of laser resonators to be applied to the case of the droplet. The nonlinearities are taken into account only in the boundary conditions. These are a nonlinear relation between the droplet curvature radius and its surface profile, and also the force of acoustic radiation pressure. The equations of slowly varying amplitudes for coupled vibrations at the fundamental frequency and second harmonic and for quasi-static component of the wave fields are derived using the perturbation theory. The simultaneous solution of these equations describes the known amplitude frequency effect with amplitude jumps on resonance curves of the same type as follows from the solutions of Duffing's differential equation. The feature of oscillating system under study is that this is a multimode nonlinear system with distributed parameters, with closely-spaced and partly overlapping resonance peaks of adjacent modes, that implies a possibility of abrupt switching from one mode of vibration to another by gradually changing the frequency of the external force. One more remarkable feature of the system under consideration is that the droplet upper surface is very easily deformable. As a consequence, the localized acoustic vibrations excited in the droplet can produce the significant stationary distortions of this surface forming the bump on it. Thus, the droplet on the substrate is a quite uncommon nonlinear resonator, in which the accumulating vibrations are able to move and to change the shape of one of reflective boundaries. This means an interesting and new possibility of abrupt switching from mode to mode by gradually changing the amplitude rather than the frequency of the external force.

Theory and experimental demonstration of a single beam acoustical tweezersD. Baresch^a, J.-L. Thomas^b and R. Marchiano^c^aINSP, IJLRDA, UPMC, 4 place Jussieu, 75005 Paris, France, Metropolitan; ^bInstitut des NanoSciences de Paris, UPMC, boîte courrier 840, 4 place Jussieu, 75005 Paris, France, Metropolitan; ^cInstitut Jean le Rond d'Alembert, 4, Place Jussieu, 75252 Paris Cedex 05, France

jean-louis.thomas@upmc.fr

The radiation pressure exerted by light or sound has long been recognized to substantially affect the dynamics of tiny particles. Optical tweezers use the radiation pressure of a single beam of light to trap a particle in three dimensions. They are excellent tools to handle particles ranging in size from a few micrometers to hundreds of nanometers but become inefficient and severely damaging on larger objects. On the other hand, at equal power, acoustical forces overtake by 5 orders of magnitude those of optical ones on macroscopic objects. Acoustical levitation is an efficient technique for container-less processing and transportation of macroscopic matter in air, while acoustophoresis has provided a powerful strategy for on-chip manipulation, sorting and mixing of many microscopic particles and living organisms. Although these ultrasonic techniques are becoming very popular, the various drawbacks in the state of the art studies using standing wave systems, have prohibited accurate manipulation of a single particle in three dimensions. For the first reported time, we demonstrate the trapping of elastic particles by the large radiation force of a single acoustical beam in three dimensions. The acoustical tweezers presented here can push, pull and accurately control both the position of a unique particle and the forces exerted under damage-free conditions. The stable potential well for elastic particles is obtained with a forward propagating helicoidal beam. Various features are promising for the development of a large variety of systems in biology, chemistry and physics where small particles play an important role, in particular, for single particle biophysical essays.

Rotating small solid objects in liquids by a focused vortex ultrasound beamO. Sapozhnikov^{a,b}, M. Terzi^a, A. Nikolaeva^c, S. Tsysar^c and A. Maxwell^b

^aPhysics Faculty, Moscow State University, Leninskie Gory, 119991 Moscow, Russian Federation; ^bCenter for Industrial and Medical Ultrasound, Applied Physics Laboratory, University of Washington, 1013 NE 40th Street, Seattle, WA 98105, USA; ^cPhysics Faculty, Moscow State University, Leninskie gory, 119991 Moscow, Russian Federation
oleg@acs366.phys.msu.ru

It is well known that sound, and generally any wave, carries energy and momentum. Dissipation of wave energy gives rise to heating of the propagation medium, whereas the existence of wave momentum becomes apparent in the radiation pressure phenomenon, in which the wave creates a force on an absorbing or scattering object. Both effects are well-known and used in many applications of acoustic waves, especially in megahertz-frequency ultrasonics. Less widely known is the fact that a sound wave may also carry angular momentum. The existence of this angular momentum can be made evident by transferring it to small absorbing or scattering particles, which are thus subjected to a torque. Such phenomena became recently popular in laser physics, e.g. in relation to the optical tweezers application. Wave beams that carry angular momentum are called vortex beams; they have a wavefront in the form of a spiral surface, so that the phase in the transverse plane increases uniformly with angle around the beam axis in a way that after a complete turn it is changed by an integer multiple of 2π . This integer is known as the 'topological charge'. The beam has typically a ring-shaped intensity distribution at the transverse plane with zero intensity at the beam axis. To create such an ultrasound beam experimentally, one may either employ a phased array or transmit a beam of a single-element source through a specially designed phase plate that creates proper distribution of the wave phase transverse to the propagation direction. Both possibilities have been employed in the current study. To create the desired ultrasound beam using an array approach, a 1.5-MHz focused transducer has been developed that consisted of 12 sectors with electrical control of the amplitude and phase applied to each element. The applied phase delay increased linearly with each adjacent sector, with a condition that the total shift around the circumference was an integer multiple of 2π . In another series of experiments, a single element 1-MHz transducer was used in combination with a plastic 12-sector plate, with the sectors' thicknesses being properly chosen to create the vortex-type phase distribution for the transmitted wave. Experiments were conducted in water tank with beams focused at spherical target beads made of different materials with diameters of several millimeters. To prevent axial motion, target beads were positioned on a flat gel in a degassed water bath, along with the transducer. In a separate experiment, the beam was focused at a free surface of water, where the target particles were floating. Theoretical modeling predicted transverse trapping at the vortex beam focal plane, with a force dependent on the incremental phase shift between elements, frequency, particle size and material. Experiments with target beads confirmed that the beads can be trapped, controllably translated along the gel surface in any direction transverse to the beam, and rotated with a different angular speed that depended on the beam topological charge. Work was supported by RFBR 14-02-00426, NIH EB16118, DK43881, DK92197, and DK07779, and NSBRI through NASA NCC 9-58.

Theoretical investigation of the mechanisms involved in the modification of the cavitation threshold by multifrequency excitations

M. Guédra^a, C. Desjouis^b, C. Inserra^c, J.-C. Béra^c and B. Gilles^c

^aINSERM, U1032, 151 Cours A. Thomas, 64424 Lyon, France; ^bLaboratoire de Mécanique des Fluides et d'Acoustique, Ecole Centrale de Lyon, 36 Avenue Guy de Collongue, 69134 Ecully, France; ^cUniversité Claude Bernard Lyon 1, INSERM U1032, 151, cours Albert Thomas, 69424 Lyon, France

bruno.gilles@inserm.fr

Stimulating cavitation activity can be interesting in a number of industrial or medical applications of ultrasound cavitation. Several studies have shown, in different configurations, that using multifrequency excitation waveforms instead of classical monofrequency waves could reduce cavitation threshold and stimulate cavitation activity beyond threshold [1 - 4]. We focus, in this study, on configurations involving similar primary frequency components, for which previous experiments [5] showed that the ratio of cavitation thresholds obtained with mono- and bi-frequency excitations depends on the value of the monofrequency threshold intensity itself: A bifrequency excitation can decrease the cavitation threshold only if sufficiently high acoustic intensities are involved, which means that nonlinear effects are involved in the process. In order to understand the mechanisms underlying such effects, numerical simulations, based on the Keller-Miksis equation for an isolated air bubble in a fluid submitted to an oscillating pressure field, have been performed. Comparison of cavitation thresholds obtained with a monofrequency excitation at 500 kHz and with several bifrequency excitations with difference frequency ranging from 5 kHz to 200 kHz, have been done. For low peak pressure excitations, in the linear or quasi-linear regime of oscillations of the bubble, weaker oscillation amplitudes of the radius $R(t)$ are observed in the case of a bifrequency excitation. As soon as the excitation level approaches the cavitation threshold, larger $R(t)$ values can be achieved with a bifrequency excitation leading to a slight decrease in the cavitation threshold for that case. For specific radii corresponding to a resonance condition at the difference frequency Δf , stronger decreases in the cavitation threshold are obtained but they don't lead to an overall reduction of the cavitation threshold in a medium with micrometric cavitation nuclei. Preliminary results concerning the influence of the difference frequency value on this decrease show that this dependence is very weak for the whole range of Δf values studied.

[1] G. Iermetti, P. Ciuti, N. V. Dezhkunov, M. Reali, and A. Francescutto. Enhancement of high-frequency acoustic cavitation effects by a low-frequency stimulation. *Ultrasonics Sonochemistry*, 4(3):263-268, Jul 1997. [2] J. Holzfuss, M. Rugeberg, and R. Mettin. Boosting sonoluminescence. *Phys. Rev. Lett.*, 81(9):1961- 1964, 1998. [3] S. Umemura, K. Kawabata, and K. Sasaki. In vitro and in vivo enhancement of sonodynamically active cavitation by second-harmonic superimposition. *Journal of the Acoustical Society of America*, 101(1):569- 77, Jan 1997. [4] B. Gilles, J.-C. Béra, J.-L. Mestas and D. Cathignol. Reduction of ultrasound inertial cavitation threshold using bifrequency excitation. *Appl. Phys. Lett.*, 89 :094106, 2006. [5] I. Saletes, B. Gilles and J.-C. Béra. Promoting inertial cavitation by nonlinear frequency mixing in a bifrequency focused ultrasound beam. *Ultrasonics*, 51 :94-101, 2011.

Factors Affecting the Cavitation Conditions ReproducibilityN. Dezhkunov^a, A. Francescutto^b, A. Nikolaev^c and A. Kotukhov^d^aBSUIR, P. Brovka st.6, 220013 Minsk, Belarus; ^bUniversity of Trieste, P. Brovka st.6, 220013 Minsk, Italy; ^cMoscow State University, Moscow, Russian, Leninskie gory 1, 119991 Moscow, Russian Federation; ^dBSUIR, P. Brovka St.6, 220013 Minsk, Belarus

dny@bsuir.by

The influence of different factors on the reproducibility of cavitation conditions have been studied experimentally. It has been shown that the most strongly influencing factors are as following: uncontrolled deviation of the resonance frequency of the transducer (transducers) from the frequency of the driving voltage, variation of conditions of reflection of the ultrasound in the reactor, variations of the gas concentration and nuclei size distribution in liquid samples, variation of the liquid height over the transducers. The deviation of the resonance frequency of the transducer is observed if the power supplier consists of the driving generator and an amplifier. Such systems are used often in experimental investigations. Reasons which may cause deviations of the transducer resonance frequency are as following. 1) Change in average mechanical stresses acting on the piezoplates of the transducer. 2) Change of the load on the transducer. It happens, for example, due to variation of the wave resistance of the liquid when bubbles concentration in cavitation zone is varied or when height of the liquid over the transducer is varied. 3) Heating the transducer due to an increase of the liquid temperature. Deviation of the resonance frequency from the frequency of the driving voltage due to above reasons leads to the increase of heat losses in transducer, its further heating and further deviation of the frequency. As a result acoustic power transferred into the liquid will drop significantly but heating of the liquid and power consumed by the transducer will not. Uncontrolled variations of the gas concentration and cavitation nuclei size distribution in the liquid sample is caused by the degassing of the liquid under ultrasound or when changing samples of the liquid in the chamber. As a result cavitation activity will be varied during an experiment or from one experiment to another even at constant ultrasound intensity. Nuclei generated during sonification strongly influence subsequent measurements, if the rest time between measurements is not long enough. Variations of conditions of reflection of the ultrasound wave in the reactor are caused by uncontrolled variations the height of the liquid in the same reactor, by introducing solid samples in the reactor, or due to the changes the sizes and geometry of reactors if measurements are produced in different reactors.

Propagation of acoustic shock waves between parallel rigid boundaries and into shadow zonesC. Desjouis^a, S. Ollivier^a, O. Marsden^b, D. Dagna^c and P. Blanc-Benon^a^aLaboratoire de Mécanique des Fluides et d'Acoustique, Ecole Centrale de Lyon, 36 Avenue Guy de Collongue, 69134 Ecully, France; ^bEcole Centrale de Lyon, 36 avenue Guy de Collongue, 69130 Ecully, France; ^cLMFA, Ecole Centrale de Lyon, 36 avenue Guy de Collongue, 36 avenue Guy de Collongue, 69134 Ecully, France

cyril.desjouis@ec-lyon.fr

The study of acoustic shock propagation in complex environments is of great interest for urban acoustics, but also for source localization, an underlying problematic in military applications. To give a better understanding of the phenomenon taking place during the propagation of acoustic shocks, laboratory-scale experiments and numerical simulations were performed to study the propagation of weak shock waves between parallel rigid boundaries, and into shadow zones created by corners. In particular, this work focuses on the study of the local interactions taking place between incident, reflected, and diffracted waves according to the geometry in both regular or irregular - also called Von Neumann - regimes of reflection. In this latter case, an irregular reflection can lead to the formation of a Mach stem that can modify the spatial distribution of the acoustic pressure. Short duration acoustic shock waves were produced by a 20 kilovolts electric spark source and a Schlieren optical method was used to visualize the incident shockfront and the reflection/diffraction patterns. Experimental results are compared to numerical simulations based on the high-order finite difference solution of the two dimensional Navier-Stokes equations.

The authors acknowledge the support of the french Agence Nationale de la Recherche (ANR), under grant ANR-12-ASTR-0038 (project LORETA).

Benchmark problems for long range atmospheric infrasound propagationR. Sabatini^a, O. Marsden^b, C. Bogey^b and C. Bailly^b^aCEA, DAM, DIF, 91297 ArpaJon Cedex, France; ^bEcole Centrale de Lyon, 36 avenue Guy de Collongue, 69130 Ecully, France

roberto.sabatini@doctorant.ec-lyon.fr

Infrasound signals have long been known to propagate over very large distances in the atmosphere. The accurate numerical prediction of waveforms is a challenging task, due both to the aforementioned long-range propagation, and also to the wide range of physical phenomena involved in the generation of the acoustic signature.

To assess numerical efficiency of propagation solvers, a set of bidimensional benchmark problems for atmospheric infrasound propagation is proposed in the present work. They are designed to underline the most important physical phenomena in a series of configurations of increasing complexity. For each of these benchmark problems, a direct numerical simulation of the full bidimensional Navier-Stokes equations has been performed. Each test case consists of an acoustic source placed at ground level in a realistic atmosphere and with variable amplitude. This acoustic source is implemented as a forcing term in the energy equation. It has a Gaussian spatial envelope with a half-width of 600 m, a dominant frequency of 0.1 Hz and a total emission duration of 10 seconds. The atmosphere is constructed through the definition of vertical temperature and wind profiles which follow the main trends observed from ground up to 160 km of altitude.

Simulations are carried out until 300 source periods on a physical domain of 600 x 160 km². The numerical algorithm is based on high-order optimized spatial finite differences in space, and a Runge-Kutta scheme for time integration. The solver is implemented in OpenCL and executed on an AMD Radeon R9 200 Series GPU, which allows a computational cost of about 5 hours per test case, for simulations with horizontal and vertical spacing of 100 m, and meshes containing about 20 million points.

Numerical results are presented and discussed. Main physical phenomena affecting the acoustic signal recorded at large distances from the source are illustrated, including the refraction due to the atmosphere's temperature gradient, the presence of additional arrivals as a result of the wind profile, and nonlinear waveform modifications.

Th. 10:00 Amphi 2

Nonlinear propagation in fluids 1

Quantitative nonlinearity analysis of model-scale jet noiseB.O. Reichman^a, K.G. Miller^a, K.L. Gee^a, T.B. Neilsen^a and A.A. Atchley^b^aBrigham Young University, Department of Physics and Astronomy, Provo, UT 84602, USA; ^bPennsylvania State University, Graduate Program in Acoustics, University Park, PA 16802, USA
atchley@psu.edu

The effects of nonlinearity on the power spectrum of jet noise can be directly compared with those of atmospheric absorption and geometric spreading through an ensemble-averaged, frequency-domain version of the generalized Burgers equation (GBE) [B. O. Reichman et al., *J. Acoust. Soc. Am.* 136, 2102 (2014)]. The rate of change in the sound pressure level due to the nonlinearity, in decibels/meter, is calculated using a form of the quadspectrum of the pressure and the squared-pressure waveforms. In this paper, this formulation is applied to data from unheated model-scale jets at both subsonic (Mach 0.85) and supersonic (Mach 2.0) velocities. These data have been previously investigated for nonlinear effects using a different quadspectrum-based metric [K.L. Gee et al., *AIP Conference Proceedings*, 1474, 307-310 (2012)] but with a qualitative rather than quantitative approach. For different jet conditions, the rate of change in level due to nonlinearity is calculated and compared with estimated effects due to absorption and geometric spreading. Reasonable bounds are placed on losses due to absorption and spreading for various frequencies and locations. Comparing these losses with the change predicted due to nonlinearity shows the presence of cumulative nonlinearity during propagation into the geometric far field for the supersonic jet.

Soil Plate Oscillator: Modeling Nonlinear Mesoscopic Elastic Behavior and Hysteresis in Nonlinear Acoustic Landmine Detection

M.S. Korman, D.V. Duong and A.E. Kalsbeek

United States Naval Academy, Physics Department, 572 C Holloway Road, Annapolis, MD 21402, USA

korman@usna.edu

An apparatus (SPO), designed to study flexural vibrations of a soil loaded plate, consists of a thin circular elastic clamped plate (and cylindrical wall) supporting a vertical soil column. A small magnet attached to the center of the plate is driven by a rigid AC coil (located coaxially below the plate) to complete the electrodynamic soil plate oscillator SPO design. The mechanical impedance Z_{mech} (force / particle velocity, at the plate's center) vs. frequency is inversely proportional to the electrical motional impedance Z_{mot} . Measurements of Z_{mot} are made using the complex output to input response of a Wheatstone bridge that has an identical coil element in one of its legs. Resonant oscillations measurements (with no soil) before and after a slight point mass loading at the center help determine effective mass, spring, damping and coupling constant parameters of the system. "Tuning curve" behavior of $\text{real}\{Z_{\text{mot}}\}$ and $\text{imaginary}\{Z_{\text{mot}}\}$ at successively higher vibration amplitudes of granular materials (dry sifted masonry sand, table salt, uncooked brown rice), are compared. They exhibit a decrease "softening" in resonance frequency and an increase in the quality Q factor. A bilinear hysteresis model predicts the tuning curve shape for this nonlinear mesoscopic elastic SPO behavior - which also models an actual plastic "inert" VS 1.6 buried landmine. In experiments where a VS 1.6 is buried 8 cm deep in a layer of masonry sand that is supported by a sand foundation placed on a thick concrete slab, the backbone curve (a plot of the peak amplitude vs. corresponding resonant frequency from a family of tuning curves) exhibits mostly linear behavior for "off target" soil surface vibration measurements of a soil layer resonating over a rigid boundary. Backbone curves for "on target" measurements exhibit significant curvature when a soil layer resonates over the compliant top-plate of the landmine. An oscillator with hysteresis modeled by a distribution of parallel spring elements each with a different threshold slip condition seems to describe the "off target" behavior [W. D. Iwan, Transactions of the ASME, J. of Applied Mech., **33**, (1966), 893-900], while a single bilinear hysteresis element describes the "on target" results [T. K. Caughey, Transactions of the ASME, J. of Applied Mech., **27**, (1960), 640-643]. When "off target" resonances have a different backbone curvature than "on the mine" backbone curves, then false alarms may be eliminated due to resonances from the natural soil layering. See [R.A. Guyer, J. TenCate, and P. Johnson, "Hysteresis and the Dynamic Elasticity of Consolidated Granular Materials," Phys. Rev. Lett., **82**, (1999), 3280-3283] for recent models of nonlinear mesoscopic behavior.

3D TREND for crack orientation characterization

P.-Y. Le Bas, T. Ulrich and B. Anderson

Los Alamos National Laboratory, Geophysics Group (EES-17), M/S: D446, Los Alamos, NM 87545, USA

pylb@lanl.gov

In some Non Destructive Evaluation techniques, detecting a crack is only the first step. Some applications like monitoring of used nuclear fuel canister also requires the characterization of the orientation of the cracks if any exist. Here, we show experimental results that expand the Time Reversal Elasticity Nonlinear Diagnostic method (TREND) to obtain the crack orientation information. TREND is based on using time reversal to focus energy at a point of interest and then quantifying the nonlinearity at this point. We will show how Time Reversal can be used to select the orientation of the focus wave to any desired direction and how this, in turn, allows measuring different nonlinear responses according to this orientation and how this could be used to determine the orientation of cracks. This work is supported by the US Department of Energy via the used fuel disposition campaign of the nuclear energy program.

Bulk strain solitons in rods, plates and shells

A. Samsonov, G. Dreiden, I. Semenova and A. Shvartz

The Ioffe Institute, 26, Polytekhnicheskaya st., 194021 St.Petersburg, Russian Federation

samsonov@math.ioffe.ru

Elastic behavior of basic elements of structures - rods, plates and shells - is exhaustively studied, and they are widely used in many applications. However, it is mostly valid for linear elasticity, whereas dynamic nonlinear theory of these elements is still far from being completed. We consider the problems of nonlinear elastic bulk wave generation and observation in these elements in order to show how the waves can be used in various applications in physics and mechanics, in non-destructive evaluation etc. Nowadays the nonlinear dynamic elasticity of rods and plates seems to be developed, and the longitudinal strain solitons can be generated and observed in many problems of nonlinear dynamics and acoustics. We studied recently the soliton propagation along lengthy wave guides, and remarkably small attenuation of solitons was proven in physical experiments. Many laminated composite wave guides (structure elements) are used nowadays for various applications, e.g., aerospace and automotive industries. Being subject to delamination, lengthy layered elements are to be tested, and bulk strain solitons are among prospective instruments for NDT. However, the theory and experiments for strain soliton in a shell remained an unsolved problem until recently, and study of nonlinear bulk wave propagation in a shell attracts essential interest, being related to stability of thin shells and tentative NDT approach. We considered the axially symmetric deformation of an infinite nonlinearly elastic cylindrical shell without torsion. The problem for bulk longitudinal waves is reducible to the one equation, if a relation between transversal displacement and the longitudinal one is found. However, the simplest hypothesis lead to unsatisfactory accuracy in the boundary conditions on free lateral surfaces. We refined the abovementioned relation, providing the validity of the boundary conditions with the desirable accuracy. We applied the Hamilton principle, derived the only nonlinear equation for longitudinal strain and shown that the equation has, amongst others, a bidirectional solitary wave solution, which lead to successful physical experiments. We performed new physical experiments, observed first the compression solitary wave in the duct-like PMMA shell and proved, that there is no tensile area behind the wave, the bulk soliton propagates on a distance many times longer than its wave length, while both its shape and amplitude remain unchanged. Being aimed to propose the bulk strain solitons as an instrument for NDT in solids, we studied numerically the evolution of them, e.g., in a cylindrical shell with local defects of the cross section and shown that the strain soliton undergoes changes in amplitude, phase shift and the shape, that can be estimated. To sum up, now we are able to propose a new NDT technique based on bulk strain soliton propagation in structural elements. Acknowledgement. The support of this study by the Russian Scientific Fund grant no. 14-12-00342 is gratefully acknowledged.

Th. 11:00 Amphi 2

Plenary lecture 5: Douglas Drob

Infrasound remote sensing of the atmosphere

D. Drob

Naval Research Laboratory, Space Science Division, Naval Research Laboratory, Washington, Dc, AK 20375, USA
douglas.drob@nrl.navy.mil

This talk discusses recent research on infrasound acoustic tomography to improve knowledge of the atmosphere from 35 to 150 km. Several recent theoretical and field studies indicate that it is indeed possible to use infrasound signals from geophysical sources such as bolides and volcanic eruptions to revise a-priori estimates of upper atmospheric winds. In these approaches linear ray theory is used to adjust a parameterized atmospheric wind profile to minimize the difference between predicted and observed time delays and direction of arrivals. In this lecture we first describe the current state of a-priori information about the atmosphere. We then examine the appropriateness of simplifying assumptions such range dependence and linear ray theory in these acoustic tomography approaches. In partially we address one of the most important factors neglected in these approaches, the influence of sub-grid scale atmospheric buoyancy oscillations (atmospheric gravity waves). Observations show that their behavior is inherently non-linear as gravity-wave spectral amplitudes saturate in the middle-atmosphere, as well as can become so large as to become dynamically unstable and break-internally with the secondary wave energy generating cascading down into small smaller scales, as well as depositing their momentum into the mean-flow. Recent work has shown that these waves have non-negligible consequences for the prediction of observed acoustic shadow zones, signal-travel times, and observed waveforms. We use quasi-linear gravity wave theory, range dependent acoustic linear ray theory, acoustic Parabolic Equation Fourier waveform synthesis methods, and thermospheric acoustic attenuation models to examine the implications of these waves in the context of both linear- and non-linear acoustic wave theories. We conclude with an example of how the local spectral characteristics of the atmospheres gravity spectrum (known to be intermittent and also vary with season, time-of-day, as well as geographic location) might be inferred from observed infrasound signals.

Acoustic wave equation in bubbly liquid

B. Miao and Y. An

Department of Physics, Tsinghua University, Haidian, 100084 Beijing, China

anyuw@mail.tsinghua.edu.cn

In some cases, a bubbly liquid may be treated as a two-phase fluid mixture and acoustic wave in the bubbly liquid is described by a linear wave equation with sound speed of the two-phase fluid mixture. Since bubble pulsation driven by the acoustic wave exists, the treatment of two-phase fluid mixture is an approximate. More accurate description of acoustic wave in bubbly liquid should be a nonlinear wave equation conjunction with the bubble pulsation equation. As an example, we investigate normal incidence of ultrasonic wave in water to a bubbly liquid layer. Two different methods, with the linear wave equation of two-phase fluid mixture and with the nonlinear equations, are employed in the present numerical simulation. Calculated results show the severe differences exist between two different methods in many cases, even for the case that far away from the resonance frequency. Besides, the numerical results show abundant nonlinear phenomena.

Th. 14:00 Amphi 1 bis

Bubbles and cavitation 2

Dynamics of an aspherical bubble oscillating near a rigid sphere

E. Kurihara

Oita University, Dannoharu 700, 870-1192 Oita, Japan

kurihara@oita-u.ac.jp

In this paper, it is investigated that behaviour of a non-spherical bubble oscillating near a rigid sphere in the framework of the Lagrangian formalism and multi-pole expansion of the bubble boundary.

In this study, modes of shape oscillations are taken into account up to the third oscillation mode (octupole mode) to illustrate the liquid jet formation on the bubble surface.

To account for interaction between the bubble and the rigid sphere, corrections of the velocity potential in a liquid containing the bubble and the sphere will be considered up to terms of fifth order in the inverse separation distance.

Derived equations describes typical bubble behaviour such as volume oscillations, translation, and shape oscillations.

This paper presents the motion of the bubble in the vicinity of the rigid sphere by using numerical computations of the equations.

In particular, it is discussed that the dependencies of bubble behaviour on the density and radius of the sphere.

Nonlinear activity of acoustically driven gas bubble near a rigid boundary

A. Maksimov

Pacific Oceanological Institute, 43, Baltic Street, 690041 Vladivostok, Russian Federation

maksimov@poi.dvo.ru

Although a great deal is known about bubble oscillations in unbounded liquids, it is not very clear to what extent these results are applicable to the sediments acoustics and biomedical technologies that use microbubble contrast agents. In actual practice, contrast agent microbubbles mainly oscillate in the vicinity of, or in contact with a boundary. Experimental studies reveal that the presence of a boundary can produce considerable changes in the oscillation amplitude of the bubble and its scattered echo. The bubble pulsating near a rigid surface is equivalent to two bubbles pulsating in phase in a free space. The effect of a rigid wall on gas bubble dynamics has been evaluated in this approach by accounting for only monopole interactions between the bubble and its mirror image. The theoretical model for the bubble activity near the rigid boundary has been proposed and an analytical solution has been derived. The present study thus fills a gap in the literature, in that it is concerned theoretically with the bubble activity at relatively small distances from the rigid boundary. Our objective is to obtain a closed-form, leading order solution for different modes of bubble oscillations, assuming the long wavelength limit. The derivation uses the Laplace equation for the velocity potential as a starting point. It was shown that the bi-spherical coordinates provide separation of variables and are more suitable for analysis of the dynamics of these constrained bubbles. This coordinate system has been successfully used by Oguz & Prosperetti (1990) in analyzing bubble dynamics near a free surface. Explicit formulas have been derived which describe the dependence of the bubble emission near a rigid wall on its size and the separation distance between the bubble and the boundary. Above the critical pressure threshold, an air bubble driven by ultrasound can become shape-unstable through a parametric instability. The influence of a constraining interface on the threshold of parametric excitation of surface modes has been analyzed. The presence of a bounding surface breaks the symmetry inherent to the problem of oscillations of a single bubble in an unbounded space, and leads to a reduction of possible types of patterns that are formed on the bubble surface above the threshold of parametric instability. Identifying possible patterns provides the interpretation of experimental (optical and acoustic) observations of bubble dynamics near an ultrasonic horn (Birkin et al. 2011). The main purpose of the present study was to reveal how the distance to the boundary affected the parameters of the bubble oscillations. It has been shown that the traditional method taking into account only the monopole component in the interaction between the bubble and its mirror image has a limited range of applicability and can't be applied at distances compared with the size of the bubble.

Th. 14:40 Amphi 1 bis

Bubbles and cavitation 2

Derivation of the nonlinearity parameter B/A of saturated, unconsolidated marine sediments via a statistical approachH. Lee^a, E. Noh^a, W.-S. Ohm^b and O.-C. Kwon^c^aYonsei University, 50 Yonsei-ro, Seodaemun-gu, 120-749 Seoul, Republic of Korea; ^bYonsei University, 50, Yonsei-ro, Seodaemun-gu, 120-749 Seoul, Republic of Korea; ^cAgency for Defense Development, 18 Hyun-dong, Jinhae-gu, 645-600 Changwon, Republic of Korea

ssevi2@yonsei.ac.kr

Marine sediments are known to exhibit the nonlinearity parameter B/A that is a few orders of magnitude greater than that of homogeneous fluids and solids. The enormous value of B/A is particularly sensitive to the state of grain contacts. Early works [Hovem, 1979 and McDonald, 2009] theoretically investigate the B/A of marine sediments. However, few studies have addressed how the random nature of grain contacts affect B/A . Here we develop a model for the B/A of saturated, unconsolidated marine sediments, which accounts for the random grain contacts. The number of contacts on each grain, the distribution of contact stress between grains, and the grain size distribution are treated statistically. The quadratic nonlinearity of the equivalent suspension of grains and the interstitial fluid is then combined with the nonlinearity arising from the random Hertzian contacts. Predictions of B/A seem to compare favorably with the measured values based on the second harmonic generation.

Development of Nonlinear Acoustic Propagation Analysis Tool toward Realization of Loud Noise Environment in Aeronautics

M. Kanamori, T. Takahashi and T. Aoyama

Japan Aerospace Exploration Agency, 7-44-1, Jindaijihigashi-machi, Chofu, 182-8522 Tokyo, Japan

kanamori.masashi@jaxa.jp

Due to a slight nonlinearity but relatively low amplitude of pressure fluctuations, it is one of the most difficult situations to numerically predict loud noise environment generated from a propulsion system of aircrafts or rockets. Propulsion devices attached on such systems make tremendous amount of noise, the level of which reaches more than 150dB OASPL. Needless to say, predictions based on the linear theory are of course useless in such an environment. As a result, one has to find other techniques which can take the effect of nonlinearity into account like computational fluid dynamics (CFD) analyses. However, it is quite a tough work for CFD analyses to compute the sound because the amplitude of such loud sounds is much smaller compared with the atmospheric pressure itself. One therefore must conduct the analyses with the combination of highly accurate computational scheme (e.g. compact differencing schemes) and sufficient amount of grid point. According to the brief estimate, prediction of the sound environment around the launch pad up to the frequency of 2kHz requires ten billions of grid point even with the use of highly accurate compact difference schemes, which is not realistic from a view point of engineering. Such a situation is just within the scope of nonlinear acoustics. Shown in this paper is an introduction of an innovative tool for realizing sufficiently accurate simulations of such an environment with a devastating speed compared with CFD analyses, which can be achieved by means of HOWARD approach proposed by Dagrau et al. in 2011. In HOWARD approach, so-called one-way form is introduced by transforming the model wave equation into a parabolic equation and considering the equation in the frequency or wavenumber spaces in time or spatial domain. This indicates that, in order to obtain an accurate result, only one sweep in space is sufficient, which is mainly due to the introduction of the omission of back scattering waves. This kind of approximation is justified in the area of the aerospace because the effect of back scattering is vanishingly small; the locations of sound sources and receivers are explicitly separated and the obstacles impeding the sound propagation can be negligible. Reflection and diffraction around obstacles are also considered in this tool as a heterogeneous media by inputting CAD data directly, which indicates that one does not have to prepare computational grids around the obstacles. As a result, real scale analyses with high resolution up to 2kHz can be achieved even with a single workstation, which can never be realized by means of CFD analyses on any supercomputer in existence.

Th. 14:00 Amphi 2

Nonlinear propagation in fluids 2

Structures of lee waves over combined topography

J. Maltseva and N. Makarenko

NSU, Lavrentyev Inst. of Hydrodynamics, Lavrentyev ave., 15, 630090 Novosibirsk, Russian Federation

maltseva@hydro.nsc.ru

The problem of finite amplitude internal waves arising in a steady exponentially stratified flow over an combined bottom is considered. Semi- analytical model deals with asymptotic solutions of the Euler equations of uniformly stratified fluid. Approximate solutions are constructed by the perturbation method complementing the Fourier method of modal expansion. We work with both the first-order linear solution, and the second-order non- linear solution (see [1,2]). Numerical calculations reveal the fragmentation effect which occurs for near-field wave patterns forced by multi-bumped topography of finite extension. In this paper we explain analytically the existence of distinct fronts which separate the flow domains having different wave scales. The results are illustrated numerically via modeling of wave structures generated by real mountain range.

References [1] N. Makarenko, J. Maltseva, Interference of lee waves over mountain ranges, NHESS, 2011, 11, 27-32. [2]

N. Makarenko, J. Maltseva, Steady waves in a stratified flow over a combined obstacle, JAMTP, 2014, 55(2), 311-317.

Second Harmonic Coupling Coefficient in Resonant Nonlinear Generation of Water Surface Waves

A. Bettucci, A. Alippi and M. Germano

Sapienza University of Rome, Via A. Scarpa, 14, 00161 Rome, Italy

andrea.bettucci@uniroma1.it

Works on nonlinear effects in water surface waves are complementary stimulated by interest in understanding the spectral composition of oceanic waves and feasibility of local detection of physical parameters. On the other side, water surface waves are composite waves contributed both by surface tension and gravity, such that study of nonlinear phenomena are theoretically severe and different approaches are available, that variously attempt to consider transverse or dilational stresses, mode resonant interactions, solitons etc. In the present work, a phenomenological approach is done, that simply moves from the detection of amplitude and phase of the harmonic components present along the propagation direction of the waves, to define a coupling coefficient between fundamental and first harmonic waves. This is obtained by considering that any harmonic component is locally generated through proper coupling coefficient of the interacting modes and then propagates by integration of the local effect along the propagation direction. That causes the harmonic components to be highly dependent upon the dispersion properties of the wave, though the coupling coefficient are not. The effect is here put into evidence by detecting harmonic production at different frequencies around the so-called resonant condition, where fundamental and second harmonic share the very same velocity, maintaining a matched phase condition along the propagation direction.

Th. 14:40 Amphi 2

Nonlinear propagation in fluids 2

The Study of Some Factors on Sound Wave Propagation in the Air

K. Han, X. Zeng, D. Chen and X. Ma

National University of Defense Technology, No.137, Yanwachi Street, 410073 Changsha, China

shunzhihan@sohu.com

In this paper, we have studied the effects of medium, wind field, temperature field on the propagation of sound wave. Firstly, the viscid wave equation is deduced, and then sound absorption coefficient and complex sound velocity are introduced. Combined with the theoretical method, we built up numerical models of the sound wave propagation. The results show that it is convenient for numerical calculation by adopting complex sound velocity which represents the absorption. Secondly, based on the staggered-grid pseudo-spectral method, we simulate the effects of average wind field, wind gradients, layered temperature field and temperature gradients on the propagation of sound wave. The results show that this gradient wind field makes the shape of sound field change, it is not a circularity at all. On the effect of temperature field, the direction of sound propagation is changed, and sound wave moves to low temperature (accordingly low velocity) areas. Finally, we simulate the sound wave propagation in the effects of various factors, and discuss the effect of SPL by wind field. It is shown that the ratio of sound wavelength and size of barrier is the important factor when sound wave is under the influence of barriers. The effect on the high frequency sound is larger than that on the low frequency one.

Irreversible Nonlinear Sound-Matter Interaction in Granular Media

X. Jia

Institut Langevin, ESPCI ParisTech, 1 rue Jussieu, 75005 Paris, France

xiaoping.jia@espci.fr

Granular materials are ubiquitous in everyday life, ranging from industrial applications to geophysical processes. Static properties and dense flow of granular materials strongly depend on the solid frame of the particles assembly, resulting from the confining pressure [1]. Elastic wave propagation offers a powerful and sometimes unique probe of this inhomogeneous and fragile contact network. The long-wavelength coherent waves give access to the elastic modulus whereas the short-wavelength scattered waves are sensitive to any rearrangement [2].

In this talk, we review the acoustic probing of dry and wet granular media such as the elastic modulus [3], the dissipation [4] and the shear band detection [5]. We show that beyond certain amplitude in the irreversible nonlinear regime elastic waves not only serve as probe but also as a controlled perturbation to fluidize the jammed granular media [6, 7]. Particular attention is paid to weakly compressed packings (e.g. under gravity), investigating both compressional [8] and shear waves [9]. Perturbation of the yield-stress rheology of amorphous interface by nonlinear shear ultrasound is also discussed [10], together with possible geophysical applications.

[1] H.M. Jaeger, S.R. Nagel and R.P. Behringer, *Rev. Mod. Phys.* 68, 1259 (1996) [2] X. Jia, C. Caroli and B. Velicky, *Phys. Rev. Lett.* 82, 863 (1999); X. Jia, *Phys. Rev. Lett.* 82, 863 (2004) [3] V. Langlois and X. Jia, *Phys. Rev. E* 89, 0223206 (2014) [4] T. Brunet, X. Jia and P. Mills, *Phys. Rev. Lett.* 101, 138001 (2008) [5] Y. Khidas and X. Jia, *Phys. Rev. E* 85, 051302 (2012) [6] P. Johnson and Jia, *Nature* 437, 871 (2005) [7] X. Jia, T. Brunet and J. Laurent, *Phys. Rev. E* 84, 020301(R) (2011) [8] S. Wildenberg, M. van Hecke and X. Jia, *Europhys. Lett.* 101, 14004 (2013) [9] J. Brum et al, *Phys. Rev.* (2014, under review) [10] J. Léopoldès, G. Conrad and X. Jia, *Phys. Rev. E* 91, 012405 (2015)

Modeling of non-linear interaction of waves in rocks

C. Larmat^a, R. Guyer^b, P.-Y. Le Bas^c, P. Johnson^b and J. Ten Cate^c

^aLos Alamos National Laboratory, Bikini Atoll Rd, EES-17, MS D452, Los Alamos, AK 87545, USA; ^bLos Alamos National Laboratory, MS D446, Bikini Atoll Rd, Los Alamos, Nm, AK 87545, USA; ^cLos Alamos National Laboratory, Bikini Atoll Rd, EES-17, MS D446, Los Alamos, 87545, USA

carene@lanl.gov

In situ imaging of elastic nonlinearity is coming closer to reality. Non-linear properties of solids have been extensively studied in laboratory samples and it has been shown that non-linearity in compound materials like rocks and concrete are two or three orders of magnitude higher than in mono crystalline solids (Ostrovsky & Johnson, 2001, Payan et al., 2009). We are using numerical modeling to explore the non-linear interaction of waves in rock with the ultimate goal to determine ways to do imaging of the elastic nonlinearity. We focus on the cross-beam geometry that was validated by early experiments conducted by Rollins et al. (1964), and later in rock by Johnson et al. (1987). In this geometry, two non-collinear beams are mixed at prescribed angles, and a third beam at the difference frequency is created in the intersection volume, probing the non-linear properties in this volume. This third beam's trajectory is determined by selection rules that depend on the angle between the primary beams, their frequency ratio and the local poisson ratio. The signature of the non-linearity is embedded in the amplitude of the third beam. Accurate full wave modeling is necessary to assess the efficiency of the third beam to be used as probe of the non-linearity. We will show results of 2D Finite Difference modeling and 3D spectral Element method modeling, with some attempts of theoretical validation. The characteristics of the third beam will be studied in regards to characteristics of the primary beams and properties of the surrounding medium such as a complex layered velocity structure.

Modulation of P-waves by S-waves in rocksA. Malcolm^a, J. Ten Cate^b, X. Feng^c and M. Fehler^c^aMemorial University of Newfoundland, 300 Prince Philip Ave, St John'S, AB, Canada a1b3x5; ^bLos Alamos National Lab, Mail Stop D446, Geophysics, EES-17, Los Alamos, AK 87545, USA; ^cMassachusetts Institute of Technology, 77 Massachusetts Ave, Cambridge, 02139, USA

amalcolm@mun.ca

The modulation of sound by sound refers to an old set of experiments done both in Russia and the US in the 1950s to 1970s. The best demonstration of the effect was when a small high frequency acoustic plane wave "probe" travelled collinearly along with a low frequency finite amplitude wave "pump" in a fluid like air or water. The nonlinear distortion of the finite amplitude wave modulated the probe wave, speeding up and slowing down different parts of the probe causing a frequency modulation which could be easily measured. We've used similar ideas to do a completely different experiment in a rock. Here a short high frequency probe pulse is timed and launched in such a way that it travels through different parts of a perpendicularly travelling shear wave pump, which effectively speeds up or slows down the arrival time of the probe. Or so we initially thought. The experiment is straightforward, the results easy to reproduce. The interpretation is, however, challenging and illustrates just how much richer wave propagation is in a rock. We'll report on a series of experiments in an anisotropic sandstone and discuss interpretations of our results. We are grateful to Weatherford for both financial support and useful discussions.

Th. 15:40 Amphi 2

Sonic boom propagation

Lateral Cutoff Analysis and Results from NASA's Farfield Investigation of No-boom ThresholdsL. Cliatt^a, E. Haering^a, S. Arnac^b and M. Hill^c^aNASA Armstrong Flight Research Center, P.O. Box 273, Mail Stop 2228, Edwards, CA 93523, USA; ^bNASA Armstrong Flight Research Center, P.O. Box 273, Mail Stop 2134, Edwards, CA 93523, USA; ^cNASA Armstrong Flight Research Center, P.O. Box 273, Mail Stop 4840A, Edwards, CA 93523, USA

larry.j.cliatt@nasa.gov

In support of the ongoing effort by the National Aeronautics and Space Administration (NASA) to bring supersonic commercial travel to the public, the NASA Armstrong Flight Research Center and the NASA Langley Research Center, in partnership with other industry organizations, conducted a flight research experiment to analyze acoustic propagation at the lateral edge of the sonic boom carpet. The name of the effort was the Farfield Investigation of No-boom Thresholds (FaINT). The test helped to build a dataset that will go toward further understanding of the unique acoustic propagation characteristics near sonic boom carpet extremity. FaINT was the first such known effort that collected measured sonic boom data across the entire lateral cutoff transition region.

The FaINT test was a NASA collaborative effort with several industry partners. Domestic partners included The Boeing Company (Chicago, Illinois); Gulfstream Aerospace Corporation (Savannah, Georgia); Wyle (El Segundo, California); The Cessna Aircraft Company (Wichita, Kansas); and Pennsylvania State University (University Park, Pennsylvania). FaINT also benefited from collaborations with international partners The Japan Aerospace Exploration Agency (Chōfu, Tokyo, Japan) and Dassault Aviation (Paris, France).

A major objective of the effort was to investigate the acoustic phenomena that occur at the audible edge of a sonic boom carpet, including the transition zone. The transition zone is the lateral area between the sonic boom carpet and the shadow zone, while the shadow zone may encompass all space beyond lateral ray propagation where an audible disturbance is detectable. A NASA F-18B aircraft made supersonic passes such that its sonic boom carpet transition zone would intersect a linear 60-microphone, 7500 ft. long array and a 62-microphone, 2000 ft. diameter spiral array. A TG-14 motor glider equipped with a microphone on its wing also attempted to capture the same sonic boom rays that were measured on the ground, at altitudes of 3000 - 8000 ft. above ground level.

Examining acoustic propagation at the lateral edge of the sonic boom carpet will help the industry realize the full extent and ranges of noises generated by a supersonic aircraft. Considerable sound levels can be experienced far beyond the sonic boom carpet predicted by computer models due to the difficulty in accurately modeling the evolution of N-waves within the sonic boom carpet and evanescent waves that propagate in the shadow zone. Understanding the entire physical area affected by supersonic aircraft will be critical in determining target flight profiles and aircraft designs for future commercial supersonic aircraft.

This paper focuses on quantifying the lateral extent of a sonic boom's carpet; analyzing the change in sonic boom levels as a function of distance from flight path using appropriate metrics for transition and shadow zone pressure signatures; changes in sonic boom rays near lateral cutoff from the midfield to the ground; and comparisons between real sonic boom measurements and a modeling software.

Numerical Model of Sonic Boom in 3D Kinematic Turbulence.F. Coulouvrat^a, D. Luquet^b and R. Marchiano^c

^aCNRS - Institut Jean Le Rond d'Alembert (UMR 7190), Université Pierre et Marie Curie, 4 place Jussieu, 75005 Paris, France; ^bUniversité Pierre et Marie Curie, d'Alembert, boîte 162, 4 place Jussieu, 75005 Paris, France; ^cInstitut Jean le Rond d'Alembert, 4, Place Jussieu, 75252 Paris Cedex 05, France
francois.coulouvrat@upmc.fr

Sonic boom is one of the key issues to be considered in the development of future supersonic or hypersonic civil aircraft concepts. The classical sonic boom, typical for Concorde with an N-wave shape and a ground amplitude of the order of 100 Pa, prevents overland flight. Future concepts target carefully shaped sonic booms with low amplitude weak shocks. However, sonic boom when perceived at the ground level is influenced not only by the aircraft characteristics, but also by atmospheric propagation. In particular, the effect of atmospheric turbulence on sonic boom propagation near the ground is not well characterized. Flight tests performed as early as the 1960's demonstrated that classical sonic booms are sensitive to atmospheric turbulence. However, this sensitivity remains only partially understood. This is related to the fact that i) turbulence is a random process that requires a statistical approach, ii) standard methods used to predict sonic booms, mainly geometrical acoustics based on ray tracing, are inadequate within the turbulent planetary boundary layer. Moreover, the ray theory fails to predict the acoustical field in many areas of interest, such as caustics or shadow zones. These zones are of major interest for sonic boom acceptability (highest levels, lateral extent of zone of impact). These limitations outline the need for a numerical approach that is sufficiently efficient to perform a large number of realizations for a statistical approach, but that goes beyond the limitations of ray theory. With this in view, a 3D one-way numerical method solving a nonlinear scalar wave equation established for heterogeneous, moving and absorbing atmosphere, is used to assess the effects of a 3D kinematic turbulence on sonic boom in various configurations. First, a plane N-wave is propagated in the free field through random realizations of kinematic fluctuations. Then the case of a more realistic Atmospheric Boundary Layer (ABL) is investigated, with a mean stratified wind superimposed to a 3D random turbulent realization. Propagation is performed either in the case of a shadow zone or of an atmospheric waveguide. To model the turbulent ABL, the mean flow and the fluctuations are handled separately. The wind fluctuations are generated using the Random Fluctuations Generation method assuming a von Kármán spectrum and a homogeneous and isotropic turbulence. The mean stratified wind is modeled based on the Monin-Obhukov Similarity Theory (MOST). To illustrate the method, the typical case of a sunny day with a strong wind has been chosen. Statistics are obtained on several parameters. It shows the importance of turbulence, which leads to an increase of the mean maximum peak pressure in the shadow zone and to its decrease in the waveguide. Moreover, the formation of random caustics that can lead to an increase of the noise perceived locally is outlined. [Work performed within the European Union ATLLAS II Project - Grant 263913 ; D. Luquet benefits from a PhD grant co-funded by Direction Générale de l'Armement - France].

Th. 16:20 Amphi 2

Sonic boom propagation

Measured N-Wave Sonic Boom Events and Sensitivity in Sonic Boom MetricsJ. Palmer^a and V.W. Sparrow^b^aPenn State, 201 Applied Science Building, University Park, PA 16802, USA; ^bThe Pennsylvania State University, 201 Applied Science Building, University Park, PA 16802, USA

jdp995@psu.edu

Various sonic boom noise metrics have been calculated for a number of sonic boom, N-wave signatures. The newly computed metrics utilized high-quality recordings from both the Superboom Caustic Analysis and Measurement Program (SCAMP) and Farfield Investigation of No-boom Thresholds (FaINT) experiments conducted by NASA. With both signature datasets comprised of microphone measurements by long linear arrays, one can assess the waveform variability due to atmospheric turbulence influences across the arrays. Preferred boom events from these NASA datasets were then chosen after review of the flight conditions, flight objectives and actual waveforms generated in order to study only the non-focused, N-wave sonic boom signatures. The sonic boom noise metrics calculated for the preferred boom events include Stevens Mark VII Perceived Level (PLdB), un-weighted Sound Exposure Level (SELz) as well as Sound Exposure Level with A, B, C, D, and E weightings applied to the waveforms. The results show, for example, that the A-weighted sound exposure levels and Steven's Mark VII Perceived Levels had standard deviations in the range of 3 dB to 9 dB for both the SCAMP and FaINT measurements. Such sensitivity results should be helpful in assessing the applicability of sonic boom metrics for use in future en-route certification standards for civilian supersonic aircraft. [The opinions, findings, conclusions, and recommendations expressed here are those of the authors and do not necessarily reflect the views of sponsors of the ASCENT Center of Excellence including the Federal Aviation Administration.]

Slow Dynamics in Granular Media: Theoretical Models and ExperimentsP. Johnson^a, A. Lebedev^b, L. Ostrovsky^c and J. Riviere^a^aLos Alamos National Laboratory, MS D446, Bikini Atoll Rd, Los Alamos, Nm, AK 87545, USA; ^bInstitute of Applied Physics, ulitsa Ulyanova, 46, 603600 Nizhny Novgorod Oblast, Russian Federation; ^cNOAA ESRL/PSD, 325 Broadway, R/PSD99, Boulder, AK 80305, USA

paj@lanl.gov

In the last two decades much effort has gone into characterizing dynamically-induced elastic nonlinearity in mesoscopic media such as rock, unconsolidated granular materials and soil [1]. In addition to nonlinear elastic effects taking place during dynamic wave excitation, experiments demonstrate that in media with complex structure the elastic response is characterized by a long-time relaxation (slow dynamics). In spite of considerable study, the mechanisms of this effect are not fully understood. Recently we suggested [2] a simplified description of a granular material with an adhesion-governed contact potential having a barrier separating two minima-where the primary minimum is responsible for the near-field forces such as the Van-der Waals forces, and a second minimum responsible for weak interactions (e.g., entropy forces). During dynamical excitation some contacts are forced over the barrier into the nearby, metastable potential wells. After a fast recovery, a small number of contacts remain in the "excited" state near the second, shallow minimum. Using the Arrhenius law for the rate of strain change and supposing that the Gibbs potential strongly exceeds the thermal kinetic energy, it is shown that after a short impact, the strain relaxes logarithmically in time. To explain the logarithmic behavior of weak probe oscillations on the background of slow relaxation, one must add the classical quadratic nonlinearity. From this model, characteristic scales of the contact were estimated to be of the same order of 101 Å for many materials.

Recently experiments were conducted exploring the early time relaxation (of the order of 15 s) and the dependence on the strength of the initial dynamic forcing in various rocks. We find a non-logarithmic recovery in this regime. Based on these results we modified the relaxation model applying the fraction of contacts remaining after this initial stage. Finally, we discuss possible applications of the above effects in the non-destructive testing of the materials.

References: 1. Guyer, R.A., and Johnson, P.A. Nonlinear mesoscopic elasticity: the complex behaviour of rocks, soil, concrete. Wiley-VCH, 2009. 2. Lebedev, A. and L. Ostrovsky, A unified model of hysteresis and long-time relaxation in heterogeneous materials, *Acoust. Physics*, 60, 555-561, 2014.

Th. 16:00 Amphi 3

Granular media 2

In Situ Acoustoelastic Testing: A Passive Monitoring Approach to Study Crustal and Fault Zone Rocks

G. Hillers

Institut des Sciences de la Terre, 1381 rue de la Piscine, UJF BP 53, 38041 Grenoble, France

gregor.hillers@ujf-grenoble.fr

Testing strategies targeting the behavior of geomaterials under controlled laboratory conditions in response to a variety of stimuli range from (quasi-) static over cyclic to dynamic stress histories or deformation protocols and include acoustic and resonant excitation. This can induce linear and nonlinear elastic or nonelastic behavior, where the response type is critically governed by the distribution and properties of voids or (micro-) cracks within the probed material, i.e., by its damage state. The scale dependence poses a fundamental problem in formulating constitutive relationships and in applying lab-based results to in situ rock properties, because sample size and the potentially variable distribution of defects control the macroscopic rheology of composite Earth materials.

In situ observations covering a large range of spatiotemporal scales are therefore essential for a better understanding of rock behavior, and important for the assessment of scalability of lab-results. Focusing on measurements of in situ responses to Earth tides is an appealing strategy because of the evident tidal effect on crustal deformation and the well understood stress history. Building on the analysis of Green's function estimates constructed from the ambient seismic wavefield, we present a passive approach to measure relative velocity variations (dv/v) in response to tidal deformation by analyzing noise recorded by a dense seismic array at the site of the Pinon Flat Observatory, Southern California. We focus in our discussion on the effect of multiple, simultaneously acting loading mechanisms. We discuss strategies to separate different contributions to obtained dv/v measurements for better sensitivity estimates and the possibility to resolve in situ hysteresis.

We observe a clear dependence of the response on the component of wave motion and noise correlation coda lapse time. Measurements on the vertical correlation component indicate reduced wave speeds during periods of volumetric compression, whereas data from horizontal components show the opposite behavior, compatible with previous observations. The in situ nonlinearity across the differential strain range of $\sim 6e-8$ is consistent with the response induced by similar strains in the laboratory. However, the observed complex anisotropic in situ rheology indicates limits to the scalability of laboratory-derived observations. Our passive in situ acoustoelastic testing method has the potential to become a building block of observational tools to investigate velocity response types of crustal and fault zone materials to continuous, periodic, and transient deformation of variable duration and amplitude.

Observations of the Nonlinear Interaction of Two Waves Intersecting at Angles in Earth MaterialsJ. Ten Cate^a, P.-Y. Le Bas^b, C. Larmat^c, P. Johnson^d and R. Guyer^d

^aLos Alamos National Lab, Mail Stop D446, Geophysics, EES-17, Los Alamos, AK 87545, USA; ^bLos Alamos National Laboratory, Geophysics Group (EES-17), M/S: D446, Los Alamos, NM 87545, USA; ^cLos Alamos National Laboratory, Bikini Atoll Rd, EES-17, MS D452, Los Alamos, AK 87545, USA; ^dLos Alamos National Laboratory, MS D446, Bikini Atoll Rd, Los Alamos, Nm, AK 87545, USA

tencate@lanl.gov

When two waves interact in a nonlinear solid, it has been shown that the interaction produces sum and difference frequencies. When those two waves are collinear, the analogue of the parametric array in a fluid results in the solid. However, *unlike* interactions in a fluid, when those waves interact at angles in a solid, the physics dictates that only under special conditions will you get nonlinearly generated waves. The geometry has to be right (i.e. “selection rules” must be followed) and (2) the kinds of waves that interact must be specified as well (e.g., compressional P waves and shear S waves)—see [Korneev and Demcenko, *J. Acoust. Soc. Am.*, **135**, 591ff (2014)]. Theory and experiments done in the 1960s demonstrated these concepts at MHz frequencies in fused silica, polycrystalline aluminum and polycrystalline magnesium [Rollins, *Appl. Phys. Lett.* **2**, 147 (1963)]. We have recently done several experiments in more unusual solids, large blocks of sandstone, where the waves are produced by arrays of transducers and the difference frequency wave is detected with a noncontact laser vibrometer. We will show and discuss the results of these experiments.

Fr. 9:00 Amphi 2

Plenary lecture 6: Peter Coen

Breaking the Sound Barrier: Achieving Overland Supersonic Flight without Sonic Boom Disturbance

P. Coen

NASA Langley research Center, MS 264, Hampton, AK 23662, USA

peter.g.coen@nasa.gov

International research and development in 1940's provided engineering knowledge that overcame the myth of a "sound barrier" at Mach 1.0. However, those early successes soon revealed another more challenging barrier to acceptable supersonic flight over land: that of unacceptably loud sonic boom noise. In the decades since, dedicated researchers have chipped away at this "barrier". In the last 10 years, research in the United States and elsewhere has made strides that have brought the prospect of supersonic flight with minimal sonic boom noise closer than ever to reality. The presentation will summarize these accomplishments and outline research needed to replace the current restrictions on sonic boom and overland flight with a certification standard that will "break the barrier" to supersonic commercial aviation.

Fr. 10:00 Amphi 2

Perception of sonic boom

An investigation into the effect of playback environment on perception of sonic booms when heard indoors

D. Carr and P. Davies

Purdue University, Ray W. Herrick Laboratories, 177 S. Russell Street, West Lafayette, IN 47907-2099, USA

djcarr@purdue.edu

Manufacturers of business jets have proposed designing and building a new generation of supersonic jets that produce shaped sonic booms of lower peak amplitude than booms created by the previous generation of supersonic aircraft. To determine if these "low" booms are less intrusive and the noise exposure is more acceptable to communities, new testing to evaluate people's responses must occur. Because of the limitations on commercial supersonic flight overland in the US, and the lack of precise control of noise exposure in those settings, these studies must initially be done in a laboratory setting. To guide aircraft design, objective measures that predict human response to modified sonic boom waveforms and other impulsive sounds are needed. In previous research, it was also found that, for outdoor booms, startle and annoyance were highly correlated. Loudness alone did not fully explain annoyance or startle judgments, and so recent research was focused on startle and annoyance model development. Models that include maximum loudness, rise time, and sharpness metrics predict responses well to sounds heard outdoors. The next research phase is focused on understanding how people will react to booms when heard inside. House type and the indoor acoustic environment modify the outdoor booms, and this must be considered when predicting indoor sounds and annoyance ratings. A test was conducted in NASA Langley's Interior Effects Room (IER), with the collaboration of NASA Langley engineers. This test was focused on the effects of low-frequency content and of vibration, and subjects sat in a small living room environment. Thirty subjects living in the Hampton, Virginia area participated in this test. A second test was conducted in a sound booth at Purdue University, using similar sounds played back over earphones. The sounds in this test contained less very-low-frequency energy due to limitations in the playback, and the laboratory setting is a less natural environment. In both tests some of the sounds were transient sounds that might be heard indoors, but were not simulated interior booms. These were included in order to compare the responses to booms to responses to sounds with which the general population is more familiar. Their inclusion also increased the range of sound characteristics heard, which is helpful in development of human response prediction models, and which broadens the range where the model is applicable. In the Purdue test, binaural simulations of the interior sounds were included to compare responses to those sounds with responses to playback of binaural recordings taken in the IER, where the simulations and recordings were both derived from the same outdoor sound. In the simulations, the characteristics of the IER were used in modeling transmission and reverberation behavior; head related transfer functions were also included. Thirty subjects participated in the Purdue test; these were students and staff working at Purdue University. The design of the test, the signals and the simulation are briefly described and the results of both tests will be presented.

Fr. 10:20 Amphi 2

Perception of sonic boom

Influence of chair vibrations on indoor sonic boom annoyance

J. Rathsam, J. Klos and A. Loubeau

NASA Langley Research Center, Mail Stop 463, Hampton, VA 23681, USA

jonathan.rathsam@nasa.gov

One goal of NASA's Commercial Supersonic Technology Project is to identify candidate noise metrics suitable for regulating quiet sonic boom aircraft. A suitable metric must consider the short duration and pronounced low frequency content of sonic booms. For indoor listeners, rattle and creaking sounds and floor and chair vibrations may also be important. The current study was conducted to examine the effect of such vibrations on the annoyance of test subjects seated indoors. The study involved two chairs exposed to nearly identical acoustic levels: one placed directly on the floor, and the other isolated from floor vibrations by pneumatic elastomeric mounts. All subjects experienced both chairs, sitting in one chair for the first half of the experiment and the other chair for the remaining half. Each half of the experiment consisted of 80 high energy, impulsive noises played at the exterior of the sonic boom simulator. The results suggest that annoyance varied more with chair order than with vibration isolators. Nevertheless, higher annoyance ratings were reported in the non-isolated chair for higher amplitude sounds when vibration levels were only partially attenuated by the isolators.

A New Evaluation of Noise Metrics for Sonic Booms Using Existing DataA. Loubeau^a, Y. Naka^b, B.G. Cook^c, V.W. Sparrow^d and J.M. Morgenstern^e

^aNASA Langley Research Center, Mail Stop 463, Hampton, VA 23681, USA; ^bJapan Aerospace Exploration Agency, 6-13-1 Osawa, Mitaka, 181-0015 Tokyo, Japan; ^cGulfstream Aerospace Corp., 500 Gulfstream Road, Savannah, GA 31408, USA; ^dThe Pennsylvania State University, 201 Applied Science Building, University Park, PA 16802, USA; ^eLockheed Martin Aeronautics Company, 1011 Lockheed Way, B611 MC1142, Palmdale, CA 93599, USA

a.loubeau@nasa.gov

An evaluation of noise metrics for predicting human perception of sonic booms was performed. Thirty metrics were chosen from standards and from the literature in an effort to include all potentially relevant metrics. Five different databases of sonic boom waveforms and associated human response were chosen to span a variety of signals, including traditional N-waves with various shock shapes and rise times, and predicted waveforms from designs of low-boom aircraft for a variety of aircraft sizes. These databases were derived from laboratory studies conducted in sonic boom simulators at NASA Langley Research Center and JAXA. Simulations of booms experienced in both outdoor and indoor environments were included by using different facilities or modifications to facility configurations. American and Japanese test subjects participated at NASA and JAXA, respectively, with instructions and rating systems in English and Japanese, respectively. Ratings of loudness using a magnitude estimation technique and ratings of annoyance, loudness, and other descriptors using a category line scaling method are included. The evaluation consists of linear correlations of human response data with the objective noise metrics. Results are presented for each study with a ranking of metric performance.

Fr. 11:20 Amphi 2

Perception of sonic boom

Understanding Sources of Uncertainty and Bias Error in Models of Human Response to Low Amplitude Sonic BoomsJ. Gavin^a, M. Collmar^b, B.G. Cook^c, R. Cowart^b and D. Freund^d^aGulfstream Aerospace Corporation, 500 Gulfstream Rd., Savannah GA. USA, 31408, Savannah, GA 31408, USA;^bGulfstream Aerospace Corporation, 500 Gulfstream Rd, Savannah, GA 31408, USA; ^cGulfstream Aerospace Corp., 500 Gulfstream Road, Savannah, GA 31408, USA; ^dGulfstream Aerospace Corporation, 500 Gulfstream Rd, Savannah,

AK 31408, USA

robbie.cowart@gulfstream.com

A pool of 200 subjects was exposed to a library of waveforms consisting of example signatures of low boom aircraft. The signature library included intentional variations in both loudness and spectral content, and were auralized using the Gulfstream SASS-II sonic boom simulator. Post-processing was used to quantify the impacts of test design decisions on the "quality" of the resultant database. Specific lessons learned from this study include insight regarding potential for bias error due to variations in loudness or peak over-pressure, sources of uncertainty and their relative importance on objective measurements, robustness of individual metrics to wide variations in spectral content, and statistical significance of resultant correlations across the distribution function of individual judgments. Results provide clear guidance for design of future large scale community surveys, where one must optimize the complex tradeoffs between the size of the surveyed population, spatial footprint of those participants, and the fidelity/density of objective measurements.

AUTHOR INDEX

Adachi, Hideo	90	Didenkulov, Igor	64
Adachi, Shizuko	28	Doc, Jean-Baptiste	116
Aida, Takumi	46	Dos Santos, Serge	89
Aleshin, Vladislav	95, 113	Dragna, Didier	124
Alippi, Adriano	137	Dreiden, Galina	96, 129
Amghar, Abdellah	55	Drob, Douglas	130
An, Yu	131	Duong, Dang V.	127
Anderson, Brian	128	Elster, Anne	34
Andreev, Valeriy	18	Fan, Tingbo	80
Andriyakhina, Yulia	24	Farr, Navid	23
Andronova, Natalja	58	Fehler, Michael	141
Angelsen, Bjørn	34	Feng, Xuan	141
Annenkova, Elena	101	Foucault, Eric	51
Aoyama, Takashi	135	Francescutto, Alberto	123
Arnac, Sarah	142	Freund, Don	152
Atchley, Anthony A.	126	Fuster, Daniel	116
Bader, Kenneth	78	Gainville, Olaf	103
Bailey, Michael	24	Garandet, Jean-Paul	68
Bailliet, Hélène	51, 53, 67	Garnier, Vincent	93
Bailly, Christophe	125	Gavin, Joseph	152
Baltean-Carlès, Diana	69	Gavrilov, Leonid	38
Baresch, Diego	120	Gee, Kent L.	126
Barriere, Christophe	117	Germano, Massimo	137
Basset, Olivier	35, 77, 88	Giammarinaro, Bruno	91
Begar, Anna	119	Gilles, Bruno	98, 122
Ben Hadid, Hamda	68	Golubkova, Irina	18
Béra, Jean-Christophe	63, 98, 122	Gomez, Thomas	104
Bernard, Adeline	88	Gong, Xiufen	56, 59, 60
Bessis, Rémi	53	Gopin, Alexander	58
Bettucci, Andrea	137	Guédra, Matthieu	100, 122
Biwa, Tetsushi	40, 42	Gurbatov, Sergey	87
Blanc-Benon, Philippe	63, 106, 108, 124	Guyer, Robert	140, 147
Blanloeuil, Philippe	44	Haering, Edward	142
Bogey, Cb	125	Hamilton, Mark	19, 21, 49
Botton, Valéry	68	Han, Kaifeng	138
Bou Matar, Olivier	95, 113	Hatanaka, Megumi	71
Bulanov, Alexey	109	Hayashi, Hiroyuki	28
Cachard, Christian	35, 77, 88	Henry, Daniel	68
Cain, Charles	22	Hertl, Michael	46
Callé, Samuel	114	Hill, Michael	142
Camarena, Francisco	86	Hillers, Gregor	146
Campos-Pozuelo, Cleofé	66	Holland, Christy	78
Carr, Daniel	149	Hu, Bo	39, 61, 99
Chaix, Jean-François	93	Huber, Grégory	98
Chaline, Jennifer	89	Hughes, Derke	110
Chavrier, Françoise	37	Hyodo, Hiroaki	42
Chen, Dan	138	Ilinskii, Yurii	19, 48, 49
Cleveland, Robin	17, 76	Ilyin, Sergey	38
Cliatt, Larry	142	Ino, Yoshihiro	115
Coen, Peter	148	Inserra, Claude	63, 122
Collmar, Matthew	152	Ishii, Katsuya	28
Conoir, Jean-Marc	116	Izossimova, Maria	62
Cook, Brian G.	151, 152	Jackson, Edward	76
Cormack, John	21	Jaros, Jiri	81
Coulouvrat, François	84, 91, 97, 100, 104, 143	Jia, Xiaoping	139
Coward, Robbie	152	Jimenez Noe	86

Khokhlova, Vera	23, 24, 38, 79, 75, 106	Nomura, Hideyuki	90
Kido, Aiko	54	Nuttall, Albert	110
Klos, Jacob	150	Ogasawara, Toshiyuki	118
Koch, Robert	110	Ohara, Yoshikazu	115
Kokshaiskii, Alexei	20, 62	Ohashi, Noriyuki	70
Kondoh, Jun	70	Ohm, Won-Suk	85, 134
Konofagou, Elisa E.	86	Okita, Kohei	102
Korman, Murray S.	127	Olivier, Côme	41
Korobov, Alexandr	20, 62	Ollivier, Sébastien	63, 106, 108, 124
Kotukhov, Alexei	123	Ostrovsky, Lev	47, 145
Koumela, Alexandra	108	Palmer, Joshua	144
Koyama, Daisuke	71	Partanen, Ari	23
Kreider, Wayne	23, 24, 38, 50, 101	Payan, Cédric	93, 112
Krit, Timofey	18	Penelet, Guillaume	41
Kryzhanovskiy, Maxim	50	Perfilov, Sergey	20
Kurihara, Eru	132	Peruzzini, Daniele	73
Kvam, Johannes	34	Pinton, Gianmarco	32, 91
Kwon, Oh-Cho	134	Poignand, Gaele	41
Lafon, Cyril	37	Prieur, Fabrice	37
Lafond, Maxime	37	Prokhorov, Viacheslav	20
Lake, Colton	112	Pronchatov-Rubtsov, Nikolay	64
Lardjane, Nicolas	103, 104	Qian, Feng	60
Larmat, Carene	140, 147	Qiao, Shan	76
Le Bas, Pierre-Yves	112, 128, 140, 147	Quan, Li	60
Lebedev, Andrey	145	Raghunathan, Shreyas B.	82
Lee, Hunki	134	Rathsam, Jonathan	150
Lee, Jae-Wan	85	Redondo, Javier	86
Leroy, Valentin	117	Reichman, Brent O.	126
Li, Di	39	Remillieux, Marcel	112
Lim, Hyung Jin	43	Rendón, Pablo Luis	33
Lin, Fanglue	77	Rénier, Mathieu	45
Lipkens, Bart	48	Reyt, Ida	51, 53
Liu, Xiaozhou	56, 59, 60	Richoux, Olivier	92
Lombard, Bruno	92	Ridoux, Julien	104
Lombard, Olivier	117	Riviere, Jacques	145
Lott, Martin	93	Rosnitskiy, Pavel	79
Lotton, Pierrick	41	Rudenko, Oleg	87
Loubeau, Alexandra	150, 151	Rufer, Libor	108
Luquet, David	84, 143	Ryashchikov, Dmitriy	27
Ma, Xiaoming	138	Sabatini, Roberto	125
Makarenko, Nikolay	136	Sabir, Brahim	57
Maksimov, Alexey	133	Sahsah, Hassan	55
Malcolm, Alison	141	Saidoun, Abdelkrim	45
Maltseva, Janna	136	Saito, Takeru	52
Marchiano, Régis	84, 97, 116, 143, 120	Sakamoto, Shin-Ichi	54
Marsden, Olivier	124, 125	Salze, Edouard	108
Martin, Elly	81	Sambandam, Baskar	97
Matsukawa, Mami	71	Samsonov, Alexander	96, 129
Matsumoto, Yoichiro	102	Sanchez-Morcillo, Victor	86
Maxwell, Adam	23, 121	Sapozhnikov, Oleg	23, 24, 38, 50, 75, 101, 121
Menshov, Igor	28	Sarvazyan, Armen	47
Mercier, Jean-François	92	Seck, Ababacar	63
Mestas, Jean-Louis	37	Sekino, Kouichi	46
Mettin, Robert	94	Semenova, Irina	96, 129
Meziane, Anissa	44, 45	Shi, Jie	39, 61, 99
Miao, Boya	131	Shi, Shengguo	39, 61, 99
Miller, Kyle G.	126	Shim, Woosup	85
Millet, Séverine	68	Shimizu, Dai	29
Mischi, Massimo	74	Shvartz, Andrew	96, 129
Molevich, Nonna	27	Sinilshchikov, Ilya	23

Takahashi, Koji	115	Vilchinska, Nora	65
Takahashi, Takashi	135	Volkov, Alexandr	20
Takahira, Hiroyuki	118	Vos, Hendrik	73
Tanaka, Moeko	118	Vu, Quang Anh	93
Tanguy, Sébastien	98	Walaszek, Henri	45
Ten Cate, James	140, 141, 147	Wang, Xiangda	56
Terzi, Marina	121	Watanabe, Yoshiaki	54
Thomas, Jean-Louis	120	Weisman, Catherine	69
Tian, Zhangfu	30	Wijkstra, Hessel	74
Tortoli, Piero	73	Wise, Elliott	83
Toulemonde, Matthieu	88	Wu, Rongrong	59
Tournat, Vincent	31	Yamanaka, Kazushi	115
Trarieux, Chloé	114	Yang, Desen	39, 61, 99
Treeby, Bradley	81, 83	Yano, Takeru	105
Treshalina, Elena	58	Yasuda, Jun	36
Treweek, Benjamin	49	Yasui, Hajime	46
Trifonov, Andrey	95, 113	Yonemitsu, Shunsuke	52
Tripathi, Bharat	97	Yoshizawa, Shin	25, 36
Tsysar, Sergey	50, 75, 121	Yuldashev, Petr	23, 24, 38, 79, 75, 106, 108
Ueda, Yuki	52	Zabolotskaya, Evgenia	19, 48, 49
Ulrich, Tj	112, 128	Zavershinskiy, Dmitriy	27
Umemura, Shin-Ichiro	25, 36	Zeng, Xinwu	30, 138
Valière, Jean-Christophe	51, 53, 67	Zhang, Dong	80
Välimäki, Vesa	72	Zhang, Fan	45
Van Sloun, Ruud J.G.	74	Zhang, Haoyang	39, 61, 99
Vanhille, Christian	66	Zhang, Lue	56
Varray, François	35, 88	Zhao, Yun	30
Velasco, Roberto	33		
Verweij, Martin	73, 82		